LOCALIZED ADOPTIVE CELLULAR THERAPY OF *EX VIVO* EXPANDED GAMMA DELTA T CELLS FOR SOLID TUMOURS

NAMFON PANTARAT MSc (Biotech)

A thesis submitted in total fulfilment of the requirements

For the degree of Doctor of Philosophy

in

The Discipline of Surgery, School of Medicine

Faculty of Health Sciences

The University of Adelaide

July 2022

Table of Contents

Declaration.....7

Acknowledgements.....8

Abstract.....9

Conference proceedings.....11

List of Figures.....12

Abbreviations used.....15

Chapter 1.....17

Introduction.....17

1.1 Localized cancer therapy.....18

1.2 Adoptive cell therapy (ACT).....19

1.3 Gamma delta (γδ) T cells.....22

1.3.1 Ligand recognition by Vγ9Vδ2 T cells.....24

1.3.2 Mechanisms of Vγ9Vδ2 T cell cytotoxicity.....27

1.4 Nitrogen-containing bisphosphonates (NBPs).....28

1.4.1 Intracellular effect and pharmacodynamics of NBPs.....30

1.4.2 Pharmacokinetics limitations of NBPs.....32

1.4.3 Clinical applications of NBPs, particularly Zoledronate (ZOL) in cancer.....32

1.4.4 NBPs and Phosphoantigens (PAgs).....34

1.5 Clinical experience with Vγ9Vδ2 T cells.....35

1.6 ACT of *ex vivo* expanded Vγ9Vδ2 T cells for solid tumours 37

1.7 Alternative routes of administration 38

1.7.1 Intra-arterial ACT 38

1.7.2 Intrapeural ACT 38

1.7.3 Intracranial ACT 40

1.7.4 Intra-tumoral ACT 40

1.7.5 Intraperitoneal ACT 41

1.7.6 Biomaterial-based localized ACT 41

1.8 Aims and Significance 44

Chapter 2 47

Materials and Methods 47

2.1 *Ex vivo* expansion and enrichment of Vγ9Vδ2 T cells 48

2.2 Labelling Vγ9Vδ2 T cells with VivoTrack680 48

2.3 Encapsulation of Vγ9Vδ2 T cells in Matrigel and 3D cell viability assay 48

2.4 *In vitro* Vγ9Vδ2 T cell release assay – video microscopy 49

2.5 Migration-based assay for quantification of encapsulated Vγ9Vδ2 T cell cytotoxicity 50

2.6 Western immunoblotting 50

2.7 Animal study design 51

2.8 Breast cancer mouse tumour model 52

2.9 Glioblastoma cancer mouse model 53

2.10 *In vivo* fluorescence and bioluminescence imaging 53

2.11 TCR δ Immunohistochemistry and TUNEL staining 53

2.12 Flow cytometric analysis tumour explants. 54

2.13 Western immunoblotting 55

2.14 Statistics 56

Chapter 3 57

***In vitro* optimisation of local ACT of ex vivo expanded Vγ9Vδ2 T cells** 57

3.1 Chapter introduction 58

3.2 Results 60

3.2.1 Vγ9Vδ2 T cells survive following encapsulation in Matrigel scaffolds 60

3.2.2 Encapsulated Vγ9Vδ2 T cells efficiently migrate out of Matrigel scaffolds 61

3.2.3 Vγ9Vδ2 T cells released from Matrigel are cytotoxic against ZOL-pretreated breast cancer cells 64

3.2.4 Incorporation of ZOL into Matrigel together with Vγ9Vδ2 T cells was equally effective in the T cell mediated cytotoxicity of cancer cells 68

3.3 Discussion 73

Chapter 4 80

Localized immunotherapy of *ex vivo* expanded Vγ9Vδ2 T cells in combination with zoledronate in xenograft models of breast and brain cancers 80

4.1 Chapter introduction 81

4.2 Results 83

4.2.1 Localized adoptive transfer of Vγ9Vδ2 T cells embedded in Matrigel together with ZOL reduced tumour burden but failed to eliminate cancer in a subcutaneous model of breast cancer 83

4.2.2 Localized adoptive transfer of Vγ9Vδ2 T cells and ZOL embedded in Matrigel potentiated cytotoxic function of the Vγ9Vδ2 T cells but did not eliminate cancer in a mammary fat pad model of breast cancer 84

4.2.3 ZOL is not internalised by cancer cells *in vivo* following local administration in ZOL-embedded Matrigel 87

4.3 Conclusion 99

Chapter 5 102

Zoledronate enhances Vγ9Vδ2 T cell antitumour responses against human glioblastoma 102

5.2 Results 105

5.2.1 Low ZOL treatment of glioblastoma U-87 MG cells induces dramatic morphological changes when compared to MDA-MB-231 breast cancer cells. 105

5.2.2 Differential growth inhibitory effects of ZOL in glioblastoma and breast cancer cells following 72 h exposure. 107

5.2.3 U-87 MG is particularly vulnerable to ZOL enhanced Vγ9Vδ2 T cell-mediated cytotoxicity. 107

5.2.4 Higher cellular uptake of ZOL in glioblastoma cells in comparison to breast cancer cells *in vitro*. 109

5.2.5 Differential accumulation of unprenylated Rap1A following ZOL treatment among glioblastoma and breast cancer cells. 112

5.2.6 Glioblastoma cells have higher endogenous HMG-CoAR protein expression when compared to breast cancer cells. 112

5.3 Discussion 114

Chapter 6 119

Discussion, Future Directions and Conclusions 119

Bibliography 131

Declaration

Name: Namfon Pantarat **Program:** PhD

I certify that this work contains no material which has been accepted for the award of any other degree or diploma in my name, in any university or other tertiary institution and, to the best of my knowledge and belief, contains no material previously published or written by another person, except where due reference has been made in the text. In addition, I certify that no part of this work will, in the future, be used in a submission in my name, for any other degree or diploma in any university or other tertiary institution without the prior approval of the University of Adelaide and where applicable, any partner institution responsible for the joint award of this degree.

I give permission for the digital version of my thesis to be made available on the web, via the University's digital research repository, the Library Search and also through web search engines, unless permission has been granted by the University to restrict access for a period of time.

I acknowledge the support I have received for my research through the provision of an Australian Government Research Training Program Scholarship.

Signature: Date: 26/09/2022

Acknowledgements

I would like to thank everyone who has helped me throughout my PhD studies. First and foremost, I would like to express my sincere gratitude to Prof. Andreas Evdokiou for giving me the opportunity to undertake such an interesting project. Thank you for the holding my work to a high standard and constantly encouraging and supporting me to improve. This would not have been possible without your support.

I would like to thank Prof Guy Maddern for offering me the scholarship to undertake Ph.D and, hence, bringing me to Adelaide. I just cannot thank you enough for being such an important part of this chapter of my life.

Next, I would like to thank the co-supervisors (Dr. Ehud Hauben and Dr. Irene Zinonos) and the past/present members of the Breast Cancer Research Unit: Bill and Romana Panagopolous, John Licari, Haruka Yamaguchi, Alex Shoubridge, Chris Difelice and Aneta Zysk for welcoming me with open arms and always being helpful and supportive.

It has been a long journey, but I was grateful to haven taken it and would not change it for anything.

Abstract

In recent years, adoptive cellular immunotherapy has emerged as a promising approach to treat cancers, particularly haematological cancers. However, its clinical utility in solid tumours is limited partly due to the requirement of transferred T cells to travel from the intravenous injection site to the tumour bed. Local administration of transferred T cells directly into the tumour mass or in the vicinity of a freshly resected tumour may be better suited to capitalize the full therapeutic potential of T cell adoptive therapy. This study explored the therapeutic potential of local delivery of gamma delta (Vγ9Vδ2) T cells (effector cells) in combination with zoledronate (cancer cell sensitiser) when embedded into biomaterial scaffolds for the local control of solid tumours using various cellular and animal models of breast cancer and glioblastoma. *In vitro, ex vivo* expanded Vγ9Vδ2 T cells maintained cell viability in Matrigel scaffolds and time-lapse video fluorescence imaging demonstrated progressive release of large numbers of Vγ9Vδ2 T cells from the scaffolds into surrounding area within just a few hours, rapidly killing cancer cells in their path. However, unlike the strong Vγ9Vδ2 T cell-mediated cytotoxicity observed *in vitro,* the effects seen *in vivo* using xenograft models of both breast cancer and glioblastoma were highly disappointing with only marginal anticancer efficacy observed. To explore the reasons for this, FACS was used to analyse the tumours at 72 hrs after the co-delivery of fluorescently labelled Vγ9Vδ2 T cells and fluorescent ZOL in Matrigel scaffolds. The data showed that, whereas Vγ9Vδ2 T cells were abundantly present in the tumour tissue, ZOL, on the other hand, could not be detected in cancer cells but rather accumulated selectively in the tumour resident macrophages and was preferentially rooted to the skeleton of mice due to its calcium binding characteristics. Collectively the data presented in this thesis clearly indicate that ZOL given locally, is unlikely to be of sufficient benefit in potentiating Vγ9Vδ2 T cell function *in vivo* and is therefore destined to fail clinically despite the overwhelming cytotoxicity observed in many cellular

models. In this regard, the use of nanotechnology to improve cancer cell uptake of ZOL may open up a new therapeutic scenario for ZOL and Vγ9Vδ2 cell-based local immunotherapy.

Conference proceedings

Localized adoptive cellular therapy of ex vivo expanded gamma delta T cells for solid tumours, The Basil Hetzel Institute and Queen Elizabeth Hospital Research Day 2020, Adelaide, SA, Australia, 15-16th Oct 2020 (**Oral presentation**)

Hydrogel-based delivery of cytotoxic gamma delta T cells for the localized treatment of incompletely resected or inoperable tumours, The Basil Hetzel Institute and Queen Elizabeth Hospital Research Expo 2018, Adelaide, SA, Australia, 18-19th Oct 2018 (**Oral presentation**)

Hydrogel-based delivery of cytotoxic gamma delta T cells for the localized treatment of incompletely resected or inoperable tumours, 2017 Australian Society for Medical Research (ASMR) SA Scientific Meeting, Adelaide, SA Australia, 1st-9th June 2017 (**Poster presentation**)

List of Figures

Fig 1.1 Basic principles of adoptive cell therapy (ACT)……..…20

Fig 1.2 Ligand model of PAg sensing by Vγ9Vδ2 TCR…….….26

Fig 1.3 Multiple cytotoxic mechanisms of Vγ9Vδ2 T cells…….29

Fig 1.4 IPP and mechanism by which NBPs indirectly stimulate Vγ9Vδ2 T cells……..31

Fig 1.5 Comparison between intra-venous and intra-arterial injections…….……..39

Fig 3.1 Biocompatibility of Matrigel-encapsulated Vγ9Vδ2 T cells…….……...62

Fig 3.2 Microscopic evaluation (10X) of Vγ9Vδ2 T cell migration out of Matrigel scaffolds following encapsulation……63

Fig 3.3 Visualization of Vγ9Vδ2 T cell migration out of Matrigel and cytotoxicity against breast cancer cells……65-67

Fig 3.4 Inhibition of prenylation from ZOL-embedded Matrigel……....69

Fig 3.5 Cytotoxic activity of Matrigel-released Vγ9Vδ2 T cells in the presence or absence of ZOL against breast cancer cells MDA-MB231-TXSA in 3D organotypic assays……..…71

Fig 3.6. Anticancer activity of Vγ9Vδ2 T cells on ZOL-pretreated breast cancer cells in conventional 2D assay……..…72

Fig 3.7 Visualization of Vγ9Vδ2 T cell migration from Matrigel scaffolds and subsequent cytotoxicity against breast cancer cells……74-75

Fig 4.1 Matrigel embedded Vγ9Vδ2 T cells in the presence of ZOL enhance the anti-tumour efficacy of Vγ9Vδ2 T cells in a subcutaneous model of breast cancer……..…..85

Fig 4.2 Matrigel embedded Vγ9Vδ2 T cells and ZOL boost the anti-tumour efficacy of Vγ9Vδ2 T cells against a smaller number of tumour cells (representing residual tumours) in a mammary fat pad model of breast cancer……86

Fig 4.3 Kaplan-Meier survival curves of tumour-bearing animals following a single treatment with local injection of Vγ9Vδ2 T cells and ZOL in free form, Matrigel delivery of Vγ9Vδ2 T cells or ZOL alone, or Matrigel carrying both Vγ9Vδ2 T cells and ZOL…….88

Fig 4.4 Vγ9Vδ2 T cells sparingly infiltrate into breast tumours *in vivo* following localized treatment with Matrigel carrying Vγ9Vδ2 T cells and ZOL …….89

Fig 4.5 Detection of TUNEL-positive cells in tumour tissues via TUNEL staining……...90

Fig 4.6 Chemical structure of Zoledronate (ZOL) vs. Alexa Flour® 647-labelled Zoledronate (AF647-ZOL) …… ……. ……. ……..….91

Fig 4.7 Efficient ZOL uptake in breast cancer MDA-MB231-TXSA cells *in vitro*…….94

Fig 4.8 Fluorescently labelled ZOL (AF647-ZOL, represented in dark red) localized to the bone and breast cancer lesions *in vivo*…….…….95-96

Fig 4.9 Tumour associated macrophages, not cancer cells, recognise and internalise AF647-ZOL *in vivo*…….97-98

Fig 5.1 U-87 MG glioblastoma cells, but not breast cancer MDA-MB231-TXSA cells, display distinct morphological changes in response to ZOL treatment *in vitro*…….……..….106

Fig 5.2 ZOL directly inhibits the growth of human glioblastoma and breast cancer cells over 72 h *in vitro*……...….108

Fig 5.3 ZOL strongly sensitises glioblastoma U-87 MG cells to killing by Vγ9Vδ2 T cells……110

Fig 5.4 Differential ZOL uptake among three glioblastoma cell lines (U-87 MG, T98G and U-251 MG) and breast cancer cell line MDA-MB231-TXSA …… 111

Fig 5.5 ZOL treatment blocks protein prenylation in cancer cells as indicated by the accumulation of unprenylated Rap1A……....113

Fig 5.6 Upregulation of endogenous HMG-CoAR protein levels in glioblastoma cell lines...……115-116

Abbreviations used

Acronym	Definition	Alternative
ACT	Adoptive cell therapy	
ADCC	antibody-dependent cellular cytotoxicity	
AF647-ZOL	Alexa Flour® 647-labelled ZOL	fZOL
AICD	Activation induced cell death	
ALN	Alendronate	
ApppI	1-adenosin-5-yl ester 3-(3-methylbut-3-enyl) ester	
BrHPP	Bromohydrin pyrophosphate	
CAR	Chimeric antigen receptor	
DMPP	Dimethylallyl pyrophosphate	
FPP	Farnesyl pyrophosphate	
FPPS	Farnesyl pyrophosphate synthase	
GBM	glioblastoma multiforme	
hMSH2	human MutS homologue 2	
IFN-γ	interferon-gamma	
IgG	immunoglobulin G	
IL-2	Interleukin-2	
IP	Intraperitoneal	
IPP	Isopentenyl pyrophosphate	
IV	Intravenous	
LAK	lymphokine-activated killer (T cells)	

MICA/B	MHC class I polypeptide-related sequence A/B	
MHBPP	(E)-4-hydroxy-3-methyl-but-2-enyl pyrophosphate	IPH1101
MHC	Major histocompatibility complex	
MMP-9	matrix metalloproteinase 9	
NBPs	Nitrogen-containing bisphosphonates	
PAgs	Phosphoantigens	
PBMCs	Peripheral blood mononuclear cells	
TCR	T cell receptor	
TIL	Tumour-infiltrating lymphocyte	
TRAIL	TNF-related apoptosis-inducing ligand	
TNF-α	tumour necrosis factor-alpha	
ULBP1	UL16 binding protein 1	
ULBP4	UL16 binding protein 4	
ZOL	Zoledronate	Zoledronic acid

Chapter 1

Introduction

1.1 Localized cancer therapy

Despite advances in modern medicine, cancer remains the second leading cause of death worldwide [1], with 1 in 2 men and 1 in 3 women expected to develop cancer in their lifetime [2]. Three pillars of conventional cancer treatments comprise of surgery [3, 4], chemotherapy [5], radiation therapy [6], and more recently a fourth pillar of immunotherapy [7, 8]. Among these, surgery is by far the most invasive but is considered the most curative option that can be used as a mainstream strategy for most primary solid tumours. The goal of surgery is to eradicate tumours both macroscopically and microscopically. However, in many instances, surgery can be dangerous or impractical due to the size, location, and stage of the tumour. In addition, the need for a negative (clear) margin dictates if surgery is possible. Surgical techniques, as currently applied, risk leaving behind residual tumours increasing the risk of relapses and metastasis [9]. As such, patients are often treated with chemotherapy, radiation therapy and/or immunotherapy in combination with surgery to prevent cancer recurrence.

By contrast, chemotherapy, a hallmark of modern cancer treatment, is a minimally invasive treatment option; however, it is often associated with toxicity due to problems with non-specificity, undesirable side effects, and drug resistance [10]. Radiation therapy remains an integral part of cancer treatment, applied to about 50% of all cancer patients during the course of their treatment and has contributed to 40% of curative cases of cancer [6]. Immunotherapy, on the other hand, especially the immune checkpoint blockades has recently emerged as a powerful modality; however, has delivered mixed results showing drastically varying efficacy among patients with different cancer types [11].

Despite multidisciplinary advances and the global downward trend of cancer mortality rates, metastasis and relapses after surgery and adjuvant treatments still represent a major

challenge. Innovative therapies, especially for those with incompletely resected or inoperable tumours are urgently needed in order to effectively improve the patients' prognosis and survival.

1.2 Adoptive cell therapy (ACT)

In the past few decades, harnessing the immune system to recognise and destroy cancer has been the central goal of cancer immunotherapy. The idea is based on the properties of the immune cells that can be specifically activated against immunogenic tumours to provide constant surveillance and protect against cancer development and cancer relapse due to their long-lasting memory [12]. Adoptive cell therapy (ACT) is a form of immunotherapy now emerged as a promising approach to effectively treat cancer. It involves extraction, expansion, and re-infusion of patient's own immune cells to mediate the antitumour immune function. As a therapeutic modality, it has been studied since the 1980s [13] with the primary focus on how to generate more powerful and efficient T cell responses against certain types of tumours. Currently, the immune cells that are employed in ACT can be classified into three main groups (Fig 1.1), each with different modes of action, namely tumour-infiltrating lymphocytes (TIL), T cell receptor (TCR) gene therapy, and chimeric antigen receptor (CAR) modified T cells [14].

TIL therapy utilises naturally occurring T cells and has been studied over several decades with remarkable results mainly in melanoma [15], ovarian [16] and colorectal cancer [17]. The current TIL therapy protocol consists of *ex vivo* expansion of tumour resident T cells from a resected tumour and adoptive transfer back into the patient following lymphodepletion and subsequent IL-2 (a T cell growth factor) supplementation. Apart from melanoma, successful production of TIL could still be achieved in other types of solid tumours ranging

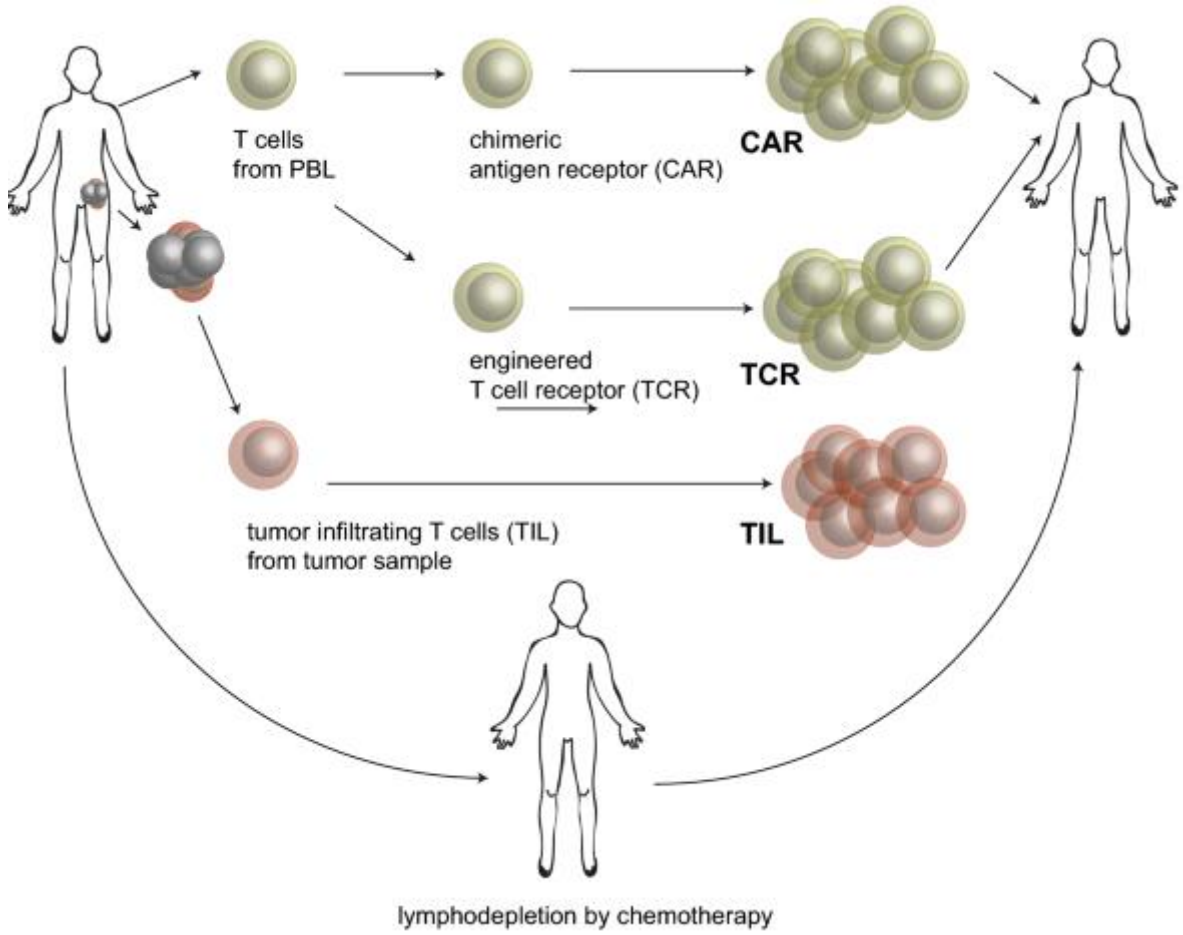

Figure 1.1 Basic principles of adoptive cell therapy (ACT).

In ACT with tumour-infiltrating lymphocytes (TIL), naturally occurring tumour-resident T cells are isolated and rapidly expanded *in vitro* following surgical resection of the tumour. The patient is then treated with a lymphodepleting conditioning regimen before intravenous adoptive transfer of the expanded T cells back into the patient. In ACT with genetic modification approaches, namely T cell receptor (TCR) and chimeric antigen receptor (CAR) therapy, peripheral blood T cells are isolated and then transduced by viral vectors to either express a specific TCR or CAR, respectively. Figure adapted from Wolf *et al*. [18]

from renal cell carcinoma [19], breast [20], pancreatic [21], and non-small cell lung cancer [22]. However, consistency in the production of reactive TIL products from tumours other than melanoma remains difficult, most likely due to the heterogeneity in mutational burden, variations amongst tumour infiltrating $CD4^+$ and $CD8^+$ T cells and other unknown factors [23]. Hence, further research in this field is needed.

In contrast to naturally occurring TILs, peripheral blood T cells can be easily isolated and genetically modified *in vitro* to express either TCRs or CARs, both of which target specific tumour antigens for their use in cell-based therapy [24]. With the TCR method, large pools of potent tumour reactive T cells can be generated [25], leading to an objective clinical response rate of up to 30% in treated patients [26]. However, the modified TCRs do require antigen presentation through the major histocompatibility complex (MHC) on tumour cells to mediated antigen recognition. The fact that many cancer types can escape immunosurveillance by downregulating their MHC expression has been a drawback of this approach.

To avoid the need for MHC-dependent tumour recognition, artificial receptors, i.e. CARs have been developed. CAR-modified T cells maintain the same effector function capacity as TCR-modified T cells but, unlike TCRs, CARs are independent of MHC expression [27]. Dramatic clinical responses and high complete remission rates have been obtained in haematological malignancies with CD19-specific CAR T cells [28], leading to the investigation of using CAR T cells in solid malignancies [29]. However, growing clinical experience with CAR T cells in haematological malignancies has shown that a substantial number of treated patients relapse shortly after remission, possibly due to poor CAR T cells persistence and/or cancer resistance arising from antigen loss or modulation [30]. In addition, severe toxicities have been observed in some patients due to on-target off-tumour effects, which are a direct attack of CAR T cells on normal tissues that share expression with the targeted tumour antigens [31].

The choice of administered T cells in ACT is based on several factors such as their antigen specificity, unwanted side effects, and potent effector functions including antitumour cytotoxic and immunomodulatory activity [32], allowing for the introduction of other types of T cells to be tested and used in ACT. Most recently, there has been an explosion of interest into human gamma delta (γδ) T cells due to their unique capacity and essential contributions to immune responses and immunopathology [33, 34]. These cells are unconventional T cells that express heterodimeric TCRs composed of γ and δ chains setting them apart from the classical and much better known CD8+ cytotoxic T cells and CD4+ helper T cells that express αβ TCRs. The γδT cells are the focus of this thesis.

1.3 Gamma delta (γδ) T cells

Since their accidental discovery in the 1980s, the crucial role of γδT cells in immunity has gradually emerged. In adults, they comprise a small proportion of 1-10% in circulating peripheral T cells [35, 36]. They appear to be more abundant in epithelial and mucosal barriers such as the intestine, making up to 20% of intraepithelial $CD3^+$ T cells in the colon [37]. Unlike their alpha beta (αβ) T cell counterparts that recognise antigens loaded onto the conventional major histocompatibility complex (MHC) molecules, γδT cells do not express the MHC class I and class II recognition molecules, CD8 and CD4 respectively. Instead, they express the γδ TCR and uniquely detect target cells independent of antigen processing and MHC restriction [33]. This property renders γδT cells attractive mediators for targeting a wide range of tumour cells, which often lack MHC molecules, enabling them to escape from (αβ) T cell-mediated immune responses (reviewed in [38, 39]).

The terminology ‘conventional’ refers to those T cells that were first identified with the ability to respond rapidly and effectively to previously encountered antigens, as opposed to the subsequent identification of a phenotypically and functionally distinct group of unconventional

T cells [40]. The conventional T cells recognize a diverse array of processed antigenic peptide presented within the grooves of MHC molecules on other cells [41]. In the ligand recognition by αβ TCRs, the extracellular domains CD4 binds to MHC class II, while CD8 binds to MHC class I. The conserved complementarity-determining regions 1 and 2 (CDR1 and CDR2) regions in individual TCRα and β chain appear to have specificity for MHC molecules, while CDR3 contacts the peptides [42, 43].

Having a more limited TCR repertoire, unconventional T cells express an alternative γδ TCR or a non-diverse αβ TCR, also known as invariant natural killer (iNKT) cells [44, 45]. These cells recognize a less diverse set of nonpeptide (e.g., stress-induced endogenous, patterned microbial, and pharmacologic exogenous molecules) in the absence of MHC molecules. In contrast to their conventional counterparts, which are the main controllers of adaptive immunity, unconventional T cells show features of both innate and adaptive immunity [40]. Several populations of unconventional T cells have been identified including γδT cells. The majority of γδT cells in the blood of healthy adults expresses Vδ2 TCR, which is exclusively paired with Vγ9 (as such referred to as Vγ9Vδ2 T cells) [46]. Other non-Vδ2 T cell subsets such as Vδ1, which can be paired with any of the six expressed Vγ genes, are found less frequently in the blood but more abundant on mucosal and epithelial surfaces [47]. γδT cells play an important role at the crossroad between the innate and adaptive immune system [48]. Their expression of clonally rearranged TCR genes assigns them into the adaptive immune system [49] while also displaying features of the innate immune system, with the lack of need for antigen processing to activate effector functions, allowing them to respond rapidly following TCR engagement [50]. In addition, γδT cells constitutively express functional receptors of innate immune cells such as natural killer cell receptor NKG2D, which can directly induce cytotoxic activity [51]. Activated Vγ9Vδ2 T cells can robustly kill a broad range of tumour cells from both solid and haematological malignancies and produce a variety of

cytokines [52]. Influenced by external stimuli, γδT cells can differentiate into Th1-, Th2- or Th-17 like cells and produce cytokines that either inhibit (such as IL-4, IL-10, IL-9, IL-17) or enhance (such as IFN-γ, TNF-α) antitumour immune responses [53-57].

While there seems to be no functional overlap between different γδT cell subsets [58], Vγ9Vδ2 is the most studied γδT cell subset and this thesis is primarily focused on *ex vivo* expanded Vγ9Vδ2 T cells from human peripheral blood.

1.3.1 Ligand recognition by Vγ9Vδ2 T cells

Although Vγ9Vδ2 T cells are one of the best-studied γδT cell subsets in humans, the exact mechanisms underlying antigen recognition by γδ TCRs remains largely unknown. To date, some diverse and relevant antigens for immune surveillance by γδT cells have been identified. Vγ9Vδ2 T cells activate and proliferate in response to small nonpeptide prenyl pyrophosphate antigens, also known as phosphoantigens (PAgs), which are intermediate metabolites of the cholesterol synthesis pathway in both microbial and eukaryotic cells. Most pathogenic bacteria and some parasites produce (E)-4-hydroxy-3-methyl-but-2-enyl pyrophosphate (MHBPP) of the non-mevalonate pathway of isoprenoid biosynthesis [59], which can exclusively activate Vγ9Vδ2 T cells in the picomolar to nanomolar ranges [60, 61]. The synthetic TCR agonist bromohydrin pyrophosphate (BrHPP) is similarly active at nanomolar concentrations [62]. Eukaryotic cells, on the other hand, produce homologous pyrophosphate molecules, specifically isopentenyl pyrophosphate (IPP) from the mevalonate pathway [63-65] although much greater concentrations into micromolar range of IPP are required to activate Vγ9Vδ2 T cells [66]. While normal cells do not produce enough IPP to activate Vγ9Vδ2 T cells, many transformed or tumour cells overproduce IPP as a result of dysregulated mevalonate pathway, allowing them to activate Vγ9Vδ2 T cells [67, 68].

Importantly, PAg activation of Vγ9Vδ2 T cells involves surface molecules found on all tumour cells, known as the butyrophilin (BTN) family of co-activators [69] and although the exact activating mechanisms are not fully understood, this process is currently under intense investigation. Landmark studies by Sandstrom *et al* [70] and Yang *et al* [71] showed PAgs directly bind to the intracellular B30.2 signalling domain of BTN3A1, triggering an "inside-out" signalling cascade to activate Vγ9Vδ2 T cells (Fig 1.2). Subsequent studies indicated that another member of the BTN family, namely BTN2A1 is required to collaborate with BTN3A1 to sensitise PAg-exposed cells to Vγ9Vδ2 TCR-mediated recognition and killing. The BTN2A1-BTN3A1 complex binds to γδ TCR at two distinct binding sites. While BTN2A1 directly binds to germline-encoded regions of the Vγ9 chain, the BTN2A1-BTN3A1 complex engages additional (unidentified) regions of the TCR, following PAg binding to the B30.2 domain [69, 72]. Taken together, it is evident that BTN2A1 and BTN3A1 proteins are critically important cell surface components to PAg-mediated activation of Vγ9Vδ2 T cells. Additional known ligands for Vγ9Vδ2 T cells include F1-ATPase in complex with apolipoprotein A-I [73] or the ectopically expressed human MutS homologue 2 (hMSH2), a DNA mismatch repair protein [74, 75].

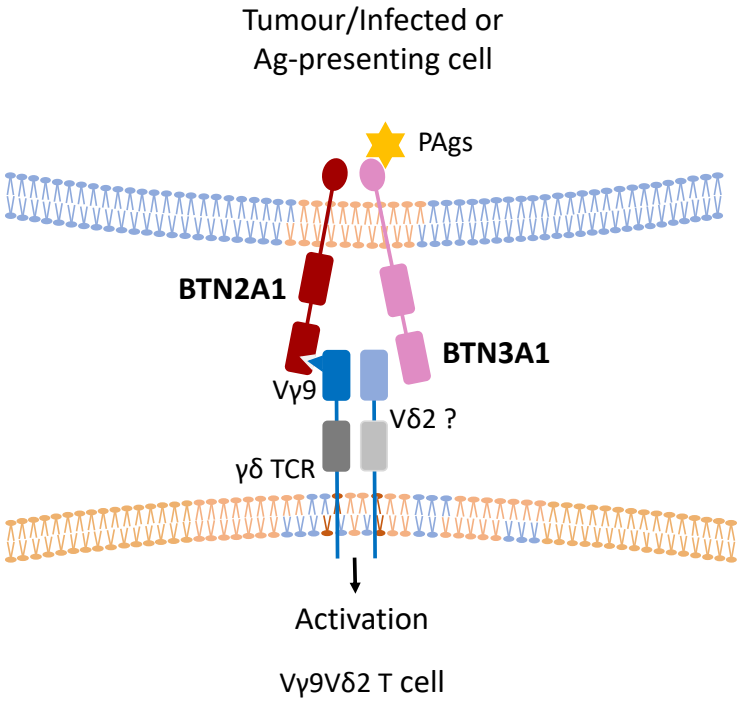

Figure 1.2 Ligand model of PAg sensing by Vγ9Vδ2 TCR.

The cell surface molecule BTN2A1 and BTN3A1 play an important role in ligand activation by Vγ9Vδ2 T cells. In infected or tumour cells, endogenous PAgs bind to the intracellular B30.2 signalling domain, while BTN2A1 binds to germ-line-encoded regions of the Vγ9 chain. This conformational change in the BTB2A1-BTN3A1 complex leads to TCR-dependent activation of Vγ9Vδ2 T cells.

Apart from the TCRs, Vγ9Vδ2 T cells usually carry other activating receptors. As previously mentioned, most Vγ9Vδ2 T cells express NKG2D receptors on their surface. Being expressed by both $CD8^+$ CTL and NK cells, NKG2D receptors detect and bind to a diverse family of stress-inducible ligands, commonly over-expressed on transformed cells, but absent on normal cells. Most solid tumours, leukemias and lymphomas constitutively express at least one of the eight NKG2D ligands (MHC class I polypeptide-related sequence A/B (MICA/B), UL16 binding protein 4 (ULBP4), and UL16 binding protein 1 (ULBP1) binding proteins [76, 77]). These NKG2D-ligand interactions lead to activation of Vγ9Vδ2 T cell cytolytic functions independently of TCR signalling [78, 79].

Although the list of potential new ligands recognised by Vγ9Vδ2 T cells will grow, the overall picture clearly indicates Vγ9Vδ2 T cells are uniquely equipped with two independent recognition pathways to detect transformed cells [78, 80], making them interesting candidates for developing cell-based therapies.

1.3.2 Mechanisms of Vγ9Vδ2 T cell cytotoxicity

Once activated, Vγ9Vδ2 T cells exhibit a cytotoxic potential reminiscent to those of NK cells and $CD8^+$ cytotoxic T cells, allowing them to kill target cells pre-dominantly through the release of soluble mediators such as perforin and granzymes [78, 81]. Secondly, they also express ligands such as TNF-related apoptosis-inducing ligand (TRAIL) and FasL, which signal through several death receptor pathways for enhanced tumour cell death in Fas- or TRAIL-receptor sensitive tumours [82]. Thirdly, activated Vγ9Vδ2 T cells produce pro-inflammatory cytokines, such as tumour necrosis factor-alpha (TNF-α) and interferon-gamma (IFN-γ) [83, 84], which enhance their antitumour activity by suppressing tumour growth while interacting with the adaptive immune system and activating NK cells [85, 86].

Importantly, γδT cells express CD16 (FcγRIIIA/B) receptor on their surface and, upon recognition of PAgs, a subset of Vγ9Vδ2 T cells upregulate CD16 [87]. CD16 is a low affinity immunoglobulin G (IgG) receptor and upon engagement to the Fc portion of IgG antibodies can lead to antibody-dependent cellular cytotoxicity (ADCC) [88], which is a process by which $CD16^+$ effector cells actively lyse target cells that have been bound by specific antibodies. *In vitro*, Vγ9Vδ2 T cells respond to activation and mediate cytolysis against tumours via ADCC with therapeutic antitumour monoclonal antibodies such as rituximab, trastuzumab and obinutuzumab [89-91]. *In vivo,* it has also been shown that stimulated Vγ9Vδ2 T cells improve cytotoxic efficacy when combined with trastuzumab against $Her2^+$ breast cancer shown in mice while breast cancer patients showed significant Vγ9Vδ2 T cell infiltration into the tumours [92].

Overall, Vγ9Vδ2 T cells utilize a variety of mechanisms as depicted in Fig 1.3 and, hence, exhibit strong cytotoxic potential against several solid and haematological cancers such as breast [93], melanoma [94], glioblastoma [95], leukaemia [96] and multiple myeloma [97] both *in vitro* and *in vivo,* encouraging further development in cell-based therapy.

1.4 Nitrogen-containing bisphosphonates (NBPs)

Nitrogen-containing bisphosphonates (NBPs) are a major class of drugs originally used to treat osteoporosis and other bone disorders associated with high bone turnover as well as bone loss in primary or metastatic skeletal cancer [98-100]. They also have other clinical utilities including antitumour activity as single agents [101] and activation of Vγ9Vδ2 T cells [102].

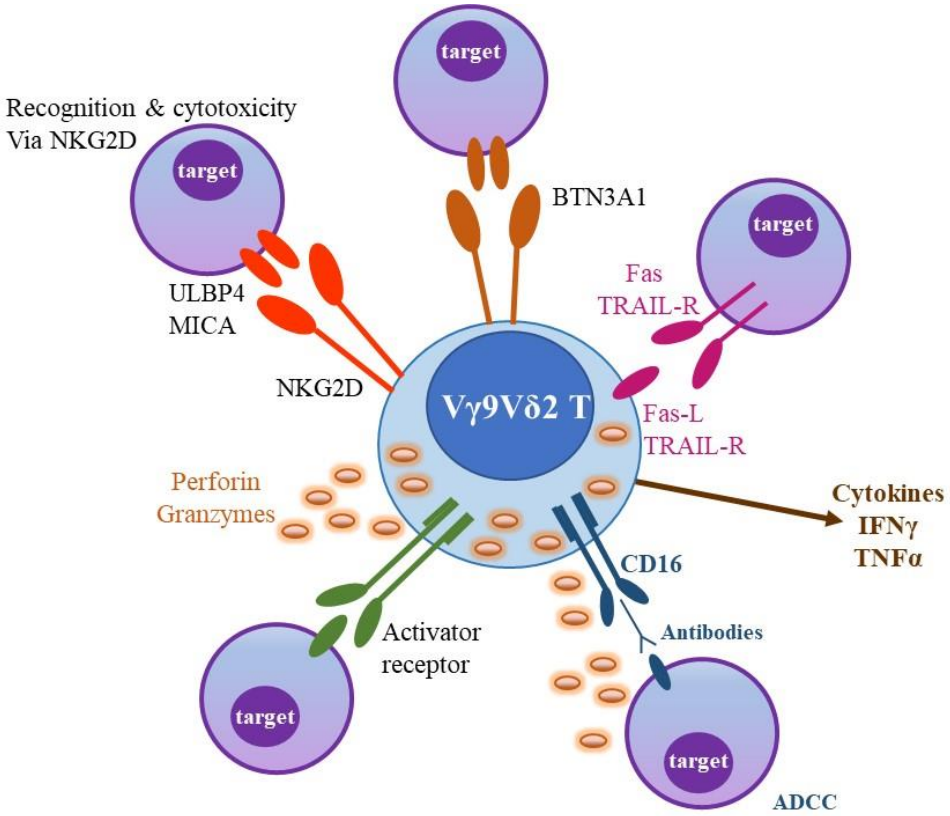

Figure 1.3 Multiple cytotoxic mechanisms of Vγ9Vδ2 T cells.

Following T cell activation via TCR and/or NKG2D, Vγ9Vδ2 T cells induce cytotoxicity via multiple methods including the release of cytotoxic granules containing perforin and granzyme, Antibody-dependent cellular cytotoxicity (ADCC), release of immune modulatory cytokines (IFNγ and TNFα) and the engagement with TRAIL and FasL to induce apoptosis. Image adapted from Braza *et al* [103]

1.4.1 Intracellular effect and pharmacodynamics of NBPs

To date, there are several NBPs that combine potent inhibition of osteoclastic bone resorption with good tolerability [104]. Many of which have been approved by the FDA including pamidronate (Aredia), neridronate (Nerizia), olpadronate, alendronate (Fosamax), ibandronate (Boniva), risedronate (Actonel) and zoledronate (Zometa) [105]. All NBPs bind tightly to the bone mineral hydroxyapatite preventing hydroxyapatite dissolution [106]; however, these physicochemical mechanisms cannot simply explain their antiresorptive effect. Rather, NBPs inhibit bone resorption through cellular effects on osteoclasts as they are internalised by osteoclasts during osteoclast-mediated bone degradation [107]. Indeed, high phagocytic activity of osteoclasts facilitates the uptake of hydroxyapatite-bound NBPs. Among clinically used NBPs, zoledronate (ZOL) is the most potent anti-resorptive NBP [108], and is the focus of this thesis.

Once internalised, NBPs act by inhibiting farnesyl pyrophosphate synthase (FPPS), an enzyme in the mevalonate pathway responsible for the conversion of PAgs such as IPP and its isomer dimethylallyl pyrophosphate (DMPP) into farnesyl pyrophosphate (FPP) (Fig 1.4). Inhibition of FPPS leads to accumulation of the upstream ATP analogue triphosphoric acid 1-adenosin-5-yl ester 3-(3-methylbut-3-enyl) ester (ApppI) within the cytosol, which then triggers apoptosis via inhibition of mitochondrial ADP/ATP translocase [109]. In addition, the activity of FPPS is also required for post-translational prenylation of small GTPases such as Ras, Rho and Rac. These small GTPases are important signalling proteins that regulate cell processes important for osteoclast function. Blocking of prenylation by NBPs leads to cell growth inhibition and activation of caspase-dependant apoptosis [110].

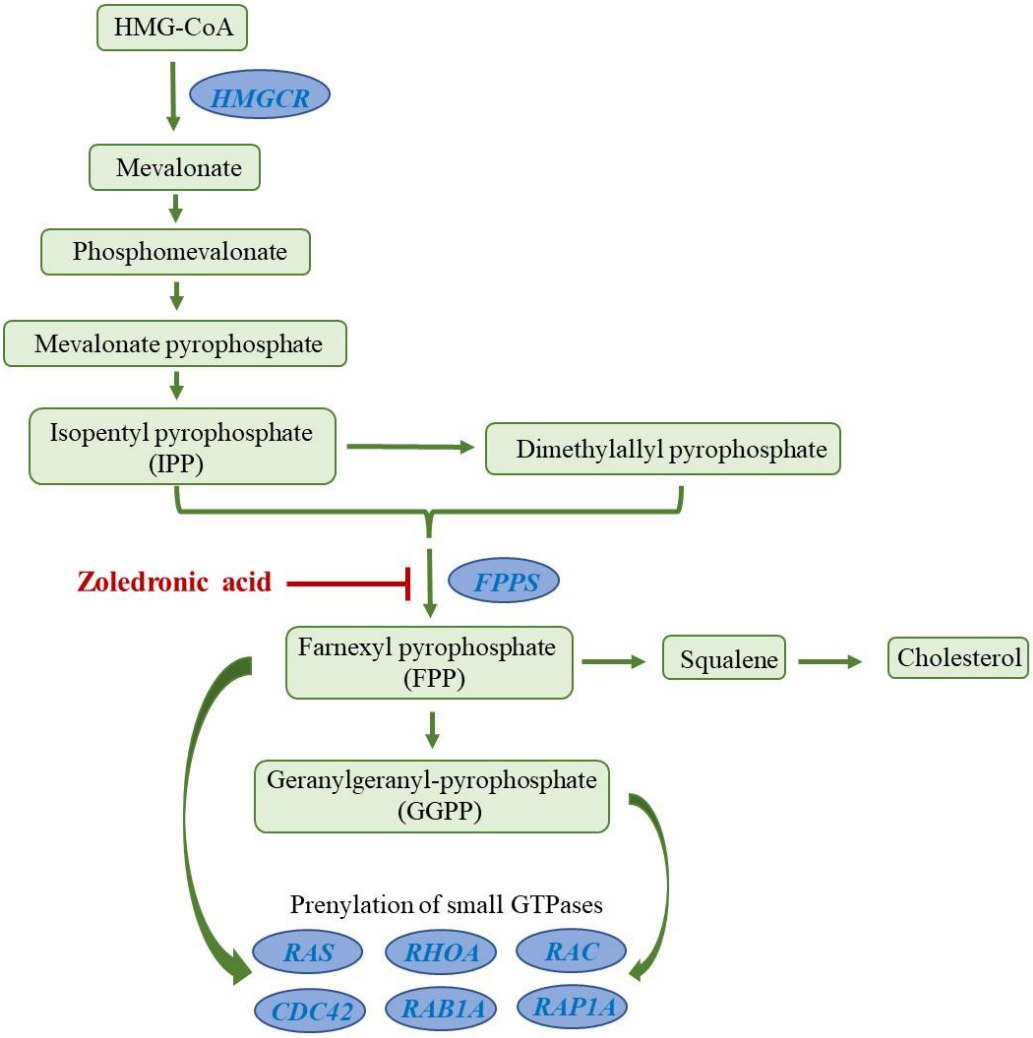

Figure 1.4 Inhibition of the mevalonate pathway by zoledronic acid.

Inhibition of the mevalonate pathway by zoledronic acid. The mevalonate pathway in mammalian cells is involved in cholesterol synthesis and the production of farnesyl and geranylgernyl groups necessary for the post-translational modification small GTPases. This image depicts that farnesyl pyrophosphate synthase (FPPS) is inhibited by zoledronic acid, which is used for the treatment of osteoporosis and bone metastasis. Inhibition of FPPS can prevent tumour cell proliferation, migration and invasion and ultimately lead to cellular apoptosis.

1.4.2 Pharmacokinetics limitations of NBPs

Due to their large size and negative charge, NBPs are poorly absorbed in the intestine hampering their transport across the lipophilic cell membrane. Hence, they are given intravenously. In a pharmacokinetic study of ZOL for the treatment of multiple myeloma and bone metastases, it was found that ZOL had a short distribution half-life (α-$t_{1/2}$) of 14 min, followed by a β-phase half-life of 1.9 h and a prolonged terminal phase half-life of 146 h, which might indicate a slow release of ZOL back into the plasma from the bone [111]. Similar results were obtained in other pharmacological studies performed on cancer patients receiving ZOL (4 mg over 15 min) [112, 113]. In these later studies, it was shown that around 55% of the initially administered dose of ZOL was retained in the bone and this was slowly released back into circulation. Other studies performed on alendronate (ALN) showed ALN concentration in noncalcified tissues reduced rapidly in 1 h following administration (5% of the initial concentration). However, its concentration in the bone continued to increase, reaching the peak at 1 h, indicating a significant redistribution of ALN from noncalcified tissues to the bone [114]. Collectively, these studies demonstrated long-lasting accumulation in bone is a common feature of NBPs.

The rapid redistribution of NBPs led to a short exposure at the noncalcified tissues while the prolonged exposure increased drug accumulation in bone. This pronounced selectivity for bone explained the antiresorptive efficacy of NBPs [115] and is the basis for their utility in clinical practice. However, owing to their intrinsic limitations at noncalcified tissues, more effort was required to increase drug accumulation at these sites in order to open new therapeutic uses for NBPs.

1.4.3 Clinical applications of NBPs, particularly Zoledronate (ZOL) in cancer

NBPs have also found clinical applications for cancer treatment. They have become an integral part of current cancer treatment used to prevent skeletal complications associated with multiple myeloma and bone metastases arising from breast, lung, prostate and other solid tumours [116]. NBPs have shown to effectively reduce skeletal-related events associated with malignancies including, hypercalcaemia and increased bone destruction [117].

A growing body of evidence indicates that NBPs exhibit direct antitumour activity on tumour cells through inhibition of cell proliferation [118], adhesion and invasion [119], and anti-angiogenesis [120]. Treatments of ZOL on some cancer cell lines have led to decreased cell viability and proliferation, as well as induction of apoptosis *in vitro*. For example, Lin *et al* has demonstrated exposure to ZOL (100 μM) markedly inhibited prostate cancer cell (PC-3, DU-145, LNCaP and CRW22Rv1) growth through apoptotic and autophagic cell death [121]. Likewise, Lan *et al* showed growth of two breast cancer cell lines (MCF-7 and MDA-MB-231) was markedly decreased following treatment with ZOL (50-100 μM) *in vitro* [122]. In addition, ZOL has also shown to synergistically augment the cytotoxic activity of paclitaxel, etoposide and cisplatin on small cell lung cancer cell lines *in vitro* [123].

On the other hand, antitumour activity of ZOL *in vivo* is more contradictory. Some pre-clinical studies showed that ZOL administration inhibited tumour growth [123-125] and progression of established bone metastasis as well as prevented the development of new bone metastasis [126-128]. Indeed, ZOL has proven to be effective against soft tissue tumours in extra-skeleton sites, showing reduction in the growth of cervical tumours in a transgenic mouse model via inhibition of pro-angiogenic protease, matrix metalloproteinase 9 (MMP-9) by tumour associated macrophages [129]. In contrast, other *in vivo* studies showed ZOL has no effects on osteosarcoma growth and fails to prevent lung metastases [130, 131].

Antitumour efficacy of ZOL in patients has been investigated. Although no clinical trials have conducted using ZOL alone, a phase II clinical study has shown ZOL administered with chemotherapy in a neoadjuvant setting led to an increase in the clearance and a decrease in the number of disseminated tumour cells in the bone marrow of patients with early breast cancer [101, 132]. Other studies, on the other hand, have shown no benefits of adjuvant ZOL treatment in early breast cancer [133]. In multiple myeloma patients undergoing chemotherapy, the use of ZOL provided treatment benefits beyond bone health, showing 16 % reduction in mortality and extended survival by 5.5 months, compared to those who received non-NBP clodronate [134]. A Cochrane review of clinical trials also confirmed ZOL has therapeutic effects in myeloma patients [135]. In addition, ZOL treatment together with androgen blockade as initial treatment has shown to improve prostate-specific antigen progression-free survival time in prostate cancer patients [136]. Various studies also confirmed the benefit of ZOL treatment in patients with bone metastasis from solid malignancies [137].

1.4.4 NBPs and Phosphoantigens (PAgs)

NBPs including ZOL are recognised as indirect acting PAgs for the activation of Vγ9Vδ2 T cells [138]. Indeed, both NBPs and PAgs are most used for *in vitro* and *in vivo* stimulation of Vγ9Vδ2 T cells. Following treatment of human peripheral blood mononuclear cells (PBMCs) with ZOL, monocytes selectively accumulate ZOL due to efficient drug uptake, resulting in the accumulation of the phosphoantigen IPP, which in turn activates Vγ9Vδ2 T cells for proliferation [139]. ZOL is the most potent FPPS inhibitor, and, hence, considered the best activator of Vγ9Vδ2 T cells [104].

Several *in vitro* and *in vivo* studies have shown that human tumour cells treated with NBPs greatly enhance their susceptibility to Vγ9Vδ2 T cell-mediated cytotoxicity [140-147]. For example, Sato *et al*. has shown a marked increase in sensitivity of small cell lung cancer

cells pre-treated with ZOL to Vγ9Vδ2 T cell lysis [148]. Another study by Mattarollo *et al*. has demonstrated that ZOL pre-treatment could overcome resistance of several solid cancer cell lines including prostate, lung, colon and breast cancer to Vγ9Vδ2 T cell-mediated cytotoxicity [149]. Taken together, these studies indicate the necessity of ZOL pre-treatment to enhance of Vγ9Vδ2 T cell cytotoxicity against target cells. Therefore, in Vγ9Vδ2 T cell-based immunotherapy, ZOL serves a double purpose. The first purpose is to induce the expansion of Vγ9Vδ2 T cells, usually in combination with IL-2, both *in vivo* and *ex vivo*. The second purpose is to sensitise cancer cells, rendering them vulnerable to Vγ9Vδ2 T cell-mediated killing.

1.5 Clinical experience with Vγ9Vδ2 T cells

Currently, a handful of early phase clinical trials using Vγ9Vδ2 T cells have been assessed against a variety of lymphoid and solid tumours such as lymphoma and myeloma [150], head and neck cancer [151], hepatocellular carcinoma (NCT00562666), clear cell renal carcinoma [152], breast and cervical cancer [153], prostate cancer [141], neuroblastoma [154], and lung cancer [155]. Notable was the immense variation amongst trial protocols, for example whether Vγ9Vδ2 T cells were expanded *in vivo* or *ex vivo* or whether various NBPs or cytokines were used in combination. However, the overall results indicated Vγ9Vδ2 T cell-based immunotherapy was generally safe and well-tolerated with minimal side effects that included fever, chills and transient flu-like symptoms [156], which were easily treated. Objective responses were observed in most trials, but the efficacy was highly variable although the rates of complete response were generally low, and long-term survival benefit was minimal.

In vivo expansion of Vγ9Vδ2 T cells occurs in patients following NBPs administration alone or in combination with IL-2. Although this strategy can be used to successfully increase the number of circulating Vγ9Vδ2 T cells, the evidence of T cell infiltration into the tumour tissue is limited. Circulating Vγ9Vδ2 T cells also showed a reduction in their response to NBPs

injection, which may be due to activation-induced anergy [157], a process by which may have occurred after T cell exposure to suboptimal NBPs concentration. In addition, repeated exposure with NBPs was shown to cause terminal differentiation and exhaustion of Vγ9Vδ2 T cells, hence reducing the number of circulating Vγ9Vδ2 T cells overtime [141, 152, 153]. During chronic exposure, Vγ9Vδ2 T cells can also undergo activation induced cell death (AICD), the process by which is mediated by Fas [158] and is crucial for maintaining proper immune function and preventing over-activation of the immune cells. In the case of Vγ9Vδ2 T cell-based immunotherapy, repeated exposure to ZOL seems to be detrimental to clinical outcomes with a decreasing number of Vγ9Vδ2 T cells, possibly due to AICD. Furthermore, the low potency of NBPs-based trials is likely to be attributed to their poor bioavailability due to rapid clearance from the plasma and absorption to bone mineral. To overcome these problems of *in vivo* expansion, protocols for expanding large number of Vγ9Vδ2 T cells using a combination of ZOL and IL-2 have been established *ex vivo* [159] and have shown to yield greater number of expanded Vγ9Vδ2 T cells achieving clinically appropriate cell numbers, especially in patients who are poor *in vivo* expanders or those receiving chemotherapy.

ACT of *ex vivo* expanded Vγ9Vδ2 T cells has been investigated in several clinical trials of haematological and solid tumours and has shown efficacy despite the number of Vγ9Vδ2 T cells still decreasing over time. Results also showed that the co-administration of ZOL and IL-2 is crucial to maintain the level and function of the transferred cells, showing better efficacy than Vγ9Vδ2 T cells alone [160]. In most clinical studies so far, autologous Vγ9Vδ2 T cells derived from peripheral blood were used; however, a few studies were carried out using allogeneic Vγ9Vδ2 T cells for which safety and promising efficacy were also noted [161, 162]. Despite considerable efforts, an average response rate of around 21% from early phase trials indicated limited potency of current ACT of *ex vivo* expanded Vγ9Vδ2 T cell protocols [150,

163, 164], most of which utilize a venous system to systemically deliver cytotoxic T cells into cancer patients.

1.6 ACT of *ex vivo* expanded Vγ9Vδ2 T cells for solid tumours

In order to successfully eradicate solid tumours, adoptively transferred T cells must travel to the tumour site [165] and infiltrate into the tumour microenvironment. Although previous studies have shown evidence of tumour-infiltrating T cells including Vγ9Vδ2 cells in various types of cancer [38], suggesting the capacity of these T cells to infiltrate the tumour mass, T cell trafficking to sites of solid tumour is relatively poor in general [166-168]. Standard protocols for ACT involve infusion of T cells through a venous catheter. The transferred T cells must then pass through the heart and pulmonary vasculature where they may become trapped in the capillary beds of the lungs [169]. A study by Fisher *et al*. [170] has clearly demonstrated an initial rapid uptake of activated T cells into the lungs of metastatic melanoma patients within 24 h post-adoptive transfer of TILs. The same study also indicated that the patients' liver and spleen act as large "sinks" for the accumulation of most administered T cells. Retention of the transferred T cells into sites outside the tumour, therefore, limits the available T cells for tumour infiltration.

The migration pattern of adoptively transferred Vγ9Vδ2 T cells with concurrent use of ZOL in patients with solid tumour has also been investigated [171]. Likewise, the results have indicated initial and transient retention of Vγ9Vδ2 T cells in the lungs, followed by movement predominantly to the liver and spleen with only a minority of these cells localized to the tumour. This finding was consistent with previous observations from CAR T cell studies and, hence, not specific to Vγ9Vδ2 T cells [170, 172].

1.7 Alternative routes of administration

Improving T cell trafficking to tumour sites is one of the major challenges for T cell-based immunotherapy. Other challenges such as identification of unique tumour target antigens, specifically for CAR T cells and inadequate expansion of transferred T cells in the immunosuppressive tumour microenvironment are discussed elsewhere and are beyond the scope of this thesis (reviewed in [173]). In this thesis, questions were raised on how to best deliver transferred T cells to optimise entry into solid tumours. Although, multiple approaches aiming at overcoming this obstacle are currently under investigation and discussed elsewhere in the literature, one approach that may achieve higher level of T-cell trafficking to solid tumours is direct T cell delivery method to the site of tumours.

1.7.1 Intra-arterial ACT

Delivering transferred T cells through the regional arterial blood supply (intra-arterial, Fig 1.5) could potentially avoid T cell trapping in the lungs and spleen as seen in intravenous delivery [174]. In a rare circumstance of regionally transferred ACT, improved antitumour efficacy in a liver metastatic melanoma patient, treated with lymphokine-activated killer (LAK) T cells was observed and was theoretically related to enhanced delivery of the LAK T cells to the tumour bed [174, 175]. Another example is a phase I clinical study (NCT02416466) in patients with unresectable CEA+ liver metastases from gastrointestinal ademocarcinoma to whom no effective treatment options were available. The results have shown a favourable safety profile with evidence of antitumour activity, encouraging further study into a phase II trial which is currently underway [176].

1.7.2 Intrapeural ACT

In pre-clinical studies with autologous CAR T cells targeting mesothelin for pleural mesothelioma or metastatic lung and breast cancer, researchers have found that the intrapleural

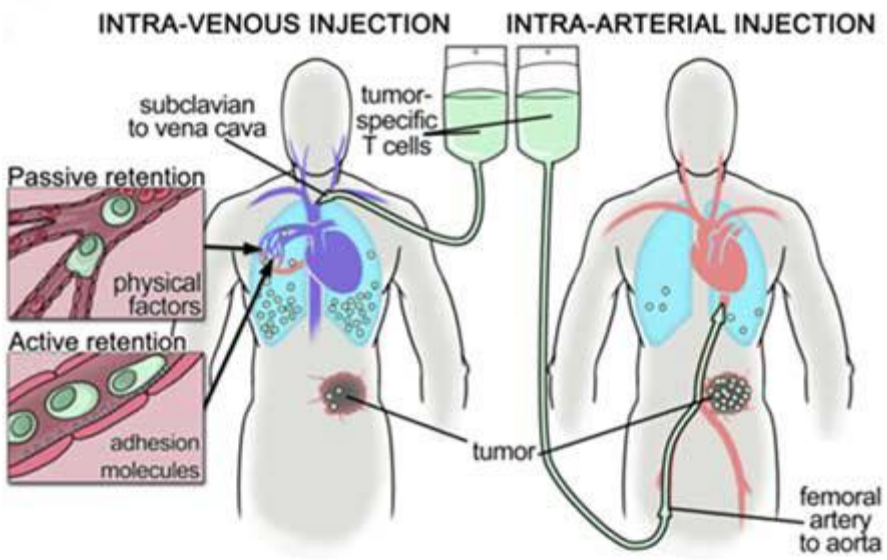

Figure 1.5 Comparison between intra-venous and intra-arterial injections.

Delivering transferred T cells directly into the arterial supply of the tumour (right) was hypothesised to increase availability of the T cells to enter tumour sites in comparison to intra-venous delivery (left). Retention of the transferred T cells in the lungs following intra-venous delivery as seen in clinical trials is multifactorial (inset). Image adapted from Visioni *et al*.[169]

delivery resulted in greater tumour eradication and survival of laboratory animals, than that seen with a 30-fold higher T-cell dose administered intravenously [177]. Likewise, systemically administered CAR T cells were found sequestered in the lungs prior to tumour infiltration. On this basis, a phase I dose escalation trial (NCT02414269) was conducted with the result indicating that intrapleural administration of CAR T cells had no evidence of toxicity while antitumour activity was observed in one patient with complete remission who had additionally received anti-PD1 therapy [178]. Further development of this approach is currently underway.

1.7.3 Intracranial ACT

Glioblastoma and brain tumour metastasis are the types of solid tumours where regional administration of transferred T cells is actively being explored (NCT03283631, NCT03500991, NCT01818323, NCT02208362) [173]. Preclinical studies have shown safety and efficacy of intracranial (infusions into the resected tumour cavity) delivery of a third generation EGFRvIII, and HER2 specific CAR T/NK cells [179-181]. Currently, among 5 patients who received multiple intrathecally (infusions into the space between the spinal cord) and/or intracranially delivered IL-13Rα2 targeting CAR T cells, one patient with recurrent multifocal glioblastoma achieved complete remission that lasted 7.5 months under continued CAR T cell treatment [182], which is remarkable for this disease.

1.7.4 Intra-tumoral ACT

Another regional ACT approach that may provide optimal therapeutic effect is intra-tumoral injection of transferred T cells. An example is the phase I trial investigating intra-tumoral injection of CAR T cells targeting ErbB for the treatment of locally advanced head and neck squamous cancer (NCT01818323). The results showed intra-tumoral injections are well

tolerated and has led to stable disease in some patients, despite having rapidly progressing tumours at the start of the trial [183].

1.7.5 Intraperitoneal ACT

Intraperitoneal (IP) delivery of transferred T cells is an ideal approach to treat peritoneal cancer metastasis due to following advantages. First, the T cells administered intraperitoneally can act immediately on cancer cells in the peritoneal cavity. Second, a higher T cell concentration will reach the peritoneal cavity as compared to intravenous administration [184]. Third, more transferred T cells can be injected by the IP route than can be tolerated by IV injection. Importantly, a pilot clinical study was conducted to assess the efficacy and safety of weekly IP injection of Vγ9Vδ2 T cells together with ZOL in patients with malignant ascites [185]. As expected, the investigators found a significant reduction in the number of tumour cells in the ascites even following the first round of the treatment and remained substantially lower throughout the course of the study [185]. Although the IP treatment did not improve overall survival in such advanced disease, the result showed a clear benefit for local control of cancer in patients whom no other treatment was available.

1.7.6 Biomaterial-based localized ACT

An exciting new approach for local delivery of adoptively transferred T cells for solid tumours is the incorporation of biopolymers to use as T cell carriers [186]. Biomaterial scaffolds preloaded with immune cells can be injected or implanted directly into a tumour resection cavity or within the vicinity of unresectable tumours, allowing an immediate opportunity for tumour infiltration as T cell trafficking is not necessary. Biomaterial-based T-cell implants are not generally designed to treat widespread metastases but to address localized, locally advanced, unresectable or incompletely resected tumours such as brain, spinal cord, head and neck, pancreatic, ovarian and breast cancer [186].

Preclinical studies to date, primarily on CAR T cells, have consistently reported significantly lower numbers of T cells required to induce tumour responses when biomaterial-based localized ACT approach was chosen over the traditional systemic delivery [187]. Unlike traditional ACT, this localized approach does not require pre-conditioning regimens such as lymphodepleting chemotherapy or cytokine support, thus limiting systemic toxicities and facilitating patient recovery [188]. In addition, as ACT is an elaborate and time-consuming procedure where T cells must be isolated from a patient and expanded in specialised laboratory facilities, the expanded T cells could become functionally exhausted before re-introduction [189]. This platform allows the addition of supplements into the scaffolds to support T cell survival and function or to offset tumour suppression and therefore, is amenable to encapsulating a variety of cells, especially those that require tightly controlled environments. Interestingly, biomaterials could also be used to co-deliver combinations of T cells and drugs. For example, a study has shown incorporation of slow-release anti-CTLA-4, an immune checkpoint inhibitor, into T cell-loaded scaffolds could intensify the T cell antitumour functions in an animal 4T1 breast cancer resection model, while systemically delivered anti-CTLA-4 failed to reject residual tumour [190]. As such, this delivery approach may be used to maximise effector function of the transferred T cells or help to stimulate the host immune system to destroy residual cancer cells all at once.

Many types of biomaterials, appropriately designed for local ACT have been explored (reviewed in [186]). Thus far investigations focussed on hydrogels composed of chitosan, polymerised alginate or hyaluronic acid [191]. Hydrogels are three-dimensional, cross-linked structures of hydrophilic polymers that can swell in water or biological fluids [192]. For the past decades, while there has been a rise in the use of hydrogels to enhance cancer vaccines [193], only recently, hydrogels have been under investigation for the improvement of cell-based therapy.

Injectable hydrogels are transformable gel-like biomaterials that can be injected into the tumour/tumour resection site to produce strong and localized antitumour immune response [194]. In 2014, Tsao and colleagues reported the development of biocompatible injectable hydrogels made of poly (ethylene glycol)-g-chitosan (PCgel), which was shown to be suitable as a T cell depot for the encapsulation and release of tumour reactive CAR T cells for the localized treatment of glioblastoma [195]. Using various laboratory techniques, the authors have shown their unique hydrogels had excellent biocompatibility and biodegradability while encapsulated tumour reactive T cells maintained their cytotoxicity against glioblastoma cells following release from the gels [195]. Despite their encouraging results, PCgel for local immunotherapy has not yet been verified in a pre-clinical model.

Two years later, a similar chitosan-based hydrogel was developed by Monette *et al*. [196]. *In vitro*, these hydrogels were shown to support survival and proliferation of $CD8^+$ TILs (expanded from renal clear cell renal carcinoma tumour) while facilitating gradual release of the encapsulated cells over a period of time [196]. More importantly, these released TILs remain cytotoxic post-encapsulation [196].

Implantable biomaterial scaffolds preloaded with immune cells can be implanted into a resection cavity or a subcutaneous space via a surgical procedure. An interesting example of implantable biomaterials is macroporous polymerized alginate-based scaffolds, developed by Stephan *et al*. [190]. Using a mouse breast cancer resection model (which mimics local and systemic recurrences arising post-surgery), this group has shown their implanted biomaterial scaffolds led to superior antitumour responses of tumour-reactive CAR T cells to eradicate tumours while systemic delivery had little effect on the tumours [190]. The results also showed massive improvement in T cell persistence, suggesting the device can also overcome the immunosuppressive barriers created by the tumours [190]. However, the drawback of this platform is in the invasive nature of the surgery to implant the scaffolds close to the tumour

site as the site of the tumour may not always be accessible by surgery and that the persistence of the scaffolds may impair normal organ function [197, 198].

The examples of biomaterials discussed here need to be tested further to confirm their therapeutic benefits; nonetheless, this platform has shown great promise in improving efficacy of local ACT for the local control of cancer.

1.8 Aims and Significance

Adoptive cell therapy (ACT) is an innovative form of cancer immunotherapy where patient's T cells are extracted and expanded outside the body and upon re-administration, these T cells traffic to recognise and kill cancer cells. Human Vγ9Vδ2 T cells have extraordinary properties including their natural ability to destroy cancer cells in an MHC-independent manner. Activated Vγ9Vδ2 T cells used in combination with zoledronate (ZOL) can effectively kill a broad range of tumour cells and shown capacity for tumour reduction in murine xenotransplant tumour models [142, 143, 199-201]. Translating pre-clinical findings to the clinic generated promising initial results but greater potency is still needed, particularly against solid tumours. Unlike blood cancers where the cancer cells are accessible through the bloodstream, transferred T cells face a unique challenge when being directed against solid tumours as they have to travel from the injection site to the tumour sites. In fact, clinical studies of ACT showed poor trafficking of systemically administered Vγ9Vδ2 T cells to localized tumours, hence limiting therapeutic outcomes.

Although systemic (intravenous) injection is the preferred route of delivery due to the ease of administration, several preclinical studies suggested regional T cell administrations may provide optimal therapeutic effects [202-204]. Among various regional delivery platforms, biomaterial-based localized ACT is an exciting new platform with therapeutic

promise [187, 190]. These biomaterial delivery systems can be in a form of scaffolds carrying transferred T cells that require to be surgically implanted into the tumour resection cavity. Alternatively, they can come in a form of gel-like materials that can be injected via a syringe directly at the site of solid tumours. These materials allow for the discrete and controlled release of transferred T cells directly at the tumour site where they can act immediately on cancer cell targets as trafficking is not required. Therefore, a hypothesis has been formed to suggest that localized T cell administration is a potential modifier for both T cell trafficking and antitumour efficacy. To date, this hypothesis has not been examined with Vγ9Vδ2 T cells.

Hence, the major aim of this thesis is to establish "proof of concept" evidence showing the efficacy of biomaterial-based delivery of *ex vivo* expanded Vγ9Vδ2 T cells in combination with zoledronate for the localized treatment of solid tumours *in vitro* and in a murine xenograft model of localized breast cancer. For the purpose of this preliminary study, commercially available Matrigel® was chosen as a T cell carrier material due to its excellent biocompatibility and cytocompatibility perfectly suited for animal tumour models.

Additionally, there is an unmet medical need for more effective anticancer drugs, particularly for those cancers that are notoriously difficult to treat with conventional cancer treatments including aggressive primary brain tumour of glioblastoma multiforme. Although the antitumour activity of Vγ9Vδ2 T cells varies against different tumour cells that were pre-treated with ZOL [205], this type of tumour may be particularly susceptible to Vγ9Vδ2 T cell-mediated cytotoxicity [206]. Killing of glioblastoma cells by Vγ9Vδ2 T cells is shown to be greatly enhanced following ZOL pre-treatment, raising the possibility of this type of tumour being targeted by localized biomaterial-based ATC of Vγ9Vδ2 T cells in combination with ZOL. This leads to the secondary aim of this thesis, which is to investigate a clinical niche for Vγ9Vδ2 T cell in combination with ZOL for brain tumour.

Overall, these studies will provide new insights into the antitumour efficacy of localized ATC of Vγ9Vδ2 T cells in combination with ZOL against solid tumours and provide pre-clinical data for the advancement of Vγ9Vδ2 T cell therapy for brain tumour.

The specific aims are:

1. To investigate Vγ9Vδ2 T cell viability and release following their encapsulation in Matrigel, and to assess their cytotoxicity upon release *in vitro*. This aim will also assess the practicality of co-delivering Vγ9Vδ2 T cells and ZOL in Matrigel scaffolds, as opposed to ZOL pre-treatment approach to enhance Vγ9Vδ2 T cell-mediated cytotoxicity *in vitro*.
2. To assess the efficacy of local ACT of Vγ9Vδ2 T cells in combination with ZOL in pre-clinical models of localized breast cancer. Specifically, this aim will:
    a. Assess the antitumour efficacy of Matrigel-encapsulated Vγ9Vδ2 T cells with or without ZOL
    b. Assess the ability of Vγ9Vδ2 T cells to infiltrate solid tumours following local delivery
    c. Assess the distribution of locally administered ZOL *in vivo*
3. To determine the efficacy of ACT of Vγ9Vδ2 T cells in combination with ZOL on various brain tumour cell lines and elucidate the underlying reasons for the robust antitumour activity of Vγ9Vδ2 T cells and ZOL in sensitive brain tumour cell lines.

Chapter 2

Materials and Methods

2.1 *Ex vivo* expansion and enrichment of Vγ9Vδ2 T cells

This study was approved by the CALHN Human Research Ethics Committee. Informed consent from healthy volunteers was obtained prior to blood collection. Vγ9Vδ2 cells were isolated and expanded as previously described [199]. Briefly, Peripheral blood mononuclear cells (PBMCs) were obtained from the whole blood by density gradient separation (Lymphoprep, Axis-Shield, Norway). The cells were cultured in CTS™ OpTmizer™ T Cell Expansion SFM (Life Technologies, Australia), 10% heat-inactivated FBS, 100 IU/mL penicillin, 100 µg/mL streptomycin, 2 mmol L-glutamin (Life Technologies, Australia), 25 mM HEPES, 0.1% β-mercaptoethanol (Sigma-Aldrich, USA), 100 IU/mL recombinant human interleukin 2 (Miltenyi Biotec, Germany) and activated with 5 µM ZOL. Cell cultures were maintained at 1-2 x 10^6 cells/mL and replenished with fresh media without ZOL every 2-3 days. At Day 7-8 of expansion, MACS negative selection (TCR γ/δ+ human T cell Isolation Kit, Miltenyi Biotec) was then performed to enrich TCR γ/δ+ T cells. Following enrichment, the percentage of γ/δ+ T cells was consistently >95%.

2.2 Labelling Vγ9Vδ2 T cells with VivoTrack680

Ex vivo expanded Vγ9Vδ2 T cells were resuspended to 2 x 10^6 cells/mL in PBS. VivoTrack 680 dye (Perkin Elmer, USA) was reconstituted to 0.1 g/mL in PBS and diluted (1:1) into PBS containing Vγ9Vδ2 T cells. Cell samples were incubated in the dark for 10-15 min at 37°C, then collected and washed three times in PBS containing 1% HI-FBS. Cell viability was assessed using trypan blue exclusion. Labelling efficacy was assessed by flow cytometry (BD FACScantoII) using appropriate lasers and filters for detection of 680 nm wavelength.

2.3 Encapsulation of Vγ9Vδ2 T cells in Matrigel and 3D cell viability assay

Ice-cold Matrigel was mixed with equal volume (50 µL) of T cell media containing 1 x 10^6 Vγ9Vδ2 T cells. ZOL (0-25 µM) was added to the mixture, followed by initiation of gelation at 37°C for 10 min. Fresh media was then added to prevent the 3D T cell cultures from drying. Matrigel-encapsulated Vγ9Vδ2 T cells were then incubated at 37°C for 24 h. Following incubation, Vγ9Vδ2 T cell viability in Matrigel was assessed using 3D CellTiter-Glo luminescent assay (Promega, Madison, USA), which quantified the amount of ATP present as a direct measurement of cell metabolism. In brief, old culture media was removed. 100 µL of CellTiter-Glo was added to each well and incubated at room temperature for 30 min in the dark to stabilize the luminescent signal before reading. The ATP content of each well was then converted into number of cells/well using previously generated ATP standard curve. Vγ9Vδ2 T cells plated directly on plastic were used as a 2D control. For observation of Vγ9Vδ2 T cell (spontaneous) release, ice-cold Matrigel (without ZOL) was mixed with Vγ9Vδ2 T cells as per described above for 3D cell viability assay. The mixture was allowed to warm up briefly at room temperature before being placed slowly to the bottom of a 24-well plate creating a convex gel surface. The plate was then kept at 37°C for 10 min to set. Fresh media was added. Migration of Vγ9Vδ2 T cells was examined with a phase contrast microscope.

2.4 *In vitro* Vγ9Vδ2 T cell release assay – video microscopy

Time-lapse video microscopy experiments were conducted to monitor the release of Vγ9Vδ2 T cells from Matrigel and their subsequent cytotoxicity toward GFP-labelled MDA-MB231-TXSA (MDA-MB231-TXSA/GFP) cells. In the first experiment, cancer cells were plated into a 24-well, black-walled Ibidi µ-plate (Ibidi, Germany) and allowed to adhere overnight. Cells were then treated with 25 µM ZOL for 24 h. Vγ9Vδ2 T cells labelled with vivoTrack680 (red) were resuspended in CTS™ OpTmizer™ T Cell Expansion SFM (Life Technologies, Australia) and infused with equal volume of Matrigel. 50 µL of the mixture was briefly allowed to warm up at room temperature and then placed directly on top of cancer cell

monolayer creating a convex gel surface. Once Matrigel was solidified, fresh media was added. Vγ9Vδ2 T cell-loaded Matrigel was monitored with an inverted time-lapse microscope equipped with a humidified chamber (37°C, 5% CO_2) and images were collected with Zeiss LSM700 confocal microscope using ZEN software (Zeiss, Germany) at 20 min intervals for 42 h using a 10x objective. Maximum projections of brightfield image stacks were computed with ZEN software. In another experiment where cancer cells were not pre-treated with ZOL, ZOL was added to the Vγ9Vδ2 T cell/Matrigel mixture instead.

2.5 Migration-based assay for quantification of encapsulated Vγ9Vδ2 T cell cytotoxicity

To properly study the interaction between encapsulated Vγ9Vδ2 T cells and target cancer cells, an organotypic 3D assay similar to the collagen-based cytotoxicity assay described by Weigelin and Friedl [207] was established. This assay consisted of cancer cell target (luciferase-tagged MDA-MB231-TXSA cells, $1x10^4$ cells), plated as monolayer at the bottom of a 96-well plate and allowed to adhere for overnight. Effector cells, i.e. Vγ9Vδ2 T cell-loaded Matrigel ($2x10^5$ cells, E:T of 20:1) $\pm$ ZOL (25 µM) were then overlayed the cancer cell monolayer. Once solidified, 100 µL of fresh media was added to the plate and incubated for 32 h at 37°C. After incubation, the cancer cells were washed in PBS, and lysates were prepared using the Cell Culture Lysis Reagent in the Luciferase Assay System (Promega, USA). Luciferase activity was measured and analysed according to the manufacturer's protocol. Cancer cell viability was calculated as a percentage. Blank Matrigel (without Vγ9Vδ2 T cells) plated directly on cancer cells were used as a control.

2.6 Western immunoblotting

A density of 1 x 10^6 MDA-MB231-TXSA and U-87 MG cells were seeded overnight to 25 cm^3 flasks. Cells were then treated with or without ZOL (0.1-25 µM) for 24 h. Lysates were prepared and separated as previously described [199]. Briefly, cells were washed with

ice-cold PBS, and lysed in 50 µL of protein lysis buffer containing 10 mM Tris HCl, pH 7.6, 150 mM NaCl, 1% Triton X-100, 0.1% sodium dodecyl sulphate (SDS), 2 mM sodium vanadate and a protease inhibitor cocktail (Roche Diagnostics, Mannheim, Germany). The protein content was quantified using the BCA™ Protein Assay Kit (Thermo Fisher Scientific, Waltham, MA, USA). An equal amount of protein from each lysed cell sample was separated on a 4-12% polyacrylamide gel and transferred to polyvinylidene difluoride membrane (GE Healthcare). The membranes were blocked with PBS containing 5% blocking reagent (GE Healthcare, UK). The following primary antibodies were used at the dilutions suggested by the manufacturer: pAB anti-RAP1A (C-17) specifically for unprenylated RAP1 (Santa Cruz Biotechnology, USA), and anti-actin mAB (Sigmal-Aldrich, USA) as a loading control. Alkaline phosphatase-conjugated anti-goat or anti-rabbit (Thermo Fisher Scientific, USA) were used as secondary antibodies. Detection of protein bands was performed using the ECF substrate reagent kit (GE Healthcare, UK) on a LAS-4000 (GE Healthcare, UK).

2.7 Animal study design

Six-week-old female non-obese diabetic severe combined immunodeficient (NOD/SCID) mice were purchased from the Animal Resources Centre (Canning Vale, WA, Australia) and housed under strict specific pathogen-free barrier practices in The Queen Elizabeth Hospital Experimental Surgical Suite (Woodville, SA, Australia). Mice were acclimatised to the animal housing facility for 1 week and monitored continuously for wellbeing using specific clinical records throughout the experiment. Monitoring criteria were body weight, general appearance such as skin, hair and breathing, as well as eating and drinking, and general behaviour. All experimental procedures were carried out with strict adherence to the rules and guidelines for the ethical use of animals in research and were approved by the Animal Ethics Committee of the University of Adelaide.

2.8 Breast cancer mouse tumour model

GFP and Luciferase-expressing MDA-MB231-TXSA cells were cultured, adjusted to 2 x 10^6cells/50µl and mixed in a 1:1 ratio with Matrigel on ice, or a 1:1 ratio with PBS (100µl total volume) and then injected into the flank of NOD-SCID mice to form a tumour over 1 week. After randomization, mice (five mice/group) were divided into five groups on the basis of different localized treatments given at the tumour site: 1) untreated control; 2) Vγ9Vδ2 T cells and ZOL in free form, i.e. solution; 3) ZOL-embedded Matrigel; 4) Vγ9Vδ2 T cells-embedded Matrigel; 5) Vγ9Vδ2 T cells and ZOL embedded Matrigel. Vγ9Vδ2 T cells were given at 5 x 10^6/animal while ZOL was given at 0.68 mg/animal. Bioluminescent imaging was performed once every 4-5 days to track cancer progression until endpoint, defined by body weight loss reaching 10% or tumour volume exceeding 1 cm^3. Data was represented as mean ± SEM. Linear mixed-effects model was used to examine the significance of differences among different groups. In the residual tumour setting of the mammary fat pad (mfp), 2 x10^5 cells/50µl was used as the inoculum cell density, which was injected into the mammary fat pad of each animal. Vγ9Vδ2 T cells were given at 1 x 10^7/animal while ZOL was given at 0.68 mg/animal.

For *in vivo* ZOL uptake studies, while five mice were used herein the whole experiment, three mice were used for bioluminescence/fluorescence imaging while the other two were used for tumour excision and FACS analysis as samples cannot be processed for both given the nature of the techniques. Breast tumours (1 x 10^6cells) were grown for 2 weeks in the flask of the animals. On Day 17, ZOL (0.68 mg) was injected at the tumour site. Two forms of ZOL were used. Non-fluorescent, biologically active ZOL was used for downstream protein analysis. Biologically inactive, fluorescently-labelled ZOL (AF647-ZOL) was used to visually observe its presence in the tumour tissue. The appropriate ZOL for each treatment group was injected either directly adjacent to the tumour in Matrigel, or intratumourally into the centre of

the tumour, in free form. Fluorescent imaging was performed immediately following injections, to locate AF647-ZOL at the site. Bioluminescent imaging was performed at Day 1, 7 and 17 to track cancer progression and 72 h after ZOL injection (Day 20). Mice were euthanized by cervical dislocation or in an atmosphere of 100% CO_2. Tumour tissue samples were prepared as viable single cell suspensions or snap frozen in liquid nitrogen for subsequent protein extraction and western blot analysis.

2.9 Glioblastoma cancer mouse model

Human glioblastoma U-87 brain cancer (U-87 MG) cells were expanded *in vitro* and adjusted to 2 x 10^6 cells/50µl. Cells were prepared with Matrigel or PBS in the same manner in the breast cancer model described above. 100 µL of cell mixture was injected subcutaneously (s.c) on the flank of mice. IVIS imaging was performed. Tumours were imaged on Day 1, 7, 14 and 17.

2.10 *In vivo* fluorescence and bioluminescence imaging

A Xenogen IVIS Spectrum Imaging System (Perkin Elmer, USA) was used to obtain non-invasive whole body bioluminescence and fluorescence images of luciferase-tagged MDA-MB231-TXSA or U-87 MG cells, with optimised settings as previously described [199]. For bioluminescence images, animals received an intraperitoneal injection of 150mg/kg D-luciferin (Perkin Elmer, USA) as a substrate, bioluminescence was acquired between 0.5 sec and 2 min with representative images showing maximum bioluminescence of each animal. Imaging was performed weekly to monitor cancer burden and progression and at Day-20, 72 h post-zoledronate injection. Images were quantified using Living Image 4.2 software (Caliper Life Sciences, Australia).

2.11 TCR δ Immunohistochemistry and TUNEL staining

Anti-human T cell receptor (TCR) δ staining was performed following a procedure adapted from Siegers *et al* [208]. Briefly, formalin-fixed and paraffin-embedded sections were melted on a slide warmer followed by de-paraffinization in fresh Xylenes. Sections were then hydrated with a series of absolute and 70% ethanol followed by brief incubation in water, then in 10 mM citrate buffer, pH 6. Antigen retrieval was next performed at 100°C for 20 min. After cooling to room temperature, sections were blocked with peroxidase block (1% H_2O_2/methanol) for 30 min. Sections were washed in PBS then blocked with 0.2% BSA in 3% normal horse serum for 1 h. Protein block was gently removed and replaced with 1:100 dilution of mouse monoclonal anti-human TCR δ antibody (clone H-41, Santa Cruz, USA). Following an overnight incubation at 4°C, sections were rinsed and washed in PBS and then incubated with secondary antibody, labelled polymer-horseradish peroxidase anti-mouse (DAKO) for 30 min at room temperature in a humidified chamber. Sections were rinsed. Visuallization was done by incubating the slides in 3,3'diaminobenzidine chromogen solution (Dako Liquid DAB+substrate Chromagen system) for a maximum of 7 min before the reaction was stopped by rinsing in water. Hematoxylin counter staining was performed and the slides were then covered with coverslips mounted with dibutylphthalate polystyrene xylene mounting medium. While there are numerous methods to detect apoptotic events in paraffin-embedded tissue sections, TUNEL staining assay (Promega, USA) has been used extensively for these types of tumour studies by our laboratory [209-211]. The assay was performed according to the manufacturer's protocol.

2.12 Flow cytometric analysis tumour explants.

Viable single cells were prepared from mouse tumour tissue by enzymatic and mechanical disaggregation using the gentleMACS Dissociator (Miltenyi Biotech), as per manufacturer's instructions. Briefly, tumours were washed in sterile room temperature PBS, placed into a petri dish and cut into quarters using a scalpel. Tumour pieces were placed into

the gentleMACS C tubes (Miltenyi Biotech) containing an enzyme mix of 1 mg/ml collagenase II and 100K unit/ml DNase I and processed using a gentleMACS Dissociator (Miltenyi Biotech) as per manufacturer's recommended program. The resulting single cell suspension was passed through 70 µm and 40 µm strainers, and the collected strained cells were washed, resuspended in 200 µl FACs wash buffer and analysed immediately. BD FACSCanto II flow cytometer was used to detect the presence of GFP-labelled tumour cells and AF647-labelled zoledronate at 488/530 and 633/660, respectively. Tumour cells from the glioblastoma model were stained with F4/80-Pacific Blue (Bio-Rad, Hercules, CA) for surface expression of murine macrophage lineage. Flow cytometric analysis was performed using a BD II cytometer with BD FACS Diva software (BD Biosciences), and data were analysed using FlowJo software.

2.13 Western immunoblotting

A density of 1 x 10^6 MDA-MB231-TXSA and U-87 MG cells were seeded overnight to 25 cm^3 flasks. Cells were then treated with or without ZOL (0.1-25 µM) for 24 h. Lysates were prepared and separated as previously described Briefly, cells were washed with ice-cold PBS, and lysed in 50 µL of protein lysis buffer containing 10 mM Tris HCl, pH 7.6, 150 mM NaCl, 1% Triton X-100, 0.1% sodium dodecyl sulphate (SDS), 2 mM sodium vanadate and a protease inhibitor cocktail (Roche Diagnostics, Mannheim, Germany). The protein content was quantified using the BCA™ Protein Assay Kit (Thermo Fisher Scientific, Waltham, MA, USA). An equal amount of protein from each lysed cell sample was separated on a 4-12% polyacrylamide gel and transferred to polyvinylidene difluoride membrane (GE Healthcare). The membranes were blocked with PBS containing 5% blocking reagent (GE Healthcare, UK). The following primary antibodies were used at the dilutions suggested by the manufacturer: pAB anti-RAP1A (C-17) specifically for unprenylated RAP1 (Santa Cruz Biotechnology, USA), and anti-actin mAB (Sigmal-Aldrich, USA) as a loading control. Alkaline phosphatase-

conjugated anti-goat or anti-rabbit (Thermo Fisher Scientific, USA) were used as secondary antibodies. Detection of protein bands was performed using the ECF substrate reagent kit (GE Healthcare, UK) on a LAS-4000 (GE Healthcare, UK).

2.14 Statistics

All in vitro experiments were performed using biological triplicates and data was presented as mean ± SEM, unless otherwise specified. Two-tailed unpaired Student's t-test was utilised and in all cases p-values <0.05 were considered statistically significant. Animal experiments were conducted using the minimum numbers of mice required to reach statistically significant results. Treatment groups typically contained 3 to 5 replicate animals and consistent results were obtained. A representative image is shown for animal bioluminescence, fluorescence and flow cytometry.

Chapter 3

In vitro optimisation of local ACT of ex vivo expanded Vγ9Vδ2 T cells

3.1 Chapter introduction

Tumour recurrence following surgical resection in patients with solid tumours represents a serious clinical problem and often results in death. In order to minimise the risk of cancer recurrence, patients are often treated with a combination of surgical and non-surgical approaches such as radiation, chemotherapy, hormonal therapy and/or immunotherapy. While most cancers respond well to this combinatorial strategy, in some patients, surgery is too dangerous or impractical due to the size and location of the tumour. Surgical approaches also risk relapse from residual tumour cells even after macroscopically complete resection, which is not only clinically relevant but also the predominant reason of treatment failure in many malignancies [212]. Thus, there is an urgent need for better treatment strategies, especially for those patients with incompletely resected or inoperable tumours.

In recent years, adoptive cell therapy (ACT) has emerged as a novel and viable immunotherapeutic approach to treat cancer. It typically utilises naturally occurring or genetically modified T cells [213]. Among these T cells, gamma delta (γδ) T cells are an extraordinary type of T cells with natural anti-tumour capacity [214]. The majority of γδT cell subset in humans are designated Vγ9Vδ2 T cells and are activated by phosphoantigens (PAgs), which are intermediate metabolites of the mammalian mevalonate pathway. These are abnormally expressed in transformed (cancer) or infected cells [102]. Following activation, Vγ9Vδ2 T cells increase the release of anti-tumour effector molecules, including perforin and granzymes [65, 83, 96, 215], secrete immunogenic cytokines including, IFN-γ and TNF-α [65, 83, 84], upregulate TRAIL death receptor [96] and increase FasL expression [82]. All of which contribute to their cytotoxic potential against a broad range of tumour cells.

Several clinically used drugs are known to improve the activity of Vγ9Vδ2 T cells against cancer [216]. Among these are the nitrogen containing bisphosphonate group of

compounds (NBPs). They are structurally related to PAgs, and indirectly act to stimulate Vγ9Vδ2 T cells by inhibiting farnesyl pyrophosphate synthase (FPPS), an enzyme of the mevalonate pathway, resulting in the accumulation of upstream metabolites of direct PAg termed IPP [217].

Zoledronate (ZOL) is a third generation NBP and is the most potent NBP to date, currently used in clinical practice for the treatment of osteoporosis and bone related malignancies. ZOL is also the most potent NBP to stimulate Vγ9Vδ2 T cells. It is well established that ZOL can sensitise many types of cancer to become vulnerable to Vγ9Vδ2 T cell-mediated cytotoxicity *in vitro* and *in vivo* [93, 145, 148, 149]. Clinical trial phase I/II of ACT has shown that Vγ9Vδ2 T cell-based therapy in combination with NBPs, especially ZOL is feasible in patients with advanced solid tumours as well as being well-tolerated [156, 171, 218]. However, the therapeutic outcome thus far has been minimal [171, 185, 219], suggesting that Vγ9Vδ2 T cell-based immunotherapy requires further optimisation. A clinical study by Nicol *et al* [171] has highlighted a number of practical issues for the use of ACT of *ex vivo* expanded Vγ9Vδ2 T cells in patients with various solid malignancies. Most importantly, it has shown that, when Vγ9Vδ2 T cells were transferred intravenously into patients only a minority reached the tumour tissue, while the majority were trapped predominantly in the lungs, liver and spleen [171], raising the issue of how to best deliver Vγ9Vδ2 T cells to optimise trafficking into solid tumours.

Although systemic delivery is a preferred route of administration, several pre-clinical and clinical studies suggested regional delivery of T cells, may provide optimal therapeutic effects [202-204]. To date, *ex vivo* expanded Vγ9Vδ2 T cells have only been delivered either intravenously or intraperitoneally. Wada *et al*. has shown intraperitoneal delivery of Vγ9Vδ2 T cells with ZOL resulted in a significant reduction in the volume of malignant ascites caused by peritoneal dissemination of gastric cancer [185].

In the context of incompletely resected or inoperable solid tumours, localized delivery of Vγ9Vδ2 T cells together with ZOL in biomaterial scaffolds would be an ideal approach. As entry into the tumour is an absolute requirement for T cell-mediated cytotoxicity, biomaterial scaffolds can provide a means of delivering a large number of therapeutic T cells directly at the tumour site while simultaneously delivering ZOL to cancer cell targets to enhance Vγ9Vδ2 T cell killing. To date, no studies have examined this treatment strategy in any well-defined *in vitro* models.

Therefore, the specific aim of this chapter was firstly to assess the ability of Matrigel to support the survival and release of the encapsulated Vγ9Vδ2 T cells and also to assess the efficacy of Matrigel carrying Vγ9Vδ2 T cells and ZOL against breast cancer cells *in vitro*. This study has shown that Vγ9Vδ2 T cells can survive in Matrigel and that they can efficiently passage through and leave Matrigel scaffolds even without external cues. Upon release from Matrigel, Vγ9Vδ2 T cells maintained their remarkable cytotoxicity against ZOL-pretreated breast cancer cells. Alternatively, the co-addition of ZOL directly into Matrigel together with Vγ9Vδ2 T cells, maintained the killing capacity of Vγ9Vδ2 T cells to that seen by ZOL pre-treatment of cancer cells highlighting the potential clinical utility of this approach for localized cancer therapy.

3.2 Results

3.2.1 Vγ9Vδ2 T cells survive following encapsulation in Matrigel scaffolds

To determine whether Matrigel encapsulation can promote Vγ9Vδ2 T cell survival, *ex vivo* expanded Vγ9Vδ2 T cells were embedded into Matrigel in the presence or absence of ZOL (0-25 μM) and cultured at 37°C for 24 h. Vγ9Vδ2 T cells plated directly into the bottom of a 96-well plate without Matrigel and without ZOL (2D, plastic) was used as a control. Following

incubation, cell viability was assessed with CellTiter-Glo® 3D cell viability assay. Results showed similar cell viability in all tested conditions (Fig 3.1). On 2D plastic, T cell viability reduced slightly to 82% at 24 h post-incubation. While not statistically significant, the encapsulation reduced Vγ9Vδ2 T cell viability to 65%. Interestingly, the addition of low dose ZOL (5 μM) into Matrigel scaffolds significantly improved cell viability to 104% ($p = 0.006$). However, as the concentration of ZOL increased, cell viability decreased reaching 65% at 25 μM ZOL ($p = 0.02$). Overall, despite the decrease in cell viability in some test conditions, Vγ9Vδ2 T cells survived relatively well following encapsulation in Matrigel scaffolds when compared to the 2D plastic control.

3.2.2 Encapsulated Vγ9Vδ2 T cells efficiently migrate out of Matrigel scaffolds

As it is essential that the encapsulated V9γVδ2 T cells can travel through and exit the scaffolds to reach their target, the ability of Vγ9Vδ2 T cells to migrate out of Matrigel was examined in a time dependent manner. A droplet of Matrigel containing *ex vivo* expanded Vγ9Vδ2 T cells was placed in the middle of a 24-well plate, forming a convex gel surface (Figure 3.2 A). V9γVδ2 T cells released from Matrigel into the surrounding media was then monitored under the microscope over time. Results showed that the encapsulated Vγ9Vδ2 T cells exited into the surrounding media as soon as incubation commenced ($t = 0$ h) but was more clearly visible from 12 h post-encapsulation onwards (Fig 3.2 B). These findings suggest Vγ9Vδ2 T cells can efficiently passage through Matrigel and exit into the surrounding medium.

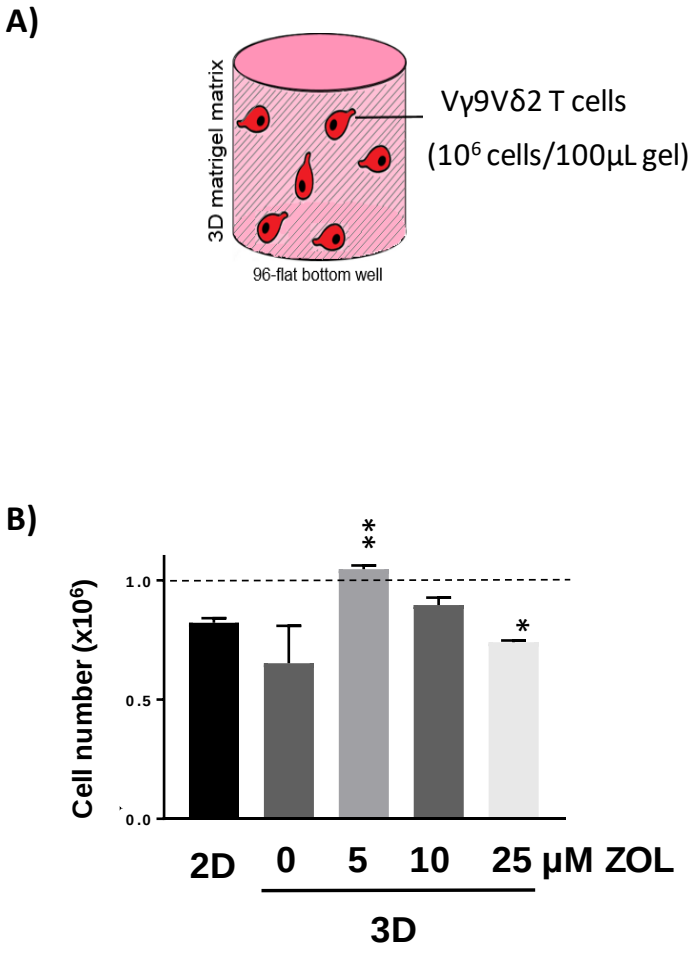

Figure 3.1 Biocompatibility of Matrigel-encapsulated Vγ9Vδ2 T cells.

A) Assay set up. One million *ex vivo* expanded V9γVδ2 T cells in 50 µL media were added to equal volume of liquid Matrigel containing 0-25 µM ZOL. Matrigel and V9γVδ2 T cells were then placed at 37°C for 5 min for Matrigel to solidify. Fresh media was added, and incubation continued for a further 24 h. Cell viability was assessed, based on the amount of ATP present by CellTiter-Glo Luminescent assay kit (Promega). V9γVδ2 T cells seeded directly on plastic (2D; without Matrigel) were used as a control. B) Cell viability at 24 h post-encapsulation. Data was pooled and normalised from two separate experiments (n = 6). Error bars indicate in SEM (*$p<0.1$, **$p<0.01$).

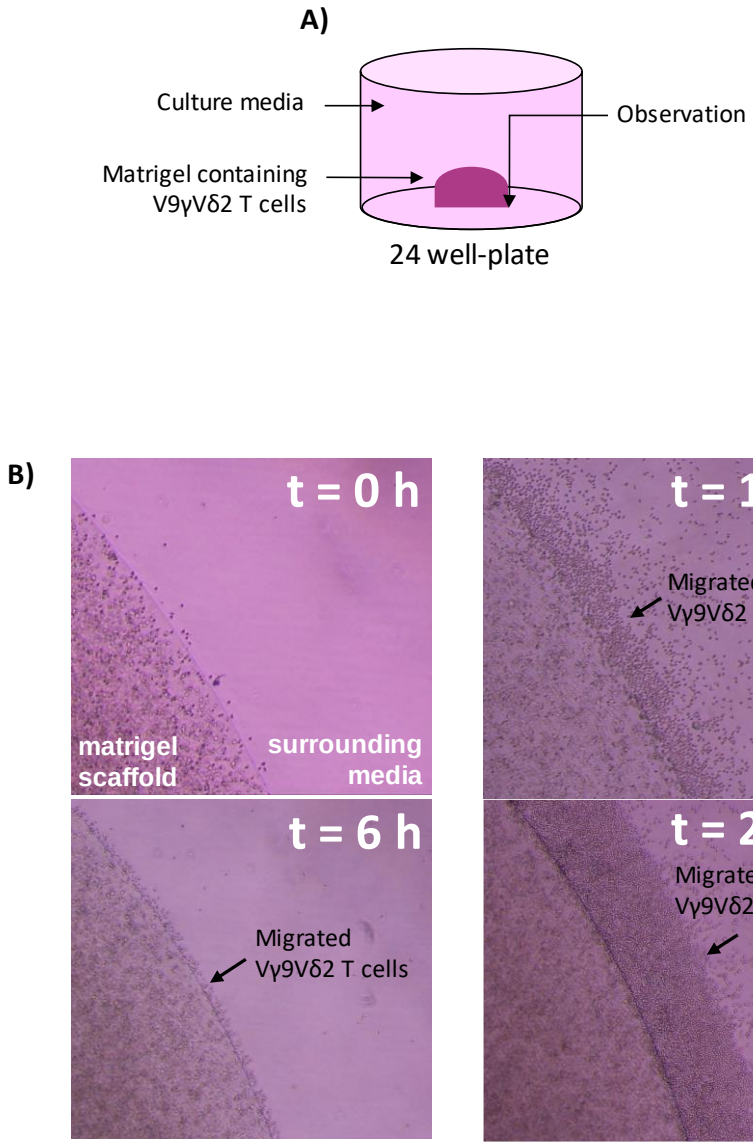

Figure 3.2 Microscopic evaluation (10X) of Vγ9Vδ2 T cell migration out of Matrigel scaffolds following encapsulation.

Equal volume of liquid Matrigel was mixed with $1x10^6$ Vγ9Vδ2 T cells. The mixture was then warmed up briefly at room temperature before being placed slowly to the bottom of a 24-well plate creating a convex gel surface. The plate was then kept at 37°C for 10 min to set. Fresh media was added. At 12 h post-incubation, substantial egress of Vγ9Vδ2 T cells into surrounding media was clearly visualized.

3.2.3 Vγ9Vδ2 T cells released from Matrigel are cytotoxic against ZOL-pretreated breast cancer cells

Vγ9Vδ2 T cell mediated cytotoxicity following release from Matrigel *in vitro* was next assessed using time-lapse fluorescence microscopy. The experimental set up was similar to that described in Section 3.2.2 but with the addition of a monolayer of GFP-labelled MDA-MB231-TXSA cells (green) at the bottom of the well. In addition, Vγ9Vδ2 T cells were labelled with VivoTrack680 dye, showing in red (Fig 3.3 A).

In the first time-lapse experiment, cancer cells were pre-treated with 25 μM ZOL for 24 h prior to the addition of Vγ9Vδ2 T cells in Matrigel. This concentration of ZOL (25 μM) was chosen because it was previously shown to be the minimum concentration required to sensitise MDA-MB231-TXSA breast cancer cells toward Vγ9Vδ2 T cell-mediated cytotoxicity *in vitro* [199]. Time-lapse fluorescence microscopy was used to monitor the area at the edge of Matrigel scaffold and cancer cell target. Immediately after the start of imaging recording, cancer cells located directly below Matrigel quickly displayed evidence of apoptosis induction such as cell shrinkage and membrane blebbing. This indicated that Vγ9Vδ2 T cells, which were initially homogeneously distributed throughout Matrigel had migrated down to the bottom of the gel and targeted cancer cells directly beneath it. The Vγ9Vδ2 T cells then avidly migrated out of the Matrigel scaffold, made contact with the nearby cancer cells and killed them before latching onto nearby cancer cells, resulting efficient killing of all cancer cells within 32 h. (Figure 3.3 B, right panel). In comparison, untreated cancer cells only occasionally showed cell death during this period and, hence, proliferated further (Figure 3.3 B, left panel).

A) Assay set up

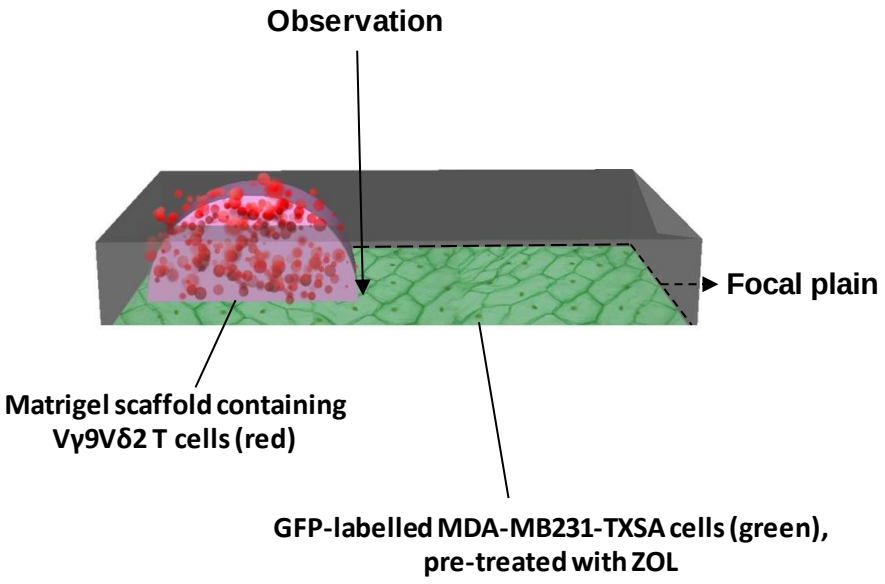

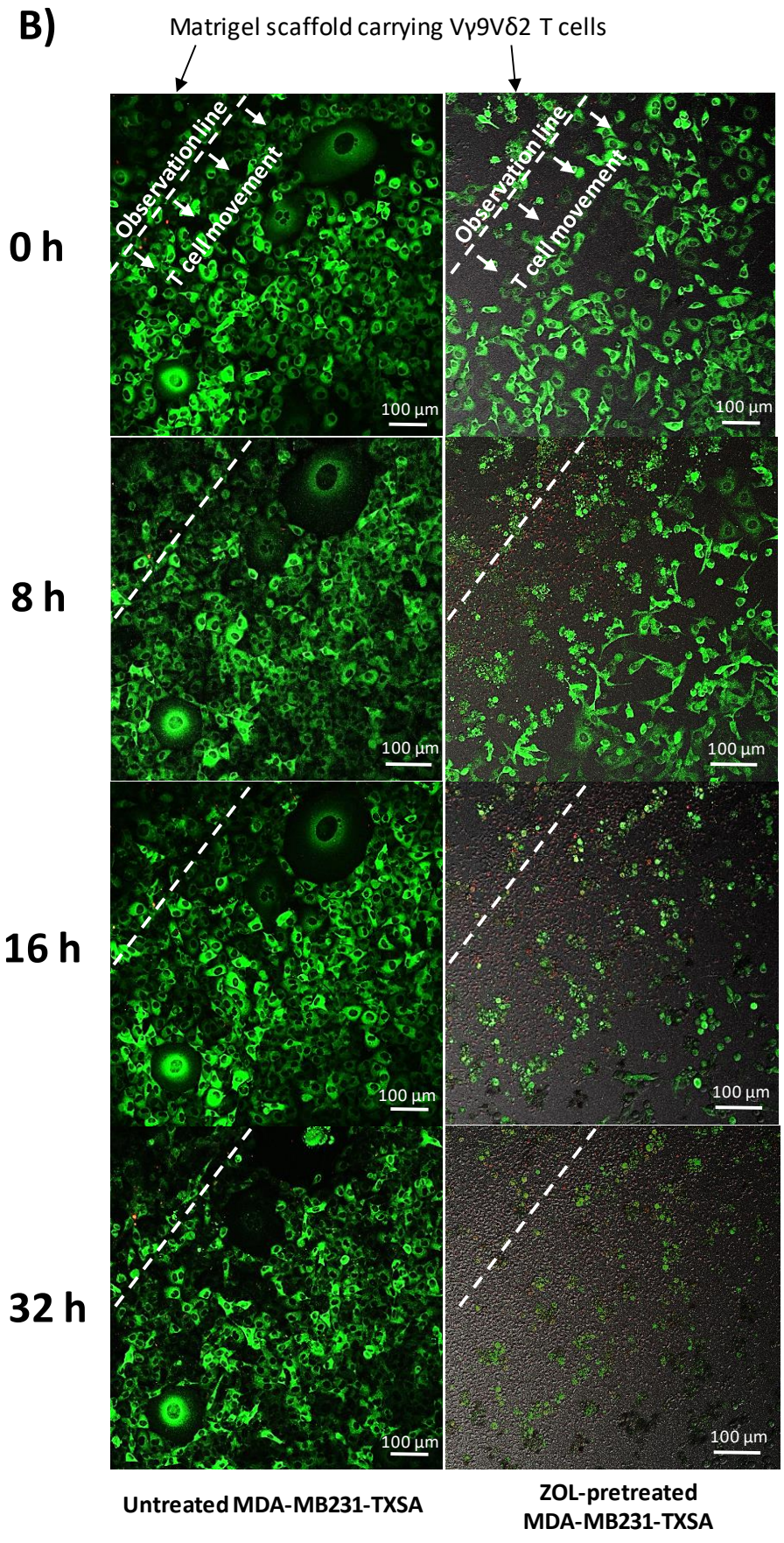
B)
Matrigel scaffold carrying Vγ9Vδ2 T cells
0 h
8 h
16 h
32 h
Observation line
T cell movement
100 µm
Untreated MDA-MB231-TXSA
ZOL-pretreated
MDA-MB231-TXSA

Figure 3.3 Visualization of Vγ9Vδ2 T cell migration out of Matrigel and cytotoxicity against breast cancer cells.

A) Assay set up. GFP-labelled MDA-MB231-TXSA cells (green) were grown to sub-confluency in 24-well plates and treated with or without 25 μM ZOL for 24 h. Vγ9Vδ2 T cells labelled with VivoTrack680 dye (red) and mixed with equal volume of Matrigel (50 μL of Matrigel + 50 μL of Vγ9Vδ2 T cells containing 10^6 cells) was placed directly on the cancer cell monolayer to form a convex gel surface once solidified. Time-lapse confocal microscopy was used to monitor subsequent killing events. B) Snapshot imaging showing Matrigel-released Vγ9Vδ2 T cells maintained cytotoxic function only against ZOL-pretreated breast cancer cells (right panel images) but are without effect against untreated breast cancer cells at 32 h post-incubation (left panel images).

3.2.4 Incorporation of ZOL into Matrigel together with Vγ9Vδ2 T cells was equally effective in the T cell mediated cytotoxicity of cancer cells

In line with the aim to develop a 3D cell culture that has dual function of delivering both Vγ9Vδ2 T cells and ZOL locally at the tumour microenvironment, the ability of ZOL embedded in Matrigel scaffolds to sensitize cancer cell target to Vγ9Vδ2 T cell-mediated cytotoxicity was examined. ZOL inhibits FPPS, a key enzyme in the mevalonate pathway, blocking prenylation of small GTPases such as Rap1A [220], leading to the accumulation of their unprenylated forms [221, 222]. Therefore, an increase in the levels of unprenylated Rap1A is commonly used as a surrogate marker for inhibition of mevalonate pathway *in vitro*.

In this set of experiments, breast cancer MDA-MB231-TXSA cells were cultured at the bottom of a 6-well plate and solidified Matrigel containing ZOL placed on the top chamber in a transwell (Fig 3.4 A), hence was not in direct contact with the cancer cells. Since ZOL was highly hydrophilic, it was assumed that it would be released immediately and almost completely from solid Matrigel into the cell culture media. For this reason, 25 µL ZOL stock solution (10 mM) was added to Matrigel. Matrigel containing ZOL was then transfer into a transwell to solidify. Once solidified, the transwell was inserted into a 6-well containing cancer cells monolayer. 1 mL of fresh culture media was added into each well of a 6-well plate and, at this volume, the final ZOL concentration would presume to be 25 µM ZOL/well/1 mL after the addition of fresh media once the gel solidified. The levels of unprenylated Rap1A in cancer cells were determined following 24 h incubation with ZOL-embedded Matrigel by Western blot analysis. MDA-MB231-TXSA cells showed an increase in unprenylated Rap1A (Fig 3B, left image) in a similar manner to that of ZOL delivered in free form at 25 µM (Fig 3B, right image) indicating the inhibitory effect of ZOL on the mevalonate pathway by both ZOL delivery methods.

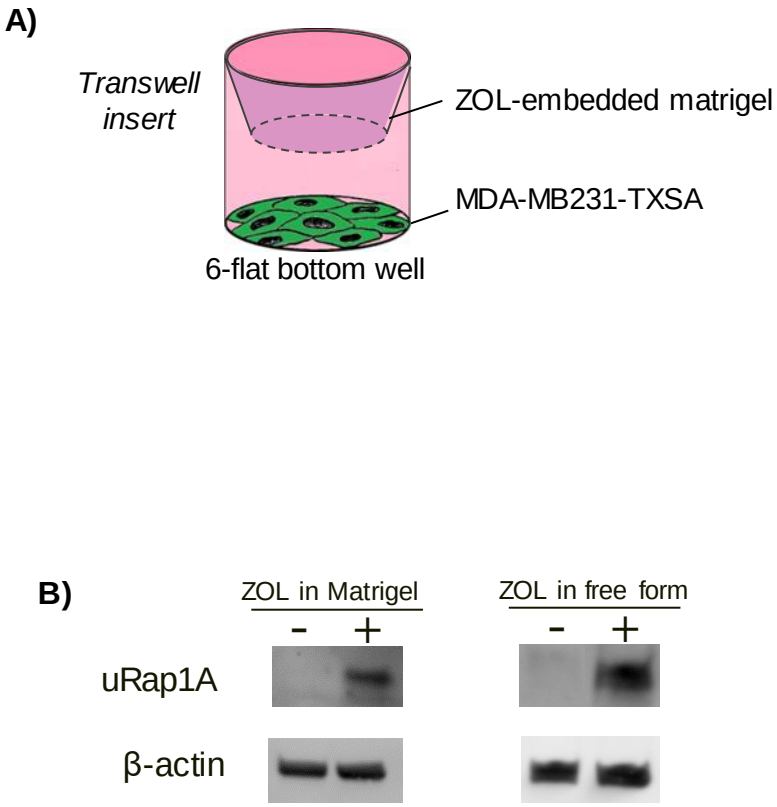

Figure 3.4 Inhibition of prenylation from ZOL-embedded Matrigel.

A) Assay set up. B) Western blot analysis showing inhibition of prenylation (uRap1A) in MDA-MB-231-TXSA cells after incubation with Matrigel containing ZOL (25 µL of 10 mM ZOL stock solution), which was placed in the top chamber of the transwell insert and not in direct contact with cancer cells, grown as a monolayer at the bottom of the plate. Upon the addition of 1 mL fresh media per well, the final ZOL concentration was presumed to be 25 µM/well. β-actin was used as a loading control. Images representative of n=2.

Having now established the ability of Matrigel embedded ZOL to inhibit the mevalonate pathway in breast cancer cells, an immune effector function assay for quantification of encapsulated Vγ9Vδ2 T cell cytotoxicity *in vitro* was developed. For this purpose, the robust migration-based T cell cytotoxicity assay previously described by Weigelin and Friedl [207] was adopted and modified. This assay consisted of the cancer cell target, being the Luciferase-labelled MDA-MB231-TXSA grown at the bottom of a 96-well plate overlaid completely with a polymerized 3D Matrigel culture containing Vγ9Vδ2 T cells with or without ZOL (Fig 3.5 A). Two dimensional (2D) co-cultures of the cancer cell target with Vγ9Vδ2 T cells (Fig 3.6 A) were used as a 2D control. Following 32 h post-incubation, the remaining target cells were assessed for luciferase activity to determine the overall cancer cell viability. As the purpose of this experiment was to test the immune effector function of encapsulated Vγ9Vδ2 T cells, only the viability of the remaining cancer cell target was measured while the cell viability of Vγ9Vδ2 T cells was not measured. Results of the 3D assay indicated neither ZOL (25 µM) nor Vγ9Vδ2 T cells alone reduced target cell viability. However, co-incubation with both ZOL (5-25 µM) and Vγ9Vδ2 T cells in Matrigel scaffolds resulted in a significant reduction in target cell viability in a ZOL-dose dependent manner (ranging from 25 % viable at 5 µM to a maximum of 0 % viability at 25 µM ZOL). On the other hand, results from the 2D assay showed about 50% killing with T cells alone, while the addition of ZOL in all concentrations tested (5-25 µM) led to an almost complete killing of the cancer cell target (Fig 3.6 B). Time-lapse fluorescence microscopy confirms breast cancer cells were killed by Vγ9Vδ2 T cells released from Matrigel.

In a similar time-lapse microscopy experiment described earlier in Section 3.2.3, Matrigel scaffolds that previously showed to favour Vγ9Vδ2 T cell migration can be combined with the ability to carry and release ZOL locally. In this experiment, soluble ZOL was co-

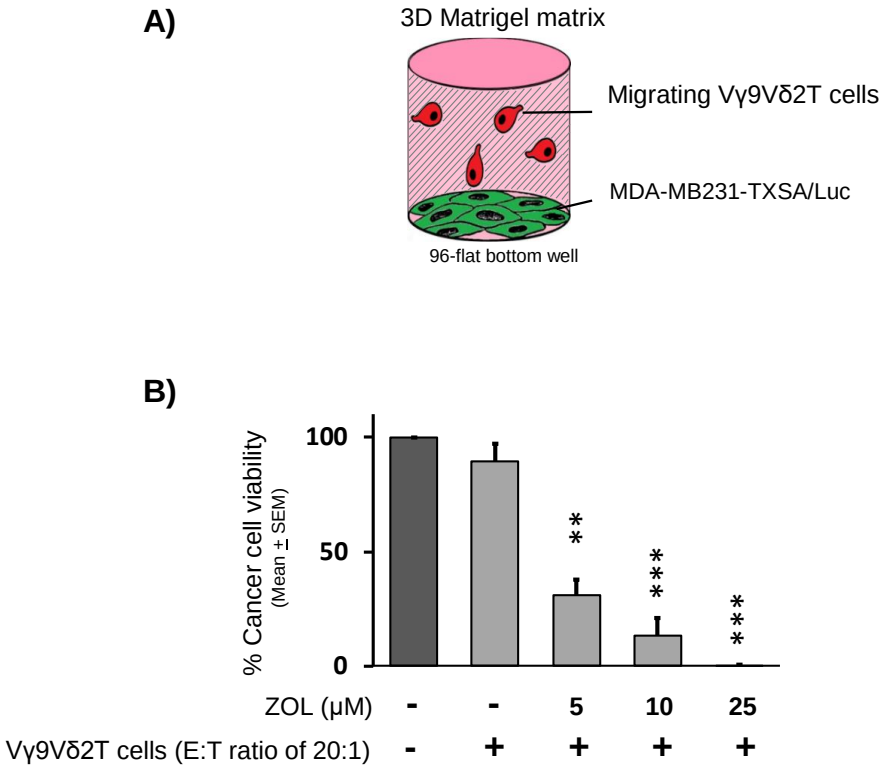

Figure 3.5 Cytotoxic activity of Matrigel-released Vγ9Vδ2 T cells in the presence or absence of ZOL against breast cancer cells MDA-MB231-TXSA in 3D organotypic assays.

A) Assay set up. **B)** Luciferase-labelled MDA-MB-231-TXSA cells were grown to confluence in 96-well plates. Preformed solidified Matrigel (100 μL) containing Vγ9Vδ2 T cells with ZOL (0-25 μM) was overlaid on top the breast cancer monolayer. Fresh media was added to each well and incubated for 24 h. After incubation, relative luciferase activity was measured and expressed as percentage cancer cell survival, compared to untreated cancer cells (100% survival). Data was pooled and normalised from two separate experiments (n=6). Error bars indicate in SEM (**p<0.01, ***p<0.001).

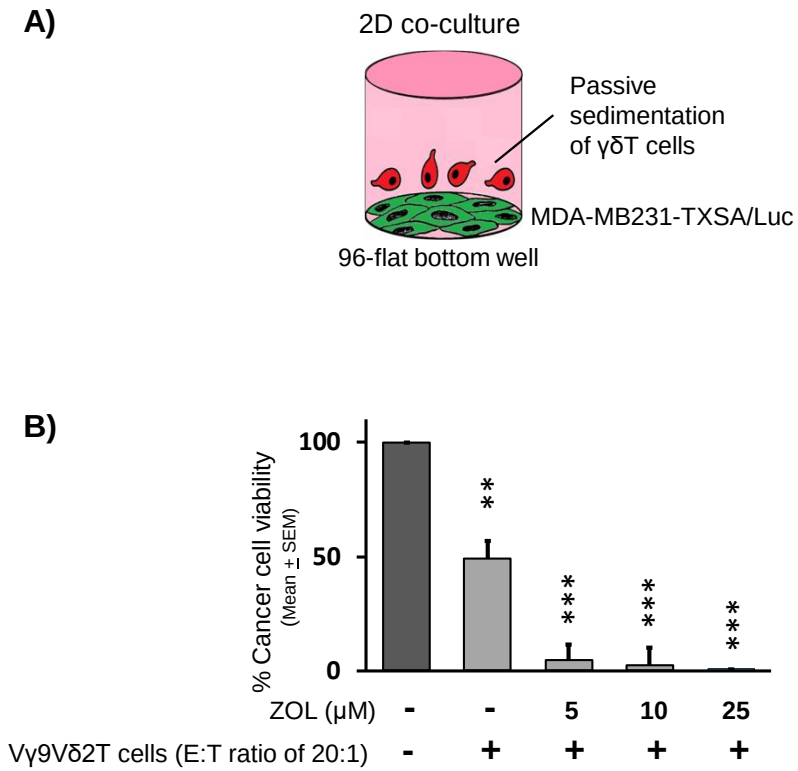

Figure 3.6. Anticancer activity of Vγ9Vδ2 T cells on ZOL-pretreated breast cancer cells in conventional 2D assay.

A) Luciferase-labelled MDA-MB-231-TXSA cells at sub-confluence were treated with 0-25 μM ZOL for 24 h. Cancer cells were then co-cultured with Vγ9Vδ2 T cells at E:T ratio of 20:1. After 24 h of incubation with ZOL, cancer cells were measured for relative luciferase activity. Results from untreated cancer cells were used as control (100% survival). Data was pooled and normalised from two separate experiments (n = 6). Error bars indicate in SEM (**p<0.01, ***p<0.001).

loaded to Matrigel-carrying T cells. The scaffold was again placed directly on top of untreated luciferase-labelled MDA-MB231-TXSA cells (represented here in green). 12.5 µL of ZOL stock solution (10 mM) was added to the scaffold. Upon the addition of 0.5 mL/well of fresh media once the gel scaffold solidified, it was presumed that the final concentration of ZOL in the media would be 25 µM. Wide-field microscopy analysis showed a delayed onset in cancer cell killing activity, which took place beginning at 3-4 h post-incubation (Figure 3.7), as opposed to rapid killing that occurred within a few minutes after the initial contact between the Vγ9Vδ2 T cell Matrigel-scaffold and ZOL pre-treated MDA-MB-231-TXSA cells seen in the previous time-lapse microscopy experiment described in 3.2.3. Subsequent to this lag time, cancer cell death was observed at the interface of the scaffold. It was then observed in the nearby and distant area, all within 40 h of incubation. Therefore, this *in vitro* study established the utility of Matrigel as a depot for the co-release of Vγ9Vδ2 T cells and ZOL simultaneously to treat localized cancers.

3.3 Discussion

The combining field where immunotherapy meets biomaterials is an ever-growing field of research with the promise to overcome current clinical limitations that restrict cell-based cancer immunotherapy. Here it is hypothesized that *ex vivo* expanded Vγ9Vδ2 T cells can be locally distributed using a hydrogel (Matrigel) carrier that is placed in the vicinity of solid tumours for local control of the disease. This method would theoretically confer several advantages, one of which is to improve localization of large numbers of T cell to the tumour bed. Additionally, therapeutic reagents (in this case ZOL) used as the cancer cell sensitiser can also be added to the carrier to enhance Vγ9Vδ2 T cell function.

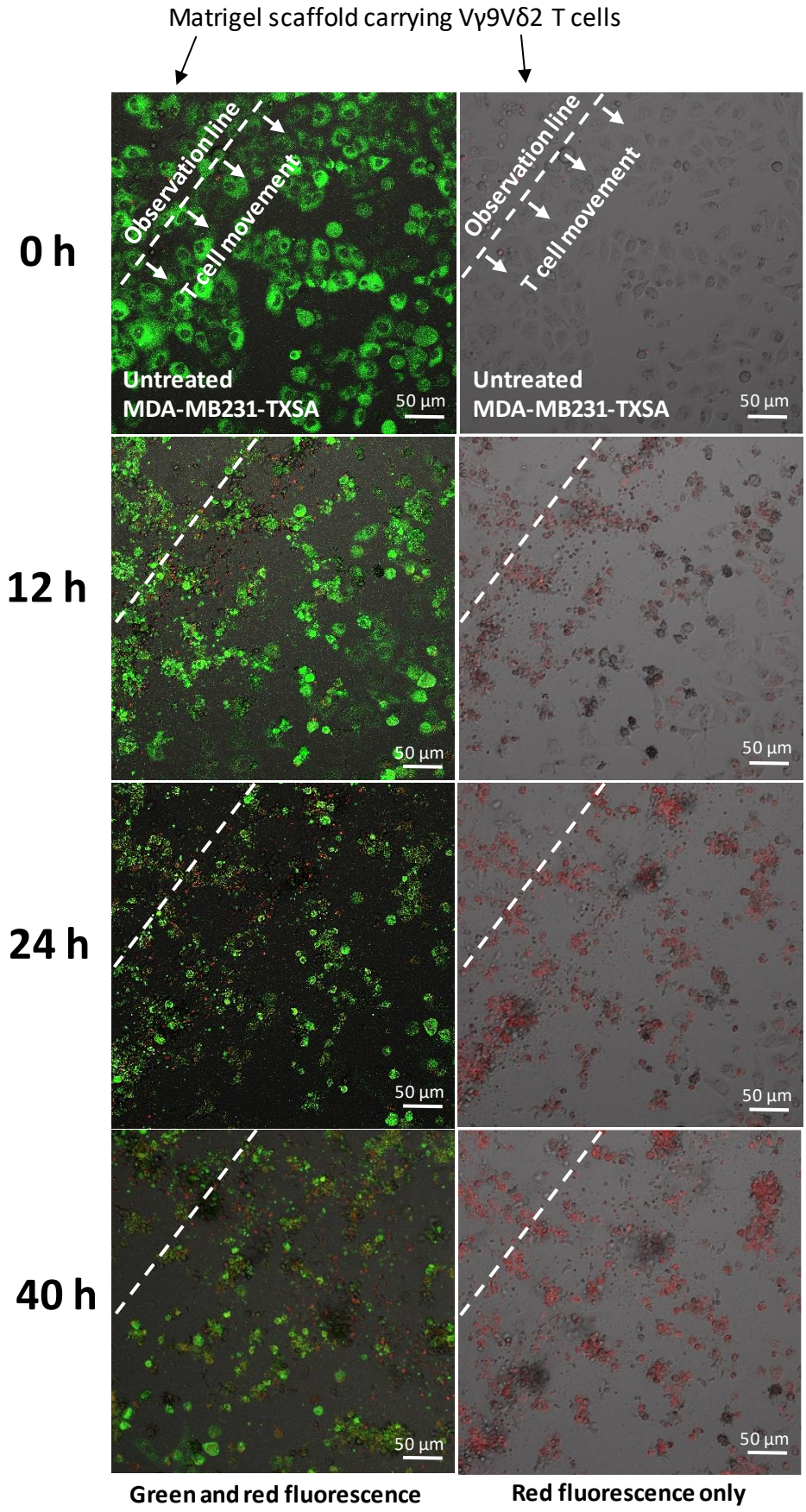
Matrigel scaffold carrying Vγ9Vδ2 T cells
0 h
12 h
24 h
40 h
Observation line
T cell movement
Untreated
MDA-MB231-TXSA
50 µm
Green and red fluorescence
Red fluorescence only

Figure 3.7 Visualization of Vγ9Vδ2 T cell migration from Matrigel scaffolds and subsequent cytotoxicity against breast cancer cells.

Unlike the previous time-lapse fluorescent microscopy experiment (3.2.3) where cancer cells were pre-treated with ZOL, cancer cells in this experiment were not pre-treated. Instead, ZOL was added directly into the Matrigel scaffolds together with the T cells. Snapshot imaging showing Matrigel-released Vγ9Vδ2 cells (red) were able to kill and eliminate breast cancer cells despite a delayed onset of cytotoxic activity (Left panel images). Extracted 2D Z-stacking images (right panel images) showing only bright field and red-fluorescent channels reveal detection of Matrigel-released T cells at 10 μm above the original focal plane, presumably on top of the cancer cell monolayer.

The findings from these *in vitro* experiments indicate that *ex vivo* expanded Vγ9Vδ2 T cells can survive within the Matrigel scaffolds and that they can efficiently and rapidly passage through and migrate out of Matrigel in large numbers in the presence or absence of external cues. To serve as temporary supports for cell growth and survival, cells can be either seeded onto prefabricated porous scaffolds or encapsulated during scaffold formation. In the former strategy, harsh chemicals may be used given that the final product is not toxic to the cells. On the other hand, cell encapsulation scaffolds must be cytocompatible (i.e. mild gelation process and suitable mechanical properties), which greatly reduces suitable materials and formulations [223]. Indeed, our group's preliminary studies have indicated a significant decrease in Vγ9Vδ2 T cell viability following encapsulation in carboxylated agarose gels and hyaluronic-based hydrogels (unpublished data). In comparison, the Vγ9Vδ2 T cell viability in 3D Matrigel scaffolds was comparable to that of 2D controls (without Matrigel), suggesting a clear benefit over other hydrogels tested in our laboratory.

Matrigel is a basement membrane extracellular matrix (ECM), consisted of gelatinous protein extracts from the Engelbreth-Holm-Swarm mouse sarcoma [224]. It is a popular choice for *in vitro* and *in vivo* scaffold-based 3D cell cultures due to its biocompatibility, stiffness, porosity and ability to be functionalised to mimic ECM [225]. Corning Matrigel® that was used in these studies is commercially available as a frozen protein solution that is then diluted to a working concentration (3-4 mg ml^{-1}) prior to use before self-assembling into a hydrogel at physiological temperatures [226]. Although Matrigel is considered a legitimate research tool by many, it is unlikely to receive approval for clinical use due to its murine origin [227] and thus not be a suitable option to use in patients. However, as a better understanding of criteria involving T cell encapsulation strategies is obtained, more successful systems could be developed that mimic Matrigel characteristics to be used in human patients.

In the context of tissue engineering and regenerative medicine, protein-based polymers such as fibrin [228] and collagen [229] are promising candidates. In particular, fibrin hydrogels are biopolymers formed from fibrinogen. In clinics, they have been used as natural scaffolds with reasonable success [230]. They are also commonly used as a bioadhesive following surgery for hemostasis, wound closure and a sealant [231, 232]. Their clinical utility relies on the fact that they are biocompatible, biodegradable and non-immunogenic [233]. Interestingly, in a recent pre-clinical study, fibrin-based gel delivery of CAR T cells within the surgical cavity of glioblastoma has shown superior antitumour activity, compared to CAR T cells regionally delivered without fibrin gels [234]. Further research is needed to prove if fibrin scaffolds will be useful in clinics.

In this current study, in addition to the cell survival and ability to migrate out of hydrogel carriers, another important factor to consider is whether the encapsulation process affects the effector function of the released T cells. Collectively the *in vitro* studies in this Chapter confirmed Vγ9Vδ2 T cells maintained their potent cytotoxicity against ZOL-pretreated breast cancer cells following their release from Matrigel scaffolds. Similarly, a study by Monette *et al* has shown encapsulated $CD8^+$ T cells maintained capacity to killing cancer cell target following released from chitosan-based thermogels *in vitro* [196]. In another *in vitro* study by Tsao *et al* [195], genetically modified $CD8^+$ T cells retained their anti-glioblastoma activity after being encapsulated into poly(ethylene glycol)-g-chitosan gels. These genetically modified T cells were even shown to be more effective at killing glioblastoma than those encapsulated in Matrigel control, which was presumably due to the more optimal pore size of chitosan gels (0.677 μm) than Matrigel (0.383 μm), which allows better T cell invasion. In addition, a study of injectable biomimetic polyisocyanopeptide (PIC) hydrogels [235] has shown these gels can support the expansion of pre-stimulated (primary) human lymphocytes *in vitro*. In a mouse model of PIC hydrogels, they have also shown to preserve the

effector/memory phenotype of adoptively transferred mouse T cells ($CD45.1^+$) without affecting the T cell function (as judged by the unchanged level of PD-1 expression following T cell encapsulation and gel formation *in vivo*). Collectively, these studies indicate that the mechanical and physical properties of T cell scaffolds are an important factor for stability during the 3D cell culture and may affect cellular behaviour. To fully understand the potential of hydrogels as a Vγ9Vδ2 T cell depot, the precise relationship between gel stiffness, gel concentration, the presence of adhesive molecules and migration propensity need to be determined. It is also crucial to consider gel stability and stiffness as these may decrease over time, permitting more cellular migration of encapsulated cells.

Currently, limiting the implementation of ZOL in Vγ9Vδ2 T cell-based immunotherapy for extra-skeleton tumours is the preferential localisation of ZOL to the bone due to the calcium binding characteristics and short plasma half-life period. An alternative concept to increase ZOL concentration in the tumour tissues is to administer the drug locally. The experiments in this Chapter show that Matrigel scaffolds can easily be adapted to simultaneously deliver this synergistic drug and cell combination. Systemic or local ACT of Vγ9Vδ2 T cells is an elaborate procedure that would normally require systemic pre-infusion or local pre-treatment with ZOL. In the later approach in this Chapter, ZOL was incorporated into the Matrigel scaffolds and, upon release locally, can act immediately on tumours nearby. Although there was a delayed onset of Vγ9Vδ2 T cell killing on cancer cells, perhaps reflecting the minimum time required for ZOL to inhibit the mevalonate pathway, various tests still showed simultaneous release of ZOL and Vγ9Vδ2 T cells in large numbers can effectively eliminate cancer cell targets.

In conclusion, the *in vitro* studies described in this Chapter provide evidence that biomaterials may be used to enhance Vγ9Vδ2 T cell localized immunotherapy and that they can practically be used to co-deliver both Vγ9Vδ2 T cells and ZOL to cancer cell target *in vitro*. Biomaterial scaffolds have previously been used to supply cells for tissue repair and

antigens to elicit immune responses, but to the best of our knowledge, this is the first time a biomaterial has been used with Vγ9Vδ2 T cells and ZOL in the context of localized tumours with promising preliminary *in vitro* results, warranting further studies in preclinical models of cancer.

Chapter 4

Localized immunotherapy of *ex vivo* expanded Vγ9Vδ2 T cells in combination with zoledronate in xenograft models of breast and brain cancers

4.1 Chapter introduction

In the previous chapter, by using a series of *in vitro* techniques, it was demonstrated that biomaterials can be used to enhance Vγ9Vδ2 T cell localized immunotherapy against breast cancer. This chapter explores further the potential of using such a novel approach to enhance the anti-cancer efficacy of Vγ9Vδ2 T cells in combination with ZOL in xenograft models of breast and brain cancers.

Working at the interface of innate and adaptive immunity, human gamma delta (γδ) T cells are highly cytotoxic immune effectors. Vγ9Vδ2 T cells, the most frequent γδT cell subset in human blood [236], can be stimulated by aminobisphosphonate drugs or synthetic phosphoantigen analogs [35]. Nitrogen-containing aminobisphosphonate drugs (NBPs) such as pamidronate and zoledronate (ZOL) act as indirect ligands for γδ TCR by modulating the expression of natural phosphoantigens in cancer and myeloid cells [237]. On the other hand, synthetic phosphoantigen analogs such as bromohydrin pyrophosphate (BrHPP) act directly as ligands for the γδ TCR and, likewise, enhance the expression of phosphoantigens both on the antigen presenting cells and the tumour cells [238-241].

The overall anti-tumour capability of Vγ9Vδ2 T cells used in combination with ZOL has prompted clinical trials of adoptive transfer of *ex vivo* expanded Vγ9Vδ2 T cells in patients with solid tumours. Although results indicated safety, clinical benefits have been inconsistent and limited, showing low objective response rates in most patients [160, 171, 185, 219, 242-246]. Our current limited understanding on γδ TCR diversity, ligands and receptor-ligand interactions could partially attribute to such failures [241] although it is beyond the scope of this thesis. Data from a trial conducted by Nicol and colleagues showed that of the large number of Vγ9Vδ2 T cells intravenously infused, only a small fraction eventually reached the tumour site, indicating poor trafficking/homing issues of systemically transferred Vγ9Vδ2 T cells to

the tumour lesions [171]. Unlike haematological malignancies where tumour cells are more accessible through the bloodstream, cells-based therapies directed against solid malignancies face a unique challenge of traveling from the injection site to the tumour site. Hence, alternate modes of cell delivery that promote efficient Vγ9Vδ2 T cell trafficking to the tumour site are required.

To take advantage of the potent cytotoxic activity of *ex vivo* expanded Vγ9Vδ2 T cells, this has led to the development of a new local delivery approach of concentrated Vγ9Vδ2 T cells in combination with ZOL in three-dimensional (3D) cell cultures using a localizable biomaterial into the tumour microenvironment akin to the tumour. The hypothesis was that the 3D T cell cultures may provide a viable option for delivery of continuous feed of Vγ9Vδ2 T cells and ZOL towards the efficient reduction of localized tumour. To this end, commercially available Matrigel (composed primarily of laminin and collagen) was chosen as a carrier material. Matrigel is a thermosensitive extracellular matrix basement membrane that undergoes a solution-to-gel transition as the temperature increases to 37°C [224]. This property allows for the injection of Vγ9Vδ2 T cells and ZOL in a liquid state and the subsequent gelation after equilibration to physiological temperature *in vivo*. In this setting, Vγ9Vδ2 T cells will be temporarily locked in the gel in large numbers readily available to act as they migrate out over time to the surrounding localized tissue.

In this *in vivo* proof-of-concept study, the ability of Vγ9Vδ2 T cells and ZOL harboured in Matrigel scaffolds in initiating specific antitumor immune responses against two different human cancers was tested. In particular, the efficacy of a single localized delivery of Vγ9Vδ2 T cells alone in solutions and in Matrigel scaffolds in the presence or absence of ZOL was examined. The results showed that at Day 7 following administration of Vγ9Vδ2 T cells, a single dose of Vγ9Vδ2 T cells alone in solution injected next to the MDA-MB231-TXSA tumours, established under the skin (subcutaneous model) had no effect on tumour growth.

When Matrigel containing Vγ9Vδ2 T cells was placed next to the tumour, there was a slight but insignificant decrease in tumour burden while the co-delivery of Vγ9Vδ2 T cells and ZOL in Matrigel reduced tumour growth further. However, as the cancer cells were not completely eliminated, the remaining cancer cells continued to grow past Day 7 and, hence, resulted in little curative effect. Similarly, in the mammary fad pat model, the results showed localized treatments with Matrigel carrying Vγ9Vδ2 T cells and ZOL produced growth retardation of the MDA-MB231-TXSA tumours but failed to eliminate them.

4.2 Results

4.2.1 Localized adoptive transfer of Vγ9Vδ2 T cells embedded in Matrigel together with ZOL reduced tumour burden but failed to eliminate cancer in a subcutaneous model of breast cancer

Once it was established *in vitro* that biomaterials may be used to enhance Vγ9Vδ2 T cell localized immunotherapy against breast cancer, a pilot study was performed to assess this treatment regimen in a pre-clinical model of breast cancer. In this subcutaneous model, immunodeficient NOD/SCID mice were inoculated with luciferase-tagged MDA-MB231-TXSA cancer cells (1 x 10^6 cells) into the flank (n=5/group). Bioluminescence imaging was obtained over time to monitor tumour burden. Treatments were commenced in the following week. Unlike previous sequential model where ZOL was given prior to Vγ9Vδ2 T cells, in this study, the tumours were not pre-treated with ZOL. Instead ZOL (25 µM) was added at the same time with *ex vivo* expanded Vγ9Vδ2 T cells (5 x 10^6 cells) into liquid Matrigel prior to administration into the animals. The rational for this strategy was that ZOL would be released from the scaffolds upon injection of the scaffolds next to the tumours and, hence, became available for uptake by the nearby cancer cells to potentiate Vγ9Vδ2 T cell anti-cancer efficacy. The *in vitro* studies described in 3.2.4 and 3.2.5 further supported this rationale. Animals

treated with a single dose of Vγ9Vδ2 T cells and ZOL injected in free form (i.e. without Matrigel) locally next to the tumours had a small inhibitory effect on tumour growth compared to untreated animals (Fig 4.1). Treatment with Vγ9Vδ2 T cell-loaded alone in Matrigel scaffolds produced a slight tumour growth reduction compared to those received Vγ9Vδ2 T cells and ZOL in free form. The animals that received Matrigel scaffolds carrying both Vγ9Vδ2 T cells and ZOL showed a superior reduction in tumour growth although this did not reach statistical significance due to the observed variability between tested groups. However, any growth inhibition effect that was observed from all treatment groups was only transient and tumour growth increased after Day 13, showing no difference in growth inhibition compared to untreated control after Day 13 (Fig 4.1).

4.2.2 Localized adoptive transfer of Vγ9Vδ2 T cells and ZOL embedded in Matrigel potentiated cytotoxic function of the Vγ9Vδ2 T cells but did not eliminate cancer in a mammary fat pad model of breast cancer

As sustained tumour inhibition was not observed in the pilot study (4.2.1), the mammary fat pad model of breast cancer with a lower tumour burden and higher Vγ9Vδ2 T cell density was conducted to re-assess the efficacy of the scaffolds in controlling tumour growth of a reduced tumour burden to mimic the presence of a small number of residual tumour cells following tumour resection. In this model, NOD/SCID mice were inoculated with 1 x 10^5 luciferase tagged MDA-MB231-TXSA breast cancer cells (one-tenth of the original inoculated cell density previous used in 4.2.1). Treatments were commenced in the following week when tumours reached 0.5 cm^2 (n=5/group). In this study, animals treated with a single dose of Vγ9Vδ2 T cells (1 x 10^7 cells) and ZOL in Matrigel effectively caused tumour growth retardation and prolong survival in mice but similar to what was observed previously in 4.2.1, this approach again failed to eliminate the tumours (Fig 4.2). Other treatments including local injection of Vγ9Vδ2 T cells and ZOL in free form, Matrigel-carrying either Vγ9Vδ2 T cells

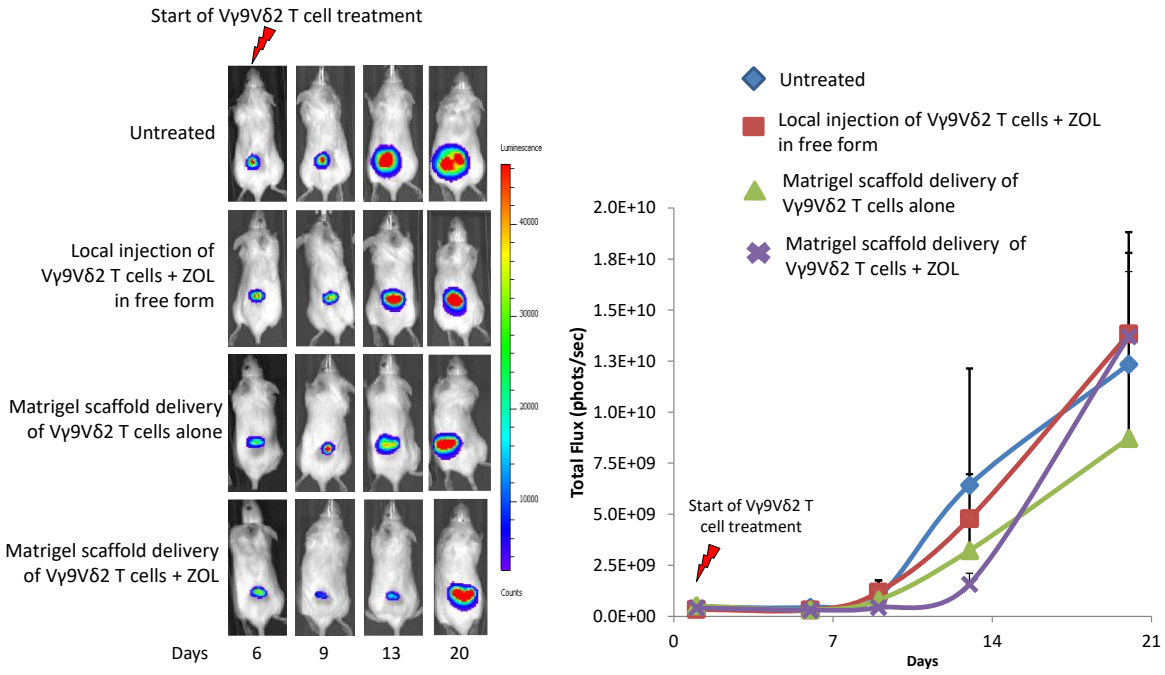

Figure 4.1 Matrigel embedded Vγ9Vδ2 T cells in the presence of ZOL enhance the anti-tumour efficacy of Vγ9Vδ2 T cells in a subcutaneous model of breast cancer.

Luciferase expressing MDA-MB231-TXSA breast cancer cells (1 x 10^6 cells) were injected subcutaneously to the flank of 5-week-old female NOD/SCID mice. Tumours grew for 7 days, then animals were assigned into three treatment groups (n=5). Animals remained untreated or were given both Vγ9Vδ2 T cells (5 x 10^6 cells) and ZOL (0.68 mg) in free form or in Matrigel scaffolds delivered locally next to the tumours. The remaining animals were given Vγ9Vδ2 T cells alone (same doses as with the previous groups) in Matrigel scaffolds. Whole body bioluminescence images were acquired on the IVIS Spectrum *in vivo* imaging system and bioluminescence signal was measured as Total Radiant Efficiency [p/s]/[μW/cm^2]. Graphs and representative images (showing one animal per group) are shown. Lines represent mean bioluminescence and bars indicate ± SEM.

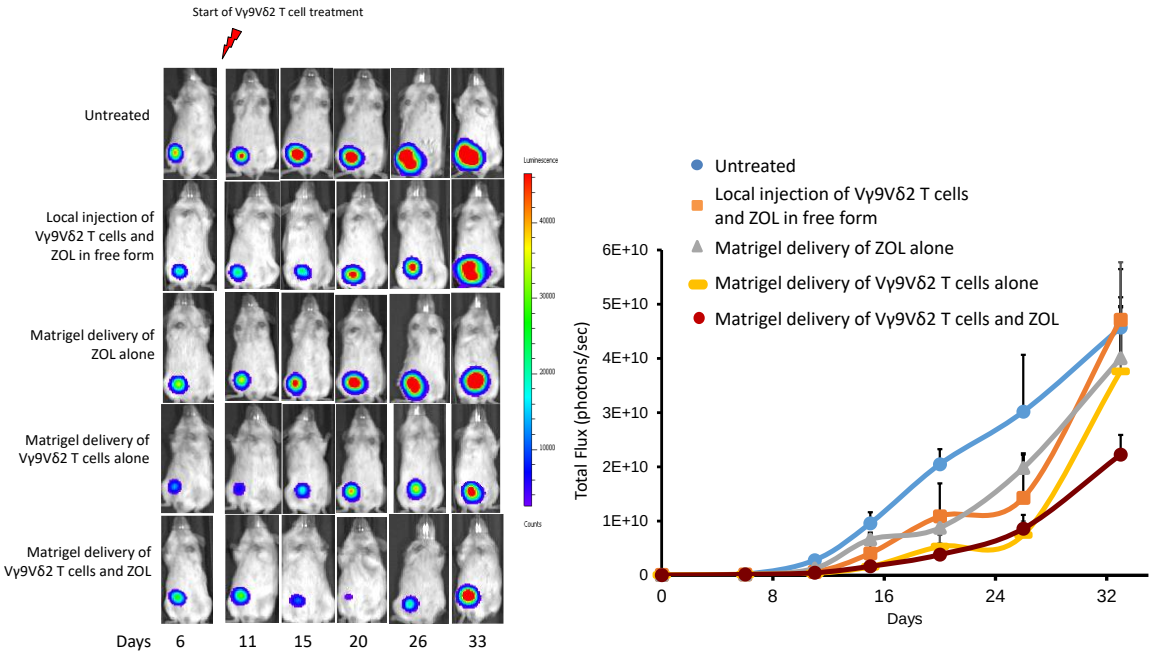

Figure 4.2 Matrigel embedded Vγ9Vδ2 T cells and ZOL boost the anti-tumour efficacy of Vγ9Vδ2 T cells against a smaller number of tumour cells (representing residual tumours) in a mammary fat pad model of breast cancer.

Luciferase expressing MDA-MB231-TXSA breast cancer cells (1 x 10^5 cells; a tenth of the original inoculated cell density previous used in 4.2.1) were injected into the mammary fat pad of 5-week-old female NOD/SCID mice. After 7 days, animals were assigned into four treatment groups (n=5). Animals remained untreated or were given a combination of Vγ9Vδ2 T cells (10^7 cells) and ZOL (0.68 mg) in free form or in Matrigel delivered locally next to the tumours. The remaining animals were given either ZOL or Vγ9Vδ2 T cells alone embedded in Matrigel. Whole body bioluminescence images were acquired on the IVIS Spectrum *in vivo* imaging system and bioluminescence signal was measured as Total Radiant Efficiency [p/s]/[μW/cm^2]. Graphs and representative images (showing one animal per group) are shown. Lines represent mean bioluminescence and bars indicate ±SEM.

and ZOL in free form, Matrigel-carrying either Vγ9Vδ2 T cells or ZOL alone slightly reduced tumour growth at first but were not able to sustain the inhibition effect over time. Collectively, this data indicates limited and insignificant antitumour responses that cannot be sustained leading to tumour recurrence.

Statistical analysis of the data revealed the median survival for untreated animals and those receiving Matrigel containing ZOL alone was 33 days (Fig 4.3). While animals that received a combination of Vγ9Vδ2 T cells and ZOL in solution survived for 39 days, and those that received this synergistic combination in Matrigel survived the longest (46 days) of all groups tested.

In the qualitative assessment of Vγ9Vδ2 T cell infiltration, the immunohistochemical analysis showed the presence of only a small number of Vγ9Vδ2 T cell infiltration in the tumours of animals received a combination of Vγ9Vδ2 T cells and ZOL embedded into Matrigel (Fig 4.4). However, the T cell infiltration was not found at all from any of the tumour samples from other treatment groups. Likewise, TUNEL-positive cancer cells, indicating apoptotic cells were only barely detected from those treated Vγ9Vδ2 T cells and ZOL embedded Matrigel scaffolds (Fig 4.5) but undetectable at all from any other groups.

4.2.3 ZOL is not internalised by cancer cells *in vivo* following local administration in ZOL-embedded Matrigel

Despite showing promising effects of localized immunotherapy of Vγ9Vδ2 T cells in combination with ZOL against breast cancer *in vitro*, this treatment strategy was limited in both subcutaneous and mammary fat pad models of breast cancer. To investigate the possible reasons, *in vivo* localization, and cellular uptake of ZOL following local administration was examined. For this purpose, Alexa Flour® 647-labelled ZOL (AF647-ZOL, Fig 4.6) was purchased from Biovinc LLC (CA, USA). This drug-dye conjugate is not able retain the

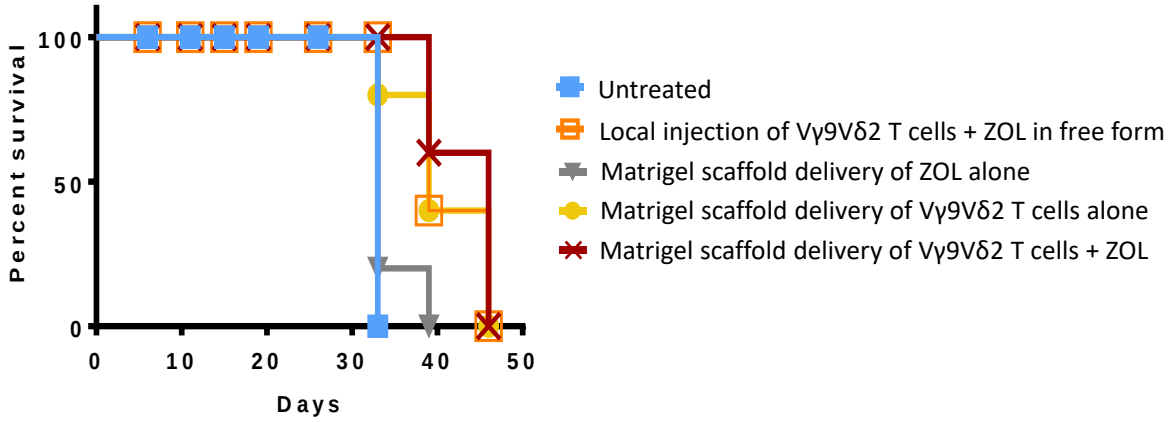

Figure 4.3 Kaplan-Meier survival curves of tumour-bearing animals following a single treatment with local injection of Vγ9Vδ2 T cells and ZOL in free form, Matrigel delivery of Vγ9Vδ2 T cells or ZOL alone, or Matrigel carrying both Vγ9Vδ2 T cells and ZOL.

In a mammary fat pad model of breast cancer in NOD/SCID mice, Matrigel carrying both Vγ9Vδ2 T cells and ZOL prolonged survival time compared with other treatment groups (n=5 per group, median survival = 46 days vs. 33 days from untreated animals and those received Matrigel carrying ZOL alone, and 39 days from those received Vγ9Vδ2 T cells and ZOL in free form).

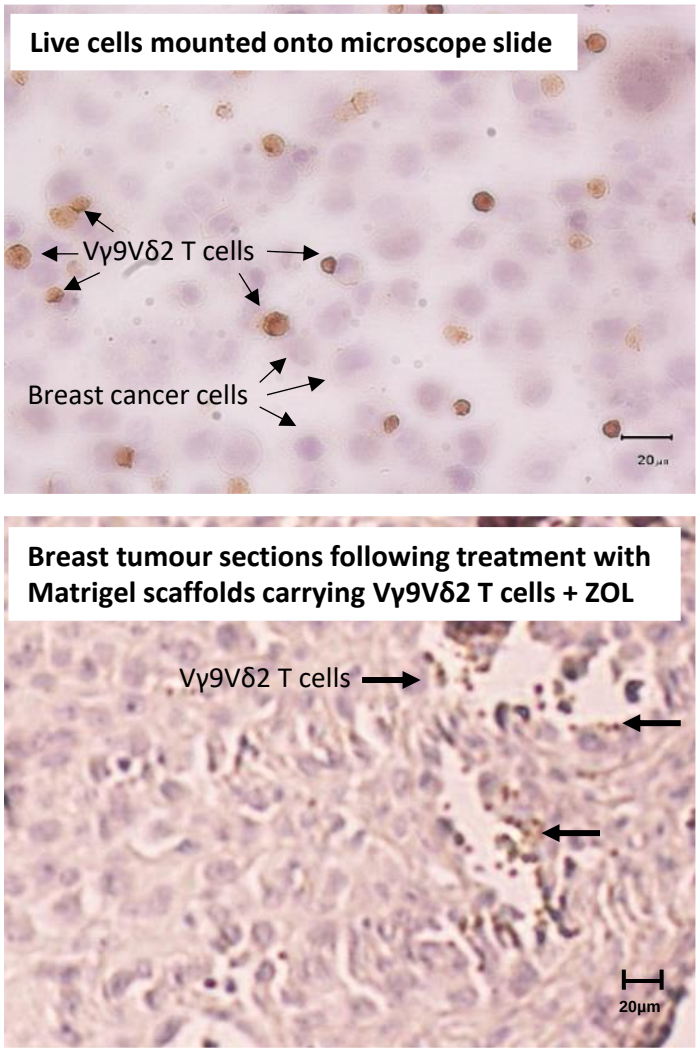

Figure 4.4 Vγ9Vδ2 T cells sparingly infiltrate into breast tumours *in vivo* following localized treatment with Matrigel carrying Vγ9Vδ2 T cells and ZOL. Immunohistochemical staining of anti-TCR monoclonal antibody H-41 [247] (Santa Cruz, USA) on live cells mounted onto microscope slide (obj. 20x, top image) and breast tumours following localized treatment of Matrigel carrying Vγ9Vδ2 T cells and ZOL (obj. 10x, bottom image).

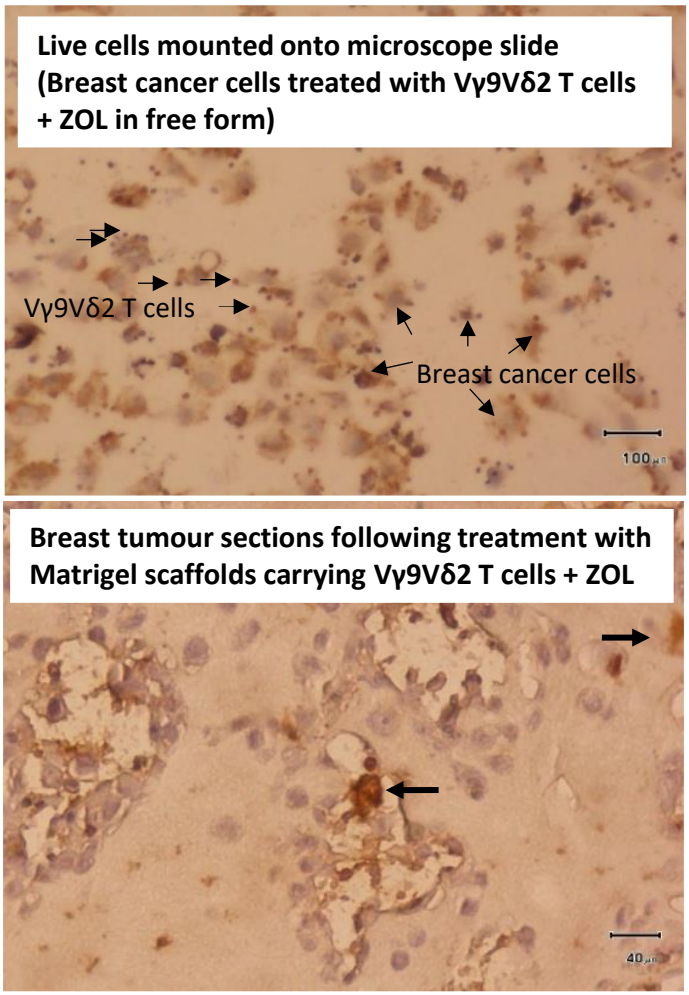

Figure 4.5 Detection of TUNEL-positive cells in tumour tissues via TUNEL staining

Apoptotic features visualised by TUNEL staining method (that is the cancer cells with dark brown edges) easily recognised on live cells mounted onto microscope slide (obj. 10x, top image) but barely detected from breast tumour samples following localized treatment of Matrigel carrying Vγ9Vδ2 T cells and ZOL (obj. 10x, bottom image).

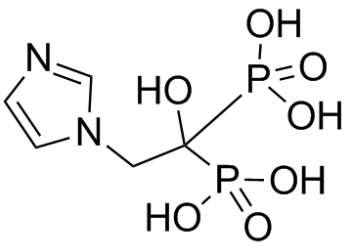

ZOL

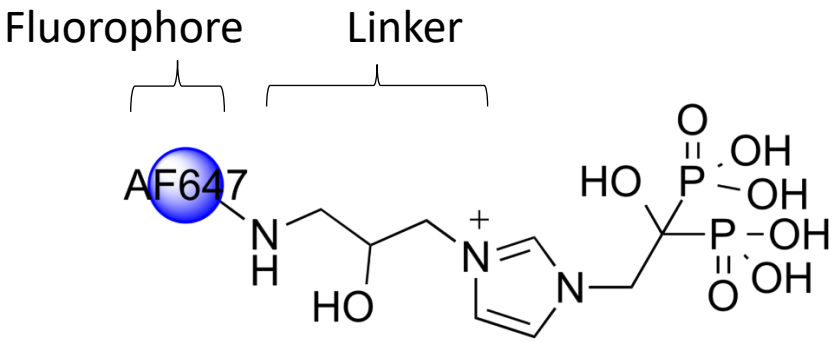

Alexa Flour® 647-labelled ZOL

Figure 4.6 Chemical structure of Zoledronate (ZOL) vs. Alexa Flour® 647-labelled Zoledronate (AF647-ZOL)

The P-C-P backbone of ZOL mimics the P-O-P backbone of naturally occurring pyrophosphate. A simple linker is introduced to link heterocyclic ZOL with AF647 dye (Image adapted from www.biovinc.com/af647-zol-1-2/)

functional ability to inhibit protein prenylation and, hence is considered pharmacologically inactive [248] and would only be used for imaging purposes. AF647-ZOL uptake was first optimized *in vitro*. Results showed efficient cellular uptake with greater than 96% of MDA-MB231-TXSA cells have taken up ZOL following 30 min incubation *in vitro* (Fig 4.7).

For *in vivo* ZOL localization and uptake studies, mice were inoculated with luciferase-tagged MDA-MB231-TXSA (1 x 10^6 cells) injected into the mammary fat pad. Once the tumours were established as determined by an increase in bioluminescence signal, AF647-ZOL (25 µM) was given locally either through Matrigel scaffolds or intratumoural injections (in free form). At 72 h following local administration of AF647-ZOL, live fluorescent images were acquired on the IVIS Spectrum *in vivo* Imaging System showing ZOL deposition in the whole MDA-MB231-TXSA tumours (Fig 4.8). The fluorescent signal was also detected at many distant calcified sites, including the femur, forearms, skull and jawbone (Fig 4.8), corresponding to the characteristic and preferential sites of bisphosphonate distribution [249]. Multi-parameter flow cytometric analysis was then performed on enzymatically digested, single-cell suspensions of the extracted tumours. Results showed that while up to a third or more of each MDA-MB231-TXSA tumour sample contained cells that expressed GFP (Fig 4.9, top row images, Q1), only a negligible number of these GPF positive (tumour) cells contained AF647-ZOL (up to approx. 4% of total cells, Fig 4.8, top row images, Q2). However, there was a notable number of GFP negative (non-tumour) cells that contained AF647-ZOL (up to approx. 10%, Fig 4.8, top row images, Q3), suggesting different cell type(s) within the tumour mass other than the cancer cells were more efficient at internalizing fluorescent ZOL. In addition, when spiked into a treated sample of tumour single cell suspensions and incubated for 30 min, AF647-ZOL was taken up by both GFP positive and negative cells in large proportions, indicated by a major shift in mean fluorescence intensity of the entire cell population (Fig 4.8, second top row image, Q2 and Q3). This suggests differential uptake of

ZOL *in vivo* by non-tumour cells whereas *ex vivo* ZOL was equally taken up by tumour and non-tumour cells.

In literature, it was shown previously that U-87 MG human glioblastoma cells are highly sensitive to the effects of ZOL [105]. Therefore, the above experiment was repeated with GFP/luciferase-labelled U-87 MG cells, to better assess cellular uptake of ZOL *in vivo*. The addition to this experiment was the use of Pacific Blue-labelled F4/80 (macrophage, myeloid lineage) antibody on single cell suspensions prior to flow cytometry analysis. Therefore, the detection of double-positive (AF647+ / F4/80+) cells indicate the cellular uptake of AF647-ZOL by mouse macrophages. Results showed that infrared images of tumour explants showed AF647-ZOL was detectable from the whole U-87 MG tumours (Fig 4.7). Tumours established from U-87 MG cells generated a largely heterogeneous mass of cells, of which there was a distinct GFP positive population of up to 7% of total cells (Fig 4.8, third row images, Q1). Of the mostly GFP negative cells, a large proportion were positive for F4/80 Pacific Blue (Fig 4.8, fourth row images, Q9), indicating that much of the tumour amounted to cells of macrophage lineage. Importantly, a significant amount of these macrophage-like cells contained AF647-ZOL, indicating efficient uptake of ZOL into these cells (Fig 4.8, fourth row images, Q10 approx. 36-56%). Similar to ZOL uptake in MDA-MB231-TXSA cells, there was a minor uptake of AF647-ZOL by U-87 MG cells, as indicated by the negligible number of double-positive (GFP+/AF647+) cells (Fig 4.8, third row images, Q2). In addition, when pharmacological active ZOL was used instead of fluorescent ZOL, Western blot analysis did not detect the unprenylated form of Rap1A in U-87 MG tumour extracts from ZOL-treated mice, thereby showing that it did not inhibit FPPS *in vivo*. Collectively, the data identified macrophage-like cells as the cell type that were more much efficient than the cancer cells at internalising ZOL following localized administration at the tumour sites.

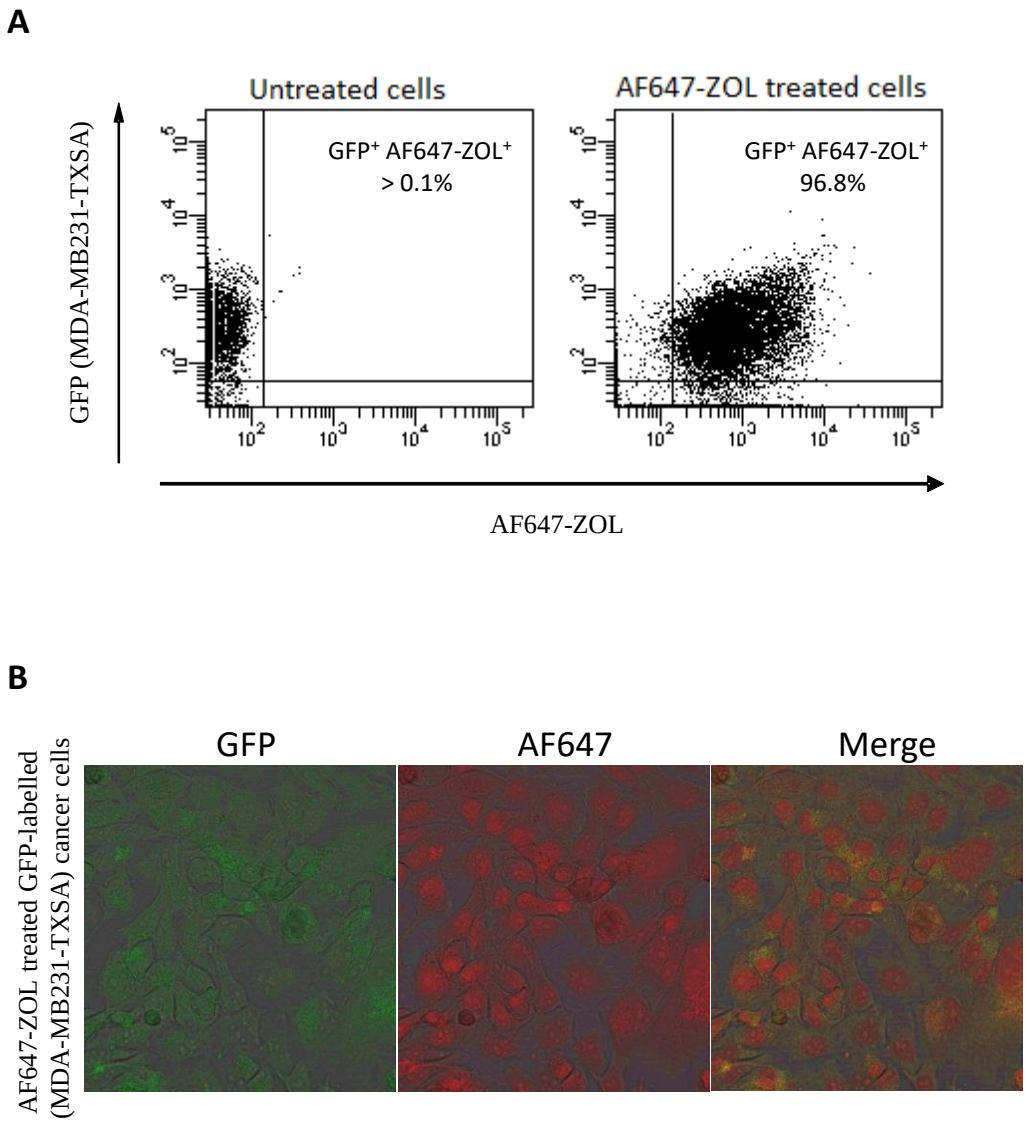

Figure 4.7 Efficient ZOL uptake in breast cancer MDA-MB231-TXSA cells *in vitro*

A. A dot plot showing flow cytometric analysis of GFP-labelled MDA-MB231-TXSA cells incubated with 25 µM ZOL for 30 min *in vitro*. **B.** Fluorescence microscopy confirmed the efficient uptake of AF647-ZOL (red) in MDA-MB231-TXSA cells (green) following incubation

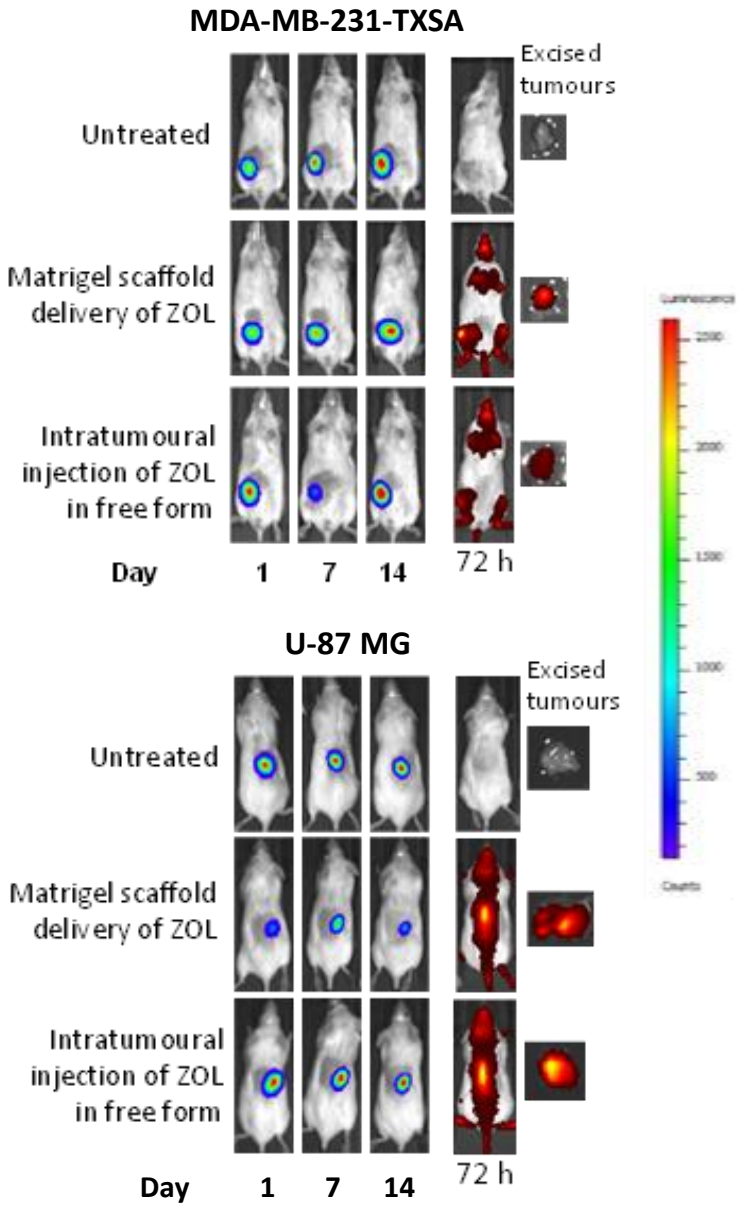
MDA-MB-231-TXSA
Excised tumours
Untreated
Matrigel scaffold delivery of ZOL
Intratumoural injection of ZOL in free form
Day
1
7
14
72 h
U-87 MG
Excised tumours
Untreated
Matrigel scaffold delivery of ZOL
Intratumoural injection of ZOL in free form
Day
1
7
14
72 h

Figure 4.8 Fluorescently labelled ZOL (AF647-ZOL, represented in dark red) localized to the bone and breast cancer lesions *in vivo*.

Following the limited efficacy of localized immunotherapy of Vγ9Vδ2 T cells and ZOL in mouse models of breast cancer, ZOL uptake in breast and brain cancer following localized delivery via Matrigel was investigated in animal models. 8-wk-old female NOD/SCID mice were injected with Luciferase/GFP-tagged MDA-MB-231-TXSA or U-87 MG cells into the mammary fat pad and flank of mice, respectively. Tumours were allowed to establish for 2 weeks. The mice were then randomised into three groups (n=5). They remained untreated or were given 25μM AF647-ZOL in Matrigel scaffolds delivered next to the tumour. The rest was given 25 μM AF647-ZOL ZOL in free form injected intratumorally. While five mice were used herein the whole experiment, three mice were used for bioluminescence/fluorescence imaging while the other two were used for tumour excision and FACS analysis. Whole body bioluminescence images were acquired on the IVIS Spectrum *in vivo* imaging system and bioluminescence signal was measured as Total Radiant Efficiency [p/s]/[μW/cm^2]. Representative images showing one animal per group are shown.

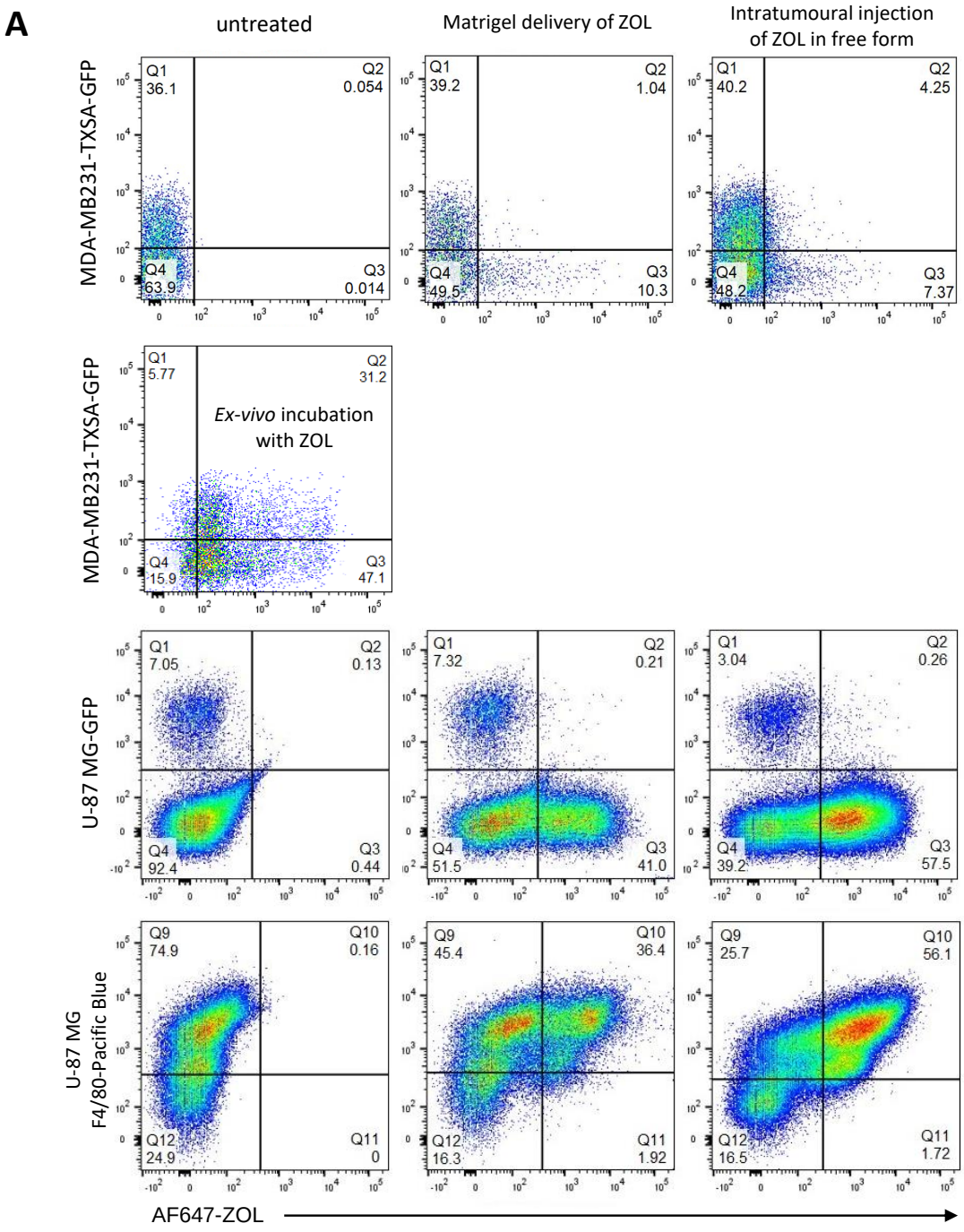
A
untreated
Matrigel delivery of ZOL
Intratumoural injection of ZOL in free form
MDA-MB231-TXSA-GFP
Q1 36.1
Q2 0.054
Q4 63.9
Q3 0.014
Q1 39.2
Q2 1.04
Q4 49.5
Q3 10.3
Q1 40.2
Q2 4.25
Q4 48.2
Q3 7.37
MDA-MB231-TXSA-GFP
Q1 5.77
Q2 31.2
Ex-vivo incubation with ZOL
Q4 15.9
Q3 47.1
U-87 MG-GFP
Q1 7.05
Q2 0.13
Q4 92.4
Q3 0.44
Q1 7.32
Q2 0.21
Q4 51.5
Q3 41.0
Q1 3.04
Q2 0.26
Q4 39.2
Q3 57.5
U-87 MG F4/80-Pacific Blue
Q9 74.9
Q10 0.16
Q12 24.9
Q11 0
Q9 45.4
Q10 36.4
Q12 16.3
Q11 1.92
Q9 25.7
Q10 56.1
Q12 16.5
Q11 1.72
AF647-ZOL
B
U-87 MG Tumour
ctrl
Active ZOL liq
Active ZOL in gel
+
Total RAP-1
uRAP-1A

Figure 4.9 Tumour associated macrophages, not cancer cells, recognise and internalise AF647-ZOL *in vivo*.

A. Flow cytometric analysis with plots showing GFP vs. AF647-ZOL or F4/80 vs. AF647-ZOL gated on viable cells from single cell suspensions from the tumour tissues of animals received local administration of AF647-ZOL. B. Western blot analysis showing inhibition of prenylation was not detectable following local administration of pharmacological active ZOL.

4.3 Conclusion

The combining field where immunotherapy meets biomaterials is an ever-growing field of research with the promise to overcome current clinical limitations that restrict cell-based cancer immunotherapy. Combined treatment modality is the sequential or simultaneous use of different treatment modality for cancer. Patients with locally or regionally advanced tumour, that cannot be cured with surgery and radiotherapy will benefit from the combined immunotherapy modality. With increased locoregional control of the tumours primary goal, the subsequential local administration of biomaterial scaffolds carrying cytotoxic Vγ9Vδ2 T cells and ZOL following surgery may lead to an additive or synergistic interaction.

This Chapter in this thesis explored the potential of biomaterial scaffolds as a 3D culture system for localized delivery of *ex vivo* expanded Vγ9Vδ2 T cells and ZOL for solid tumours *in vivo*. Previously in Chapter 3, it has been demonstrated that Matrigel can support survival and release of Vγ9Vδ2 T cells and when used in combination with ZOL in a localized setting can effectively eliminate cancer cell target. Unfortunately, the results in this current Chapter demonstrated limited efficacy of the localized treatment strategy *in vivo*, showing only moderate tumour growth suppression in animals treated with Vγ9Vδ2 T cells and ZOL embedded in Matrigel. All animals eventually developed advanced disease. Future investigations revealed ZOL was failing to be taken up by the breast and brain tumour cells *in vivo* following local delivery in Matrigel scaffolds at the tumour site. Instead cells of macrophage lineage within the tumour mass were much more efficient than the tumour cells at internalizing ZOL, in line with previous report from Junankar *et al* [250], whose unequivocal results showed ZOL targeted tumour associated macrophages (TAMs) but not 4T1 mouse mammary tumours *in vivo*.

Cellular uptake of small molecules like NBPs including ZOL is a complex process and different cell types use different routes of uptake. Cells of myeloid lineage such as peripheral blood, bone marrow monocytes, peritoneal macrophages, osteoclasts and TAMs, share a selective ability to internalise NBPs [251], which is most likely due to their capacity to phagocytose and pinocytose calcium containing complexes [107, 252, 253]. For example, studies by Thompson and colleagues have demonstrated that NBPs alendronate was taken up into osteoclasts and J774 macrophages by fluid-phase endocytosis [252] but diffused much poorer into other cell types including MCF-7 breast cancer cells *in vivo*, presumably due to their poor endocytic activity [107]. A number of recent studies showed skeleton and peritoneal macrophages took up ZOL through their high phagocytic activity; hence, the well-known fact that ZOL has the specificity to chelate calcium is highly relevant [254]. A study by Zlatev *et al* in cancer cells, on the other hand, revealed breast cancer MCF7 and T47D cells internalized ZOL *in vitro* mostly by dynamin dependent endocytosis, which requires longer time to process and hence could partly explain the fewer accumulation of ZOL in cancer cells in comparison to TAMs [255].

Several nanotechnology strategies have been explored in order to improve bioavailability of various NBPs, such as ZOL, pamidronate (PAM) and alendronate (ALD), in extraskeletal tissues. One of those strategies is to deliver them as packed in nanoparticles [256], using in particular liposomes to exploit their ability to accumulate in the reticulo-endothelial system [257]. Indeed, ZOL-encapsulating PEGylated liposomes (LIPO-ZOL) and ZOL containing self-assembly PEGylated nanoparticles (NPs) have been designed and tested [258-260]. In comparison with standard ZOL, both nanotechnology products increased anti-cancer activity against PC3 prostate tumour xenografts when given systemically. Although a direct drug distribution study was not carried out in these studies, the investigators attributed the improved cytotoxicity to higher drug penetration into the cancer cells, which consequently

enhanced the direct anticancer effects of ZOL. Indeed, NPs comprises of calcium/phosphate nanoparticle and cationic lipids, which have been commonly used to promote cellular uptake of negatively charged molecules [261]. The complexes between ZOL and NPs could potentially be taken up through endocytosis in a similar manner of DNA containing lipoplexes, leading to improved cellular uptake of ZOL.

To sum up, in this current Chapter, the *in vitro* results have clearly indicated that ZOL can be taken up into the cancer cells and efficiently sensitize them to cytolysis mediated by Vγ9Vδ2 T cells. *In vivo*, however, the antitumour effect of this localized immunotherapeutic strategy was much less effective and was most likely due to the failure of cancer cells to internalize ZOL to sufficient amount to initiate Vγ9Vδ2 T cell killing. The use of nanotechnology may open up a new therapeutic scenario for ZOL to be able to specifically accumulate in the sites where its ability to inhibit the mevalonate pathway is required.

Chapter 5

Zoledronate enhances Vγ9Vδ2 T cell antitumour responses against human glioblastoma

5.1 Chapter introduction

There is growing interest in ACT using various effector T cells for the treatment of malignant brain tumours, particularly glioblastoma multiforme (GBM). GBM is the most common and most aggressive primary brain tumour in humans (WHO grad IV, [262]), accounting for 12-15% of all brain tumours [263]. Despite advanced multimodality treatments including surgery, radiation and chemotherapy, patients with GBM have a very poor prognosis with a median survival of 12-15 months following diagnosis [264]. This dismal prognosis is attributed to the deep invasive growth nature of GBM, limited surgical efficiency and high degree of tumour heterogeneity. In addition, the unique environment of the central nervous system such as the presence of the blood brain barrier (BBB) also represents significant challenges in treating this disease. The BBB forms a physiological and pharmacological barrier that hinders the influx of molecules including NBPs such as ZOL [265] from the bloodstream into the brain. Likewise, it also prevents the entry of tumour-killing cells into the tumour bed [266].

Hence localized delivery of ZOL into the site of brain tumours is an alternative approach to overcoming the BBB. Not only does this approach offer the advantage of local exposure of high concentrations of drugs while avoiding systemic toxicities, it seems particularly appropriate to treat residue disease following tumour resection since relapses often take place within the vicinity of the original site of resection [267]. However, previous efforts to administer drugs through catheter systems were not successful due to mechanical failure of the devices, obstruction by tissue debris/clots, or infection [268]. Another variation to local delivery approach is to use sustained-release polymers. In fact, Gliadel® (chemotherapy carmustine-loaded polymers) was successfully developed as a post-operative implant, resulting in marginal increase in survival and local control in newly diagnosed GBM patients [269].

With Gliadel® as a model, many investigators are focusing on combinations of localized delivery approaches of chemotherapy and/or immunotherapy. In cellular immunotherapies, various effector T cells used for GBM have been developed ranging from lymphokine-activated killer (LAK) cells with nonspecific cytotoxicity to more tumour-specific genetically modified cytotoxic T lymphocytes (CTLs) over time. Clinical trials have then been conducted for both systemic and intracranial infusion of *ex vivo* expanded T cells, extracted from the patients' tumour, draining lymph nodes, or allogenic (HLA-mismatched) T cells from healthy donors [270] but have had limited success so far.

Among the attractive immune effectors, human Vγ9Vδ2 T cells have been shown to have spontaneous cytotoxic effects on human GBM cell lines [142, 271, 272] and primary GBM cells [272-274] both *in vitro* and *in vivo*. Unlike their adaptive αβ T cell counterpart, Vγ9Vδ2 T cells can detect, and immediately respond to, a wide variety of MHC-like stressed-induce self-antigens, many of which are found on GBM cells [275]. Indeed, due to the high heterogeneity and low immunogenicity of GBM, common adaptive effector T cells are difficult to detect and kill them. On the other hand, the Vγ9Vδ2 T cells rely on their unique γδ TCRs and do not require recognition of the MHC molecules, and therefore can effectively detect some hidden antigens and mediate a potent response against cancer cells [276].

As mentioned in previous chapters, although most antigens recognised by Vγ9Vδ2 T cells are still unknown, the most noticeable ligands are phosphoantigens (PAgs), specifically isopentenyl pyrophosphate (IPP), which could be generated endogenously as intermediates of the mammalian mevalonate pathway of cholesterol synthesis. Increase in intracellular accumulation of PAgs can occur following cell distress induced by transformation or infections. In addition, nitrogen-containing aminobisphosphonates (NBPs) including zoledronate (ZOL) are pharmacologic inhibitors of the mevalonate pathway. NBPs work by inhibiting farnesyl pyrophosphate synthase (FPPS), which is downstream from 3-hydroxy-3-

methylglutaryl coenzyme A reductase (HMG-CoAR), leading to increased IPP levels within cells with deregulated metabolism such as tumour cells including GBM [277]. IPP then activates Vγ9Vδ2 T cells. Hence, NBPs has an indirect antitumour effect by sensitizing cancer cells toward Vγ9Vδ2 T cell-mediated cytotoxicity. Interestingly, NBPs also reportedly exhibit direct antitumour effects, caused by the inhibition of prenylation of small membrane-binding proteins (GTPases) in the downstream signalling pathway via FPPS blocking [278].

To investigate the possibility of using Vγ9Vδ2 T cell-based localized immunotherapy for GBM, this Chapter explores cytotoxic effects of Vγ9Vδ2 T cells in combination with ZOL on three GBM cell lines (U-87 MG, T98G and U-251 MG) and directly compares the effects of ZOL alone on these three GBM cells and breast cancer MDA-MB-231-TXSA cells. In addition, to elucidate possible reasons behind differential sensitivity to ZOL treatment, cellular uptake of fluorescently labelled ZOL and prenylation status as determined by Western blotting analysis for the expression of unprenylated RAP1A, FPPS and HMG-CoA were conducted.

5.2 Results

5.2.1 Low ZOL treatment of glioblastoma U-87 MG cells induces dramatic morphological changes when compared to MDA-MB-231 breast cancer cells.

In this work, highly aggressive cell lines representing cancers of the nervous system (glioblastoma U-87 MG) and breast (MDA-MB231-TXSA) were selected for analysis. Treatment with 25 µM ZOL was added to the cell culture for a period of 24 h. Images were then taken using phase contrast microscopy at the end of the incubation period. Phase contrast images revealed that ZOL-treated U-87 MG cells displayed a round shape while untreated cells displayed a normal elongated, neurite-like extension shape (Fig 5.1). ZOL concentrations above 1 µM still caused morphological changes in U-87 MG cells; however, at or below 1 µM,

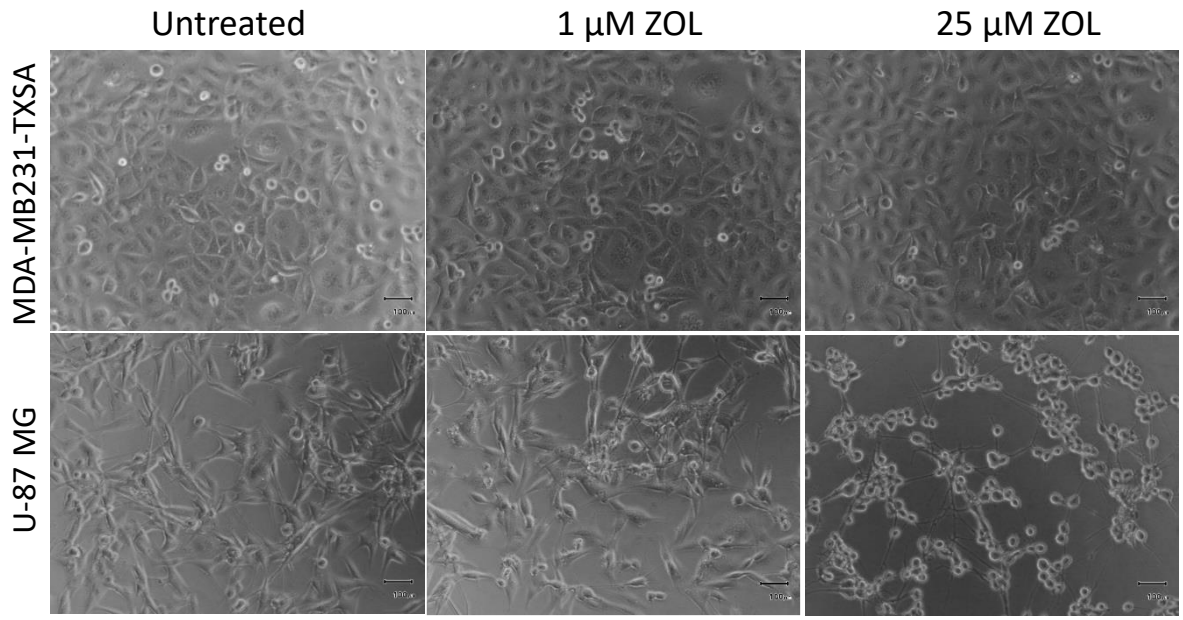

Fig 5.1 U-87 MG glioblastoma cells, but not breast cancer MDA-MB231-TXSA cells, display distinct morphological changes in response to ZOL treatment *in vitro*.

U-87 MG glioblastoma cells (1.2 x 10^4 cells/well) or MDA-MB231-TXSA breast cancer cells (1 x 10^4 cells/well) were seeded in 96-well flat-bottom plates. Cells were untreated or treated with 1-25 µM ZOL and cultures were maintained for 24 h. Representative bright field images of U-87 MG cells under treatment conditions showed changes in cell morphology following treatment of ZOL at low concentration (< 1 µM) while MDA-MB231-TXSA cells showed no changes at 25 µM.

ZOL did not cause any changes. On the other hand, cell morphology of MDA-MB231-TXSA cells did not change following exposure to as much as 25 µM ZOL (Fig 5.1). This result suggest that the glioblastoma cells are highly sensitive to ZOL when compared to the breast cancer cells.

To understand this phenomenon further, two additional glioblastoma cell lines (T98G and U-251 MG) were added for further analysis on cell morphological changes following ZOL treatment. Surprisingly, the results reveal that 25 µM ZOL did not appear to change the cell morphology of T98G and U-251 MG cell lines after 24 h of exposure suggesting that this effect was specific for U87 MG cells.

5.2.2 Differential growth inhibitory effects of ZOL in glioblastoma and breast cancer cells following 72 h exposure.

The effects of ZOL on the three glioblastoma U-87 MG, T98 G, U-251 MG cell lines and breast cancer MDA-MB231-TXSA cells were investigated *in vitro* using the alamar blue assay. Treatments with ZOL (0.1-40 µM for glioblastoma cells and 2-500 µM for breast cancer cells) produced a dose-dependent reduction of cancer cell growth following 72 h exposure (Fig 5.2). The IC_{50} for the glioblastoma cell lines was in the range of 3-4 µM whereas for breast cancer cells, the IC_{50} was 10-fold higher at approximately 30 µM.

5.2.3 U-87 MG is particularly vulnerable to ZOL enhanced Vγ9Vδ2 T cell-mediated cytotoxicity.

To test the indirect anticancer effects of ZOL when used in combination with *ex vivo* expanded Vγ9Vδ2 T cells on GBM cells, the three GBM cells (U-87 MG, T98 G and U-251 MG) and breast cancer cells (MDA-MB231-TXSA) were pre-treated at two concentrations of ZOL (1 or 25 µM) for 24 h before being treated with Vγ9Vδ2 T cells at the E:T ratio of 5:1. Cell death assays as determined by LDH release showed that incubation with 25 µM ZOL

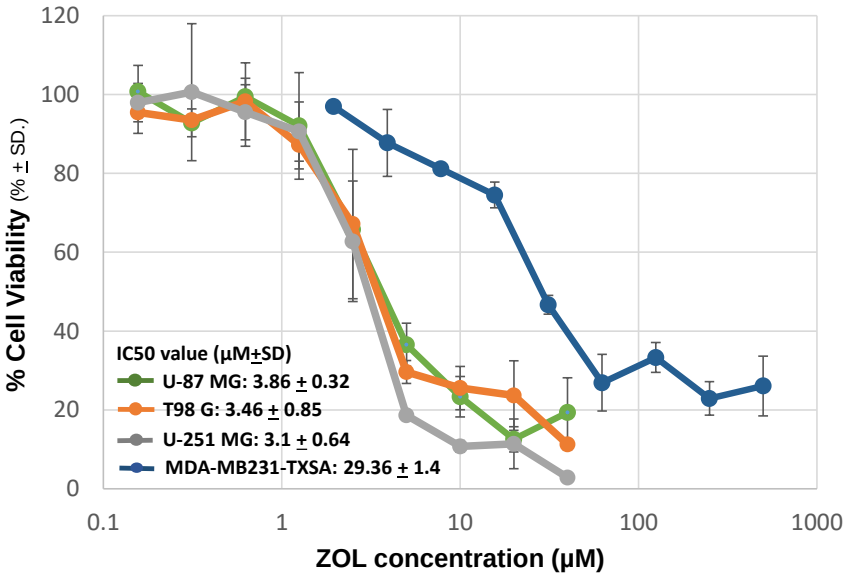

Figure 5.2 ZOL directly inhibits the growth of human glioblastoma and breast cancer cells over 72 h *in vitro*.

The cell lines U-87 MG (1.2 x 10^4 cells/well), T98 G, U-251 MG and MDA-MB231-TXSA (1 x 10^4 cells/well) were seeded in 96-well plates and incubated for 24 h. Then the cultured media was replaced with medium containing various concentrations of ZOL (0.1-40 µM for glioblastoma cells and 2-500 µM for breast cancer cells). Following 72 h of exposure, cancer cell viability was determined by the alamar blue assay. 100% was assigned to untreated control cells. Each point was the average of three replicate experiments (n=9) ± SD. IC50 for each cell line was calculated by the equation of logarithmic regression trendline.

resulted in a small but significant decrease in cell survival of U-87 MG and T98 G cells at 24 h post-incubation with ZOL alone (Fig 5.3A). Consistent with no morphological alterations at 25 µM ZOL, the survival of MDA-MB231-TXSA cells was not affected (Fig 5.3A). However, except for T98 G cells, the cytotoxic effect of ZOL was greatly enhanced in combination with Vγ9Vδ2 T cells (Fig 5.3A). In combination of ZOL and Vγ9Vδ2 T cells, U-87 MG cells were most sensitive where the combined treatment using 1 µM ZOL and Vγ9Vδ2 T cells decreased cancer cell survival down to around 10% (Fig 5.3B). U-251 MG cells were moderately susceptible where 25 µM ZOL caused about 50% cell death while no killing effects were observed in T98 G cells at all (Fig 5.3B). On the other hand, the cell survival of MDA-MB231-TXSA cells dropped to around 20% following treatment with 25 µM ZOL and Vγ9Vδ2 T cells (Fig 5.3B).

5.2.4 Higher cellular uptake of ZOL in glioblastoma cells in comparison to breast cancer cells *in vitro*.

Drug cellular uptake plays an important role in drug bioactivity in target cells. Internalisation and accumulation of drugs into cancer cells is, therefore, crucial in order to elicit their therapeutic effect against tumours. The cellular uptake of fluorescently labelled AF647-ZOL (fZOL) was examined in U-87 MG, T98G, U-251 MG and MDA-MB231-TXSA cells after 4 h of incubation at 25 µM at 37°C. As shown in Fig 5.4, the fluorescence intensity showed that ZOL was internalised by all four cancer cell lines as indicated by the shift in fluorescence intensity (using the flow cytometer's APC channel) following exposure to fZOL. Next, the extent of cellular uptake in different cell lines was quantitatively determined. Higher fluorescence intensity, which indicates higher amount of drug uptake, was found in the following order: U-87 MG > T98G > U-251 MG > MDA-MB231-TXSA. Overall, ZOL was more efficiently taken up by all glioblastoma cell lines than the breast cancer cell line, which may relate to different rates of endocytosis in different cell lines as cellular uptake of NBP

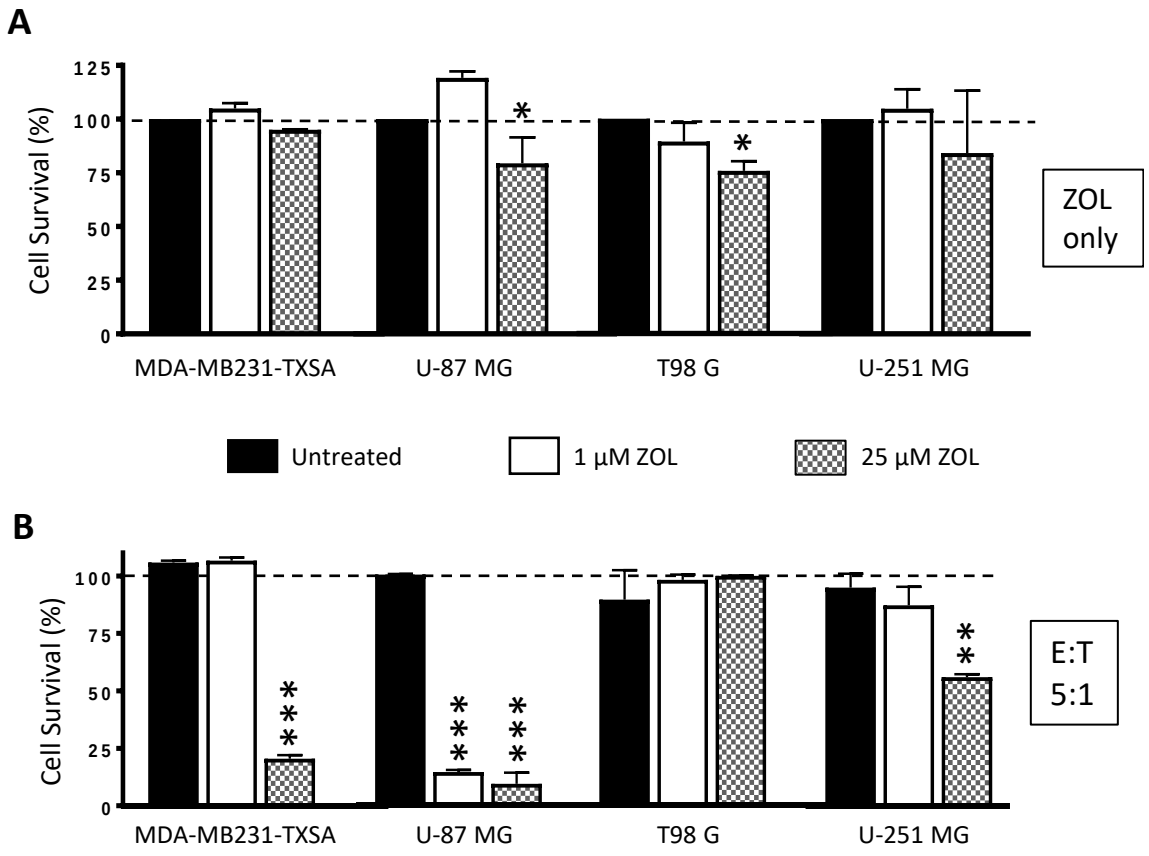

Figure 5.3 ZOL strongly sensitises glioblastoma U-87 MG cells to killing by Vγ9Vδ2 T cells

MDA-MB231-TXSA and the three glioblastoma cell lines (U-87 MG, T98 G and U-251 MG) were left untreated or pre-treated with 1 and 25 µM ZOL overnight at 37°C, then co-cultured with *ex vivo* expanded Vγ9Vδ2 T cells at the E:T ratio of 5:1 for 8 h at 37°C. Cytotoxicity was measured using the luciferase assay and expressed as percentage cytotoxicity compared to untreated cells (**$p < 0.005$, ***$p < 0.001$, two-tailed student's t-test, data represent mean±SEM, n=6)

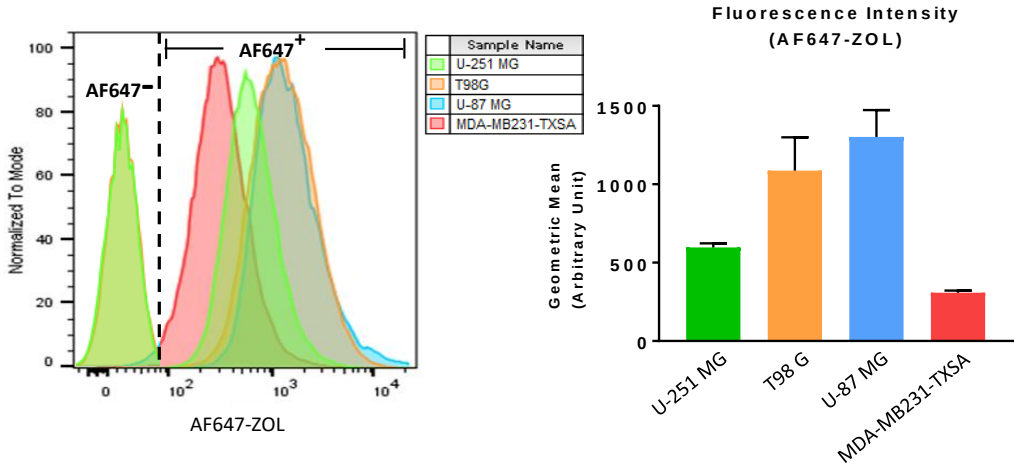

Figure 5.4 Differential ZOL uptake among three glioblastoma cell lines (U-87 MG, T98G and U-251 MG) and breast cancer cell line MDA-MB231-TXSA

Cells were incubated with 25 µM AF647-ZOL for 4 h. Cell were then washed, trypsinised and analysed by flow cytometry. Data represent the geometric means±SD from three different experiments (n=3).

drugs including ZOL requires fluid-phase endocytosis [252]. Interestingly, the sensitive cell line U-87 MG had about 5 times higher ZOL uptake than MDA-MB231-TXSA cells while the drug uptake in T98 G and U-251 MG cells was about 4 and 2 times higher than that of MDA-MB231-TXSA cells, respectively.

5.2.5 Differential accumulation of unprenylated Rap1A following ZOL treatment among glioblastoma and breast cancer cells.

ZOL acts by inhibiting farnesyl pyrophosphate synthase (FPPS), a key enzyme in the mevalonate pathway, leading to Vγ9Vδ2 T cells sensitisation. Inhibition of FPPS also blocks prenylation of downstream small GTPases such as Ras, Rho and Rap1A [220] causing intracellular accumulation of their unprenylated forms [221, 222]. In particular, increase in levels of unprenylated Rap1A have been commonly used as a surrogate marker for both cellular uptake and antitumour activity of ZOL [279]. In this study, levels of unprenylated Rap1A in the four cancer cell lines (U-87 MG, T98 G, U-251 MG and MDA-MB231-TXSA) were determined following 24 h incubation with varying concentrations of ZOL (0-25 µM). Results showed that ZOL increased accumulation of unprenylated Rap1A in all cancer cell lines in a ZOL dose-dependent manner (Fig 5.5). In the most sensitive cell line, U-87 MG, the accumulation of unprenylated Rap1A was detected following exposure to as little as 1 µM ZOL with the detection being more pronounced as the ZOL concentrations increased. For the rest of the cell lines (MDA-MB231-TXSA, T98 G and U-251 MG), unprenylated Rap1A accumulated following exposure to higher concentrations of ZOL (10-25 µM).

5.2.6 Glioblastoma cells have higher endogenous HMG-CoAR protein expression when compared to breast cancer cells.

Previous studies have shown increased endogenous expression levels and function of hydroxy-methylglutaryl-CoA reductase (HMG-CoAR), a major rate limiting enzyme of the

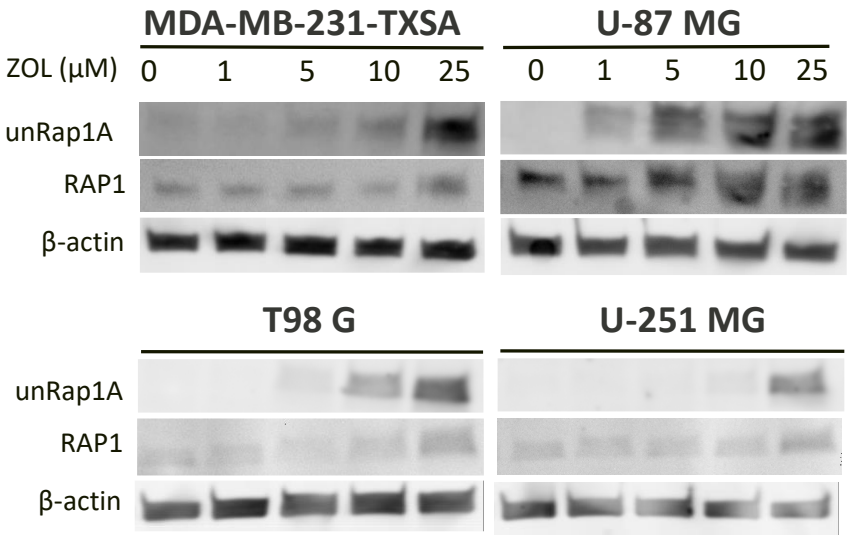

Figure 5.5 ZOL treatment blocks protein prenylation in cancer cells as indicated by the accumulation of unprenylated Rap1A.

Cells were treated with various concentrations (0-25 μM) of ZOL for 24 h. The cell lysate was subjected to Western blot analysis using antibodies that are specific for the unprenylated form of Rap1A and for RAP1. β-actin was served as loading control.

mevalonate pathway (Fig 5.6B) in haematological malignancies [280] and mammary carcinoma cells [281]. In this study, the effects of ZOL treatment at the protein levels of HMG-CoAR, FPPS and unprenylated Rap1A were examined by Western blot analysis. Blockade of HMG-CoA prevents accumulation of mevalonate metabolites and hence recognition by Vγ9Vδ2 T cells. On the other hand, when the metabolite accumulation is induced by overexpressing HMG-CoAR or by treatment with NBPs, tumour cells then acquire the capacity to stimulate Vγ9Vδ2 T cells. In Fig 5.6, representative Western blots of HMG-CoAR, FPPS and unprenylated Rap1A proteins from untreated and ZOL-treated cancer cells are shown. As expected, treatment with 25 μM ZOL greatly enhanced the expression of unprenylated Rap1A in all cell lines tested (MDA-MB231-TXSA, U-87 MG, T98 G and U-251 MG) with unprenylated Rap 1A being most pronounced in U-87 MG correlating with the results on ZOL-enhanced Vγ9Vδ2 T cell cytotoxicity on this cell line. ZOL treatment increased the protein level of FPPS, the target enzyme for ZOL in all cell lines tested. When HMG-CoAR protein expression levels were monitored, it was found that the endogenous HMG-CoAR levels were different amongst different cell lines but there were more distinctive levels in all three glioblastoma cell lines (U-87 MG, T98 G and U-251 MG) when compared to breast cancer MDA-MB231-TXSA cells. Treatment with ZOL had no significant effect on the expression of HMG-CoAR in each cell line, compared to their respective untreated control.

5.3 Discussion

GBM is a highly lethal brain tumour for which conventional treatments have failed to effectively improve survival of patients. In recent years, the development of adoptive immunotherapy (ACT) has ignited a new hope for the treatment of GBM. In particular, Vγ9Vδ2 T cells have shown to have potent cytotoxic activity against malignant glioma cells both *in vitro* and *in vivo* [142, 143, 273]. Pre-treatment with NBPs can further enhance the cytotoxic effects by Vγ9Vδ2 T cells [271, 277, 282]. ZOL, the third generation NBP, is clinically used

A

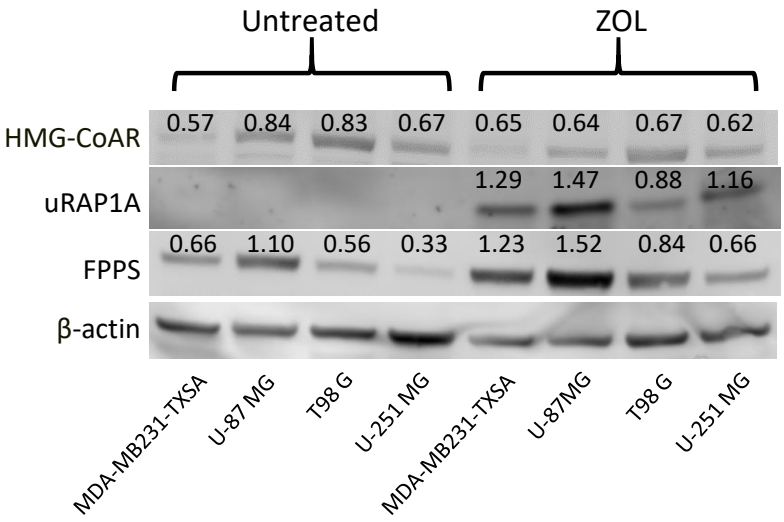
Untreated
ZOL
HMG-CoAR
uRAP1A
FPPS
β-actin
0.57 0.84 0.83 0.67 0.65 0.64 0.67 0.62
1.29 1.47 0.88 1.16
0.66 1.10 0.56 0.33 1.23 1.52 0.84 0.66
MDA-MB231-TXSA
U-87 MG
T98 G
U-251 MG
MDA-MB231-TXSA
U-87MG
T98 G
U-251 MG

B

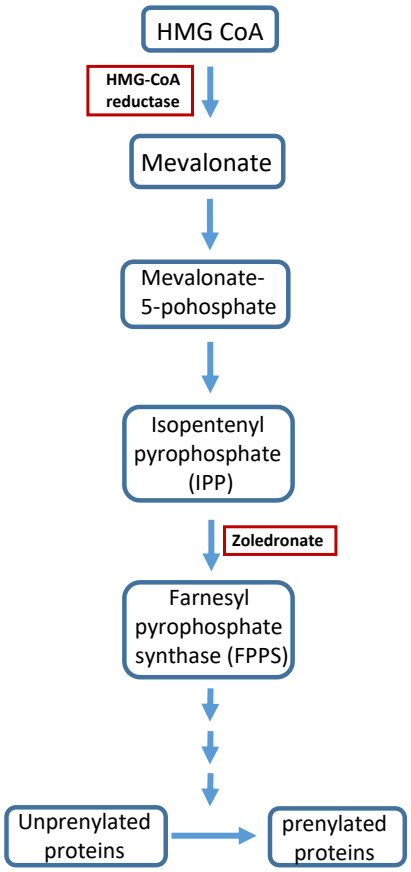
HMG CoA
HMG-CoA reductase
Mevalonate
Mevalonate-5-pohosphate
Isopentenyl pyrophosphate (IPP)
Zoledronate
Farnesyl pyrophosphate synthase (FPPS)
Unprenylated proteins
prenylated proteins

Figure 5.6 Upregulation of endogenous HMG-CoAR protein levels in glioblastoma cell line.

A. the effect of ZOL on the regulation of the mevalonate proteins in three glioblastoma cell lines (U-87 MG, T98 G and U-251 MG) and a breast cancer cell line (MDA-MB231-TXSA). Total levels of HMG-CoAR, unprenylated Rap1A, FPPS and β-actin (internal control) were determined by Western Blotting in cell lysates. The cells were incubated with 25 μM ZOL for 24 h. Representative images are shown. The blots were quantified by ImageJ software and normalized to β-actin. B. Mevalonate synthesis pathway and related metabolites.

to treat osteoporosis and osteolytic bone metastases secondary to breast and prostate cancer [283, 284]. It is an inhibitor of the mevalonate pathway, exerting its pleiotropic antitumour effects via apoptosis induction as well as modulating the immune system [285-287]. In this study, Vγ9Vδ2 T cells in combination with ZOL have shown to have different cytotoxic effects on GBM cell lines. While U-87 MG was the most responsive cell line to the combination treatment, U-251 MG and T98 G were shown to be moderately resistant and completely resistant, respectively. Interestingly, the cytotoxic effect seen on U-87 MG cells was also significantly higher than that of breast cancer MDA-MB231-TXSA cells, which was already known to show cytotoxic sensitivity [199, 200]. To investigate the reasons behind the stronger sensitizing effect on U-87 MG, cellular uptake studies showed that all glioblastoma cell lines were more efficient than MDA-MB231-TXSA at internalizing ZOL. In fact, U-87 MG and T98 G cells had the highest levels of uptake amongst all cell lines tested; hence, the increase in cellular uptake per se does not automatically imply increase in drug efficacy.

Previous studies have shown that inhibition of the mevalonate pathway played a critical role in the anticancer effect of ZOL [288, 289]. Following ZOL inhibition of FPPS, the mevalonate pathway is blocked and the IPP metabolite upstream to FPPS accumulates in conjunction with downstream inhibition of protein prenylation. While the intracellular build up of IPP makes cancer cells more amenable to Vγ9Vδ2 T cell-mediated killing, several studies have indicated the interruption of protein prenylation as a major contributor to the anticancer effects of ZOL [290-292]. In U-87 MG cells, the appearance of the unprenylated form of Rap1A in response to varying concentrations of ZOL was seemed to correlate well with ZOL-enhanced Vγ9Vδ2 T cells cytotoxicity. Furthermore, endogenous levels of FPPS were also highest in U-87 MG cells, followed by MDA-MB231-TXSA cells. In line with current literature [293], this study showed that the stronger inhibition of FPPS correlated with higher antitumour activity of Vγ9Vδ2 T cells against U-87 MG and MDA-MB231-TXSA cells.

Similarly, endogenous levels of HMG-CoAR, the rate limiting enzyme upstream to FPPS, were higher in U-87 MG than the rest of the cell lines. In U-87 MG cells, previous studies have described the up regulation of HMG-CoAR as a mechanism for drug resistance while inhibiting the HMG-CoAR-mediated mevalonate pathway can lead to cell cycle arrest and autophagy [105]. High endogenous expression of HMG-CoAR was observed in many cancers such as ductal carcinoma-in-situ, a subtype of breast cancer [294], ovarian cancer [295, 296] and glioblastoma [297], possibly reflecting an increased demand of isoprenoids to maintain cell growth advantages [298, 299].

This current study has shown that U-87 MG cells are not only highly sensitive to ZOL treatment but also showed a unique sensitivity to ZOL-induced Vγ9Vδ2 T cell killing. The increased ZOL uptake in glioblastoma resistant cell line T98 G may otherwise suggest that perhaps the sensitivity is not only achieved by increased cellular ZOL uptake but is also accompanied by the greater extent of FPPS inhibition and the high activity level of the mevalonate pathway. Likewise, the lack of ZOL-induced Vγ9Vδ2 T cell cytotoxicity could theoretically be attributed to the cancer cells' low intracellular accumulation of phosphoantigens following exposure to ZOL and possibly due to the low activity of the mevalonate pathway. In conclusion, ZOL may has a dual role against GBM by directly killing cancer cells due to inhibition of protein prenylation and also by acting synergistically with Vγ9Vδ2 T cells. For tumours that are localized within a relatively closed environment and difficult-to-access niches, post-resection administrations of Vγ9Vδ2 T cells and ZOL directly into the vicinity of primary brain tumour could be an effective method to deliver concentrated cellular immunotherapy to the site of residual malignancy.

Chapter 6

Discussion, Future Directions and Conclusions

6.1 Discussion

Harnessing the unique properties of γδT cells, particularly the Vγ9Vδ2 T cell subset for cellular immunotherapy holds considerable promise for the treatment of various solid and haematological malignancies. However, its efficacy has been limited with an average response ratio of only 21% in early phase clinical trials for the treatment of advanced tumours [164]. To overcome this sub-optimal efficiency problem of Vγ9Vδ2 T cells-based therapies, multidisciplinary approaches that provide additive or synergistic actions are required and may open novel opportunities for future cell-based cancer therapies.

Pre-treatment with NBPs such as ZOL has been shown to sensitise cancer cells toward Vγ9Vδ2 T cell-mediated cytotoxicity both *in vitro* and in pre-clinical settings. However, since ZOL is preferentially localized to the bone, its therapeutic efficacy in non-skeletal tumours is hampered. In addition, it has also been established that, with systemic delivery of Vγ9Vδ2 T cells, the lack of *in vivo* efficacy of the ZOL/Vγ9Vδ2 T cell combination is in part due to insufficient trafficking of the T cells to the tumour, especially for solid tumours, which is a well-defined problem for cellular immunotherapy. Therefore, it has been suggested that local administration of T cells directly into the vicinity of the tumours, which bypasses the requirement for T cell trafficking may potentially improve the treatment efficacy. Additionally, since a large body of studies have demonstrated the synergistic effects of biomaterials combined with immunotherapy, an elegant approach for targeting localized tumours has emerged. Improved delivery technologies using rationally designed biomaterials allowing not only for discrete localization but also for controlled release of immunotherapeutic agents may substantially improve outcomes of the ZOL/Vγ9Vδ2 T cells combination treatment against localized tumours.

There are several important points to consider for selecting a proper biomaterial for T cell encapsulation. First, as the T cells are suspended in a liquid precursor solution prior to encapsulation, the gelation process must occur in mild and cell-friendly conditions and should not influence the viability of encapsulated cells. Second, the structure and chemistry of biomaterials must support cell survival and egress over time. Lastly, T cells must be able to maintain their remarkable antitumour activity upon release from biomaterials. As proof-of-concept evidence, Corning Matrigel®, a commercially available basement membrane matrix was chosen as a biomaterial to carry Vγ9Vδ2 T cells and ZOL. Matrigel is extracted from the mouse sarcoma, which is rich in extracellular matrix proteins. It is liquid at 4°C but forms a soft gel at 37°C. The advantage of using Matrigel for this purpose is the ease of mixing both T cells and ZOL leading to *in situ* gel formation, which temporarily traps T cells and ZOL in the semirigid gel that can be injected in the vicinity of solid tumours or directly into the resection cavity following tumour resection. In addition, the *in situ* gel formation of Matrigel at physiological temperature provides soft physical properties similar to organs and have already been used extensively as the 3D scaffolds for cell culture and drug delivery in laboratories and pre-clinical studies. For the first time, the studies in this thesis have examined the anti-cancer efficacy of Matrigel scaffold-based carrying Vγ9Vδ2 T cells and ZOL against localized breast cancer using relevant *in vitro* (Chapter 3) and clinically relevant animal models (Chapter 4).

The *in vitro* results described in Chapter 3 have shown that Vγ9Vδ2 T cells and ZOL can be delivered via Matrigel scaffolds for localized cancer immunotherapy. Encapsulated T cells were compatible with Matrigel scaffolds as they maintained cell viability to that of unencapsulated cells. Furthermore, the embedded T cells were readily released from Matrigel carriers within a very short time leading to efficient cancer cell killing. The use of Matrigel in this setting was not only intended to serve as a structural support for the T cells but also to co-deliver ZOL to cancer cells. Incubation of MDA-MB231-TXSA cells with Matrigel that was

pre-loaded with ZOL (25 μM) led to an increase in unprenylated Rap1A expression in a similar manner to that seen when breast cancer cells were first pre-treated with ZOL in solution. Accordingly, Matrigel carrying both Vγ9Vδ2 T cells and ZOL could effectively kill MDA-MB231-TXSA cells, overcoming resistance of this cell line to the cytotoxicity of Vγ9Vδ2 T cells alone.

To demonstrate that the anticancer efficacy of this combinatorial approach can be recapitulated *in vivo*, a study (Chapter 4) was conducted using the subcutaneous model of breast cancer in immunodeficient mice. In this study, a single local injection of Matrigel carrying Vγ9Vδ2 T cells and ZOL directly in the vicinity of established breast tumours led to only a small but transient reduction in tumour growth. Tumour growth increased thereafter, resulting in no significant differences in tumour growth inhibition between groups. Therefore, despite the potent cytotoxic activity of this combination seen *in vitro*, the animal studies were highly unexpected. There are several factors that can modify the anti-tumour activity of adoptively transferred T cells *in vivo*. Amongst these factors is the effector to target cell (E:T) ratio. In general, transferred T cells used at higher E:T ratios exhibit higher cytotoxic activity. As such, adjustment on the number of cytotoxic T cells versus cancer cell target may be required to improve efficacy in controlling tumour growth. Therefore, in the subsequent animal experiment, twice as many Vγ9Vδ2 T cells was used while one-tenth of the cancer cells was used as a starting cell density implanted into the mammary fat pad of each animal. This adjustment resulted in improved cytotoxic function of Matrigel carrying Vγ9Vδ2 T cells and ZOL in this minimum breast cancer model but still failed to completely eliminate the cancer cells. Interestingly, tumour growth in animals received Matrigel carrying Vγ9Vδ2 T cells alone mirrored those that received Matrigel carrying both Vγ9Vδ2 T cells and ZOL for 3 weeks post-administration, before starting to grow aggressively in Week 4, while the tumours of the group that received the combination treatment in Matrigel remained relatively smaller. Nonetheless,

this may suggest the growth retardation of the tumours was primarily due to Vγ9Vδ2 T cells alone and that ZOL failed to sensitise cancer cell target *in vivo* despite being delivered locally into the vicinity of the tumours.

ZOL is a well-characterised inhibitor of FPPS, the key enzyme in the mevalonate pathway, resulting in intracellular IPP accumulation, thereby leading to increased cancer cell recognition by Vγ9Vδ2 T cells. *In vitro*, ZOL is also reported to exhibit anti-tumour effect through inhibition of tumour cell proliferation, invasion, and angiogenesis as well as induction of apoptosis in a range of cancer cell lines [123, 300-304]. However, in pre-clinical settings, the potential anti-tumour effect of ZOL remains controversial with some studies reported growth inhibition of primary tumours and metastasis [123, 124, 126-129, 305-307] while others reported ZOL had no effect [130, 131]. *In vitro*, 25 μM ZOL either in free form (solution) [199] or embedded onto Matrigel (Chapter 3) was not sufficient to directly kill MDA-MB231-TXSA cells; however, this concentration was required to sensitise MDA-MB231-TXSA cells to rapid killing by Vγ9Vδ2 T cells *in vitro* [199]. Hence, it was clearly seen that, for solid cancers such as breast cancers, ZOL failed to sensitise cancer cells to Vγ9Vδ2 T cell-mediated cytotoxicity *in vivo* (Chapter 4).

For ZOL to exert its therapeutic effects, it must first be internalised by cancer cells. Previous studies have also shown ZOL treatment *in vivo* can affect the mevalonate pathway of tumours in a subcutaneous model of breast and prostate cancer [93, 308, 309], but in these particular studies, the exact cell types within the tumour microenvironment that involved in the cellular uptake were not identified. The studies in this thesis directly compared the differences in cellular uptake of fluorescently labelled ZOL *in vitro* and *in vivo* on GFP-labelled MDA-MB231-TXSA cells following localized delivery of ZOL. For the first time, it was demonstrated that, breast cancer cells efficiently internalised ZOL *in vitro* as indicated by a complete shift of the GFP positive cancer cells to co-express fluorescent ZOL following

incubation (Chapter 4). On the other hand, breast cancer cells in tumour tissue isolated from the mammary fat pad were negative for ZOL uptake, showing only a negligible number of cells that co-expressed both GFP and fluorescent ZOL following local delivery of ZOL via Matrigel (Chapter 4). When the *in vivo* uptake experiment was repeated with the more ZOL sensitive cell line, glioblastoma U-87 MG (using a subcutaneous mouse model), similar results were also obtained. In this latter study, it was shown that ZOL was internalised mainly by tumour-associated macrophages (TAMs) but not the glioblastoma tumour cells (Chapter 4). These observations were in line with previous literature where fluorescently labelled risendronate, another NBPs, was internalised by TAMs, not cancer cells in the mammary fat pad model of T41 breast cancer. The ability of TAMs to selectively internalised NBPs including ZOL is shared with other cells of the myeloid lineage such as peripheral blood monocytes, peritoneal macrophages and osteoclasts [139, 310]. This could possibly due to a more efficient phagocytic/pinocytosis internalization capability, especially for calcium-containing complexes shared amongst these cells [252]. Hence the antitumour activities of ZOL observed in preclinical and clinical settings could be mediated indirectly through ZOL uptake into TAMs leading to their depletion and, therefore, unlikely a result of the direct uptake of ZOL into cancer cells. This was a significant finding as it does not support the use of ZOL/Vγ9Vδ2 T cell combination immunotherapy in patients with solid tumours. Further studies are required to form a new strategy to improve the effectiveness of localized immunotherapy of Vγ9Vδ2 T cells.

Many studies have previously shown NBPs such as ZOL play a dual role against many cancer cells by directly inhibiting tumour growth as well as enhancing Vγ9Vδ2 T cell antitumour immune responses *in vitro* and *in vivo* [115, 282, 311, 312]. The direct antitumour effects of NBPs *in vitro* include inhibition of tumour cell proliferation, induction of apoptosis, inhibition of tumour cell adhesion, invasion and angiogenesis [313]. Acting by inhibiting

farnesyl pyrophosphate synthase (FPPS), NBPs thereby deplete cancer cells of downstream isoprenoid lipids farnesyl pyrophosphate (FPP) and geranylgeranyl diphosphate (GPPS) [251]. Both FPP and GPPS are required for the post-translational prenylation of small GTPases of the Ras, Rac and Rho family proteins, which is important protein signalling for regulating normal cell activity and survival [220]. Consistent with previous literature in this context, this study has showed that ZOL inhibited both GBM and breast cancer cell growth, but the efficacy varied between cell lines. The IC_{50} of ZOL against GBM cell lines (U-87 MG, T98G and U-251 MG) reached in the 3-5 µM range which was significantly much lower than that of the breast cancer cell line MDA-MB231-TXSA cells, reaching at 30 µM ZOL (Chapter 5). Differences in sensitivity to ZOL in different cells were previously observed [314, 315]. Further, investigations into the exact mechanisms underlying sensitivity/resistance to ZOL induced cell death showed that these mechanisms can be varied between different cell types. For example, Mönkkönen and colleagues have shown in MCF-7 breast cancer cells, ZOL induced the formation of a cytotoxic ATP analogue, ApppI, due to FPPS inhibition. ApppI can directly induce apoptosis [316]. As there were considerably different levels of ZOL-induced Apppl formation between different cancer cell lines (MCF-7, MDA-MB 436 and RPMI 8226), the efficiency of ZOL against tumour cells may vary depending to the extent of Apppl accumulation and protein prenylation within these cells [317]. In U-87 MG cells, on the other hand, it was observed that ZOL may exert antiproliferative effects through the induction of tumour cell cycle arrest and cellular autophagy (rather than apoptosis) via depletion of GGPP, a mevalonate pathway intermediate, which in turn led to Rab protein prenylation [105]. Further studies are needed to elucidate the different pathways by which ZOL directly induces cancer cell death in many other different cancer types and to identify the molecular targets of ZOL underlying these mechanisms.

This study then focused on the effect of ZOL on sensitizing GBM cells to Vγ9Vδ2 T cell-mediated cytotoxicity. It was known that treatment with ZOL can make cancer cells including GBM more susceptible to cell lysis by Vγ9Vδ2 T cells and hence improved their antitumour activity [271, 282]. However, the *in vitro* antitumour activity of Vγ9Vδ2 T cells on ZOL-pretreated cancer cells varied greatly [94, 102, 318]. In this current study, it was found that the sensitizing effect of ZOL varied among GBM cell lines (U-87 MG, T98G and U-251 MG) with a uniquely strong effect on U-87 MG cells (Chapter 5). On the other hand, T98G and U-251 MG cells were less sensitive (Chapter 5). In U-87 MG cells as shown by Western blot analysis, there was a correlation between drug cellular uptake, ZOL-induced unprenylated Rap1A and FPPS protein expressions, and HMG-CoA reductase expression to the sensitivity of the cancer cells to ZOL/Vγ9Vδ2 T cells combination treatment. These results were in agreement with data reported by Benzaïd and colleagues [93] who showed a correlation between Vγ9Vδ2 T cell cytotoxicity and ZOL-induced IPP accumulation in breast cancer cell lines (T47D, MCF-7 and B02) both *in vitro* and *in vivo*. In sharp contrast to U87-MG cells, ZOL treatment did not strongly promote the expression of unprenylated Rap1A in T98 G cells, which may partly explain the lack of Vγ9Vδ2 T cell-mediated cytotoxicity following ZOL-pretreatment in this cell line. Overall, these results provide some support that GBM cells with higher ZOL uptake and higher inhibition of the mevalonate pathway were more likely to benefit from ZOL/Vγ9Vδ2 T cells combination treatment.

6.2 Future Direction

As adoptively transferred T cells need to infiltrate into the tumour to exert their antitumour activity, the studies in this thesis focus on localized T cell delivery method to solid tumours, which may enhance the Vγ9Vδ2 T cell migration to the tumour. While these studies provide new information in the field of localized immunotherapy, questions remain on how to best increase accumulation of mevalonate metabolites, particularly IPP *in vivo*. Accumulation

of the mevalonate metabolites in the tumour cells is a powerful danger signal but ZOL has limited *in vivo* efficacy possibly due to the unfavourable pharmacokinetic and lack of cancer specificity in terms of uptake/molecular targeting [138, 216, 319]. Hence, the development of modified PAgs and NBPs that can be readily internalised by cancer cells may overcome these restrictions and improve clinical efficacy.

6.2.1 Liposomal ZOL

As depicted earlier in this thesis, ZOL used *in vivo* displayed only marginal efficacy despite being very effective *in vitro*. The use of nanocarriers to deliver ZOL directly to cancer cells may help overcome these limitations. In fact, owing to their ability to store drugs and enhance penetration into tumour tissues, various lipid carriers such as liposomes are under investigation for the direct delivery of NBPs into cancer cells and found to increase anticancer efficacy as cytotoxic agents and immunomodulating agents for adoptive T cell immunotherapies in mouse models of cancer [320, 321]. In a study to optimise cell delivery, neridronate (NER), an NBP with relatively poor cell killing activity was chosen and shown that a liposomal formulation of NER increased cell growth inhibitory activity of human breast cancer MDA-MB-231 and glioblastoma U-87 MG cells by at least 50 times, compared to free drug [322]. Demonstrating indirectly by co-encapsulating of fluorescent dye into liposomes with the drug has also shown significant uptake into the cancer cells *in vitro*.

ZOL has been encapsulated into liposomes by a different strategy, known as stealth liposomes (lipoZOL) designed for improved tumour targeting and found to increase cytotoxic effect in prostate, breast, head and neck, lung and pancreas cancer cell lines [258]. However, another study reported that lipoZOL did not elicit any significant cytotoxic effect on cancer cells *in vitro* [323]. In this latter study, significant inhibitory effect was only found using folate-conjugated lipoZOL on cancer cells overexpressing folate receptor. Another group has investigated the *in vivo* antitumour activity of lipoZOL, developed in their laboratory, using a

prostate cancer mouse model [258, 259]. In these experiments, mice treated with lipoZOL had greater tumour growth inhibition together with increase animal survival. This group also reported the development of self-assembling nanoparticles encapsulating ZOL for which an increase in growth inhibition in comparison to free ZOL on different cancer cell lines was observed [259]. Consistently, the self-assembling nanoparticles of ZOL showed a marked reduction of tumour growth in a mouse model of prostate cancer while free ZOL did not show any significant reduction. Likewise, treatments with pegylated liposomal alendronate (PLN-alen) resulted in a dramatic increase in liposome deposition in breast cancer cells *in vivo* [324] as well as significant liposome uptake in TAMs [325]. In addition, it was also found that treatments with PLN-alen polarized TAMs toward an M1 antitumour phenotype, hence increased cytotoxic T cell infiltration into the tumour as well as increased their cytokine responses [325].

While several studies have reported the use of liposomal ZOL and liposomal alendronate as a monotherapy in cancer models, only a handful of studies have explored these drugs in combination with Vγ9Vδ2 T cells. Interestingly, a study by Hodgins and colleagues [326] has reported that pre-treatments with liposomal alendronate (PLN-alen) significantly increased trafficking/homing of Vγ9Vδ2 T cells to the mammary fat pad tumours at 48 h post-administration. Therefore, it was not surprising that PLN-alen has been reported to sensitise cancer cells to destruction by Vγ9Vδ2 T cells both *in vitro* and *in vivo* [326, 327]. For example, Parente-Pereira *et al*. has shown PLN-alen in combination with Vγ9Vδ2 T cells, following local (intraperitoneal) administration of Vγ9Vδ2 T cells resulted in growth retardation of ovarian tumours in mice [328]. Significant tumour growth inhibition was also observed when PLN-alen treatments were combined with Vγ9Vδ2 T cells in metastatic lung melanoma tumour-bearing mice following i.v. administration of both PLN-alen and Vγ9Vδ2 T cells [327]. On the other hand, lipoZOL was able to sensitise several ovarian cancer lines to Vγ9Vδ2 T cell

killing *in vitro* although its use *in vivo* was prohibited due to toxicity and sudden mice death [319, 328].

Taken together, it is reasonable to believe that the role of ZOL and other NBPs in cancer treatment appears to be underestimated. The use of nanotechnology may open a new therapeutic scenario, enabling changes in characteristics of NBPs and therefore allowing them to be preferentially accumulated in extraskeletal tumours.

6.2.2 Lipophilic pyridinium bisphosphonates

ZOL and other NBPs are extremely polar/negatively charged compounds at physiological pH which is essential for inhibition of FPPS but may limit their ability to enter cells [329] together with the C-1 hydroxyl group leading to very high affinity to the bone [330]. As such, chemical modifications to mask this negatively charge may enhance their cellular potency in soft tissues while decreasing the bone bind affinity [331]. Zhang *et al*. developed a series of six lipophilic bisphosphonates, several of which have shown to have potent antitumour activity against breast cancer MCF-7 cells [332]. In addition, some of these compounds were far more active at activating Vγ9Vδ2 T cells than ZOL and bind weakly to the bone [333]. The authors concluded that these compounds could better target both FPPS and DPPS, leading to elevated IPP levels and activation of Vγ9Vδ2 T cells due to their hydrophobic nature. However, the ability of these compounds to sensitise cancer cells have not yet been tested. Lipophilic bisphosphonates may open up a new possibility to improved efficacy of Vγ9Vδ2 T cells.

6.2.3 Nucleotidic phosphoantigens

The butyrophillin family surface antigen BTN3A1 is important in the mechanism of PAgs recognition by Vγ9Vδ2 T cells [334]. The intracellular B30.2 domain of BTN3A1 directly binds to PAgs and this binding is detected by the Vγ9Vδ2 TCR [70]. However, there is an alternative mechanism of PAg recognition, whereby some binding of PAgs occurs onto the extracellular domain of BTN3A1 [335]. While most studies have focused on pyrophosphate

phosphoantigens such as IPP and HMBPP, nucleotidic PAgs (derivatives of HMBPP) were shown to sensitise K562 and HeLa cell lines *in vitro* and induced a long-lasting stimulating ability [240]. Cancer cells sensitised with HMBPP, on the other hand, rapidly lost their stimulatory activity [240]. Further experiments indicated that these nucleotidic PAgs must convert into HMBPP before entering the cells and may directly bind to BTN3A1 intracellularly. The preferential uptake of nucleotidic PAgs by HeLa cells suggested these compounds may represent alternative compounds for Vγ9Vδ2 T cells-based immunotherapy.

6.3 Conclusion

The data presented in this thesis clearly shows that Vγ9Vδ2 T cells were abundantly present in the tumour tissues following localized adoptive transfer. However, ZOL used here as the cancer cell sensitising agent could not be internalised by cancer cells but rather accumulated selectively in the tumour resident macrophages and was preferentially rooted to the skeleton of mice due to its calcium binding characteristics. Collectively, the results of this study clearly indicate that ZOL administered locally directly in the tumour tissue is unlikely to be of sufficient benefit in potentiating Vγ9Vδ2 T cell function *in vivo* and is therefore destined to fail clinically despite the overwhelming cytotoxicity observed in many cellular models described in this thesis. In this regard, modified NBPs using nanotechnology-based carriers as well as lipophilic NBPs and synthetic nucleotide PAgs may represent alternative pharmacotherapeutic strategies to improve Vγ9Vδ2 cell-based local immunotherapy.

Bibliography

1. Parkin, D.M., *Global cancer statistics in the year 2000.* The lancet oncology, 2001. **2**(9): p. 533-543.
2. Miller, K.D., et al., *Cancer treatment and survivorship statistics, 2019.* CA: a cancer journal for clinicians, 2019. **69**(5): p. 363-385.
3. Vahrmeijer, A.L., et al., *Image-guided cancer surgery using near-infrared fluorescence.* Nature reviews Clinical oncology, 2013. **10**(9): p. 507.
4. Yan, T.D., et al., *Systematic review and meta-analysis of randomized and nonrandomized trials on safety and efficacy of video-assisted thoracic surgery lobectomy for early-stage non-small-cell lung cancer.* Database of Abstracts of Reviews of Effects (DARE): Quality-assessed Reviews [Internet], 2009.
5. DeVita, V.T. and E. Chu, *A history of cancer chemotherapy.* Cancer research, 2008. **68**(21): p. 8643-8653.
6. Baskar, R., et al., *Cancer and radiation therapy: current advances and future directions.* International journal of medical sciences, 2012. **9**(3): p. 193.
7. Gubin, M.M., et al., *Checkpoint blockade cancer immunotherapy targets tumour-specific mutant antigens.* Nature, 2014. **515**(7528): p. 577-581.
8. Couzin-Frankel, J., *Cancer immunotherapy*. 2013, American Association for the Advancement of Science.
9. Baker, D., et al., *The influence of the surgical wound on local tumor recurrence.* Surgery, 1989. **106**(3): p. 525-532.
10. Pérez-Herrero, E. and A. Fernández-Medarde, *Advanced targeted therapies in cancer: drug nanocarriers, the future of chemotherapy.* European journal of pharmaceutics and biopharmaceutics, 2015. **93**: p. 52-79.

11. Siamof, C.M., S. Goel, and W. Cai, *Moving Beyond the Pillars of Cancer Treatment: Perspectives From Nanotechnology.* Frontiers in Chemistry, 2020. **8**: p. 598100-598100.

12. Papaioannou, N.E., et al., *Harnessing the immune system to improve cancer therapy.* Annals of translational medicine, 2016. **4**(14).

13. Rosenberg, S.A., et al., *Use of tumor-infiltrating lymphocytes and interleukin-2 in the immunotherapy of patients with metastatic melanoma.* New England Journal of Medicine, 1988. **319**(25): p. 1676-1680.

14. June, C.H., S.R. Riddell, and T.N. Schumacher, *Adoptive cellular therapy: a race to the finish line.* Science translational medicine, 2015. **7**(280): p. 280ps7-280ps7.

15. Rosenberg, S.A., et al., *Durable complete responses in heavily pretreated patients with metastatic melanoma using T-cell transfer immunotherapy.* Clinical Cancer Research, 2011. **17**(13): p. 4550-4557.

16. Fujita, K., et al., *Prolonged disease-free period in patients with advanced epithelial ovarian cancer after adoptive transfer of tumor-infiltrating lymphocytes.* Clinical cancer research, 1995. **1**(5): p. 501-507.

17. Topalian, S.L., et al., *Immunotherapy of patients with advanced cancer using tumor-infiltrating lymphocytes and recombinant interleukin-2: a pilot study.* Journal of Clinical Oncology, 1988. **6**(5): p. 839-853.

18. Wolf, B., et al., *Safety and tolerability of adoptive cell therapy in cancer.* Drug safety, 2019. **42**(2): p. 315-334.

19. Andersen, R., et al., *T-cell responses in the microenvironment of primary renal cell carcinoma—implications for adoptive cell therapy.* Cancer immunology research, 2018. **6**(2): p. 222-235.

20. Lee, H.J., et al., *Expansion of tumor-infiltrating lymphocytes and their potential for application as adoptive cell transfer therapy in human breast cancer.* Oncotarget, 2017. **8**(69): p. 113345.

21. Hall, M., et al., *Expansion of tumor-infiltrating lymphocytes (TIL) from human pancreatic tumors.* Journal for immunotherapy of cancer, 2016. **4**(1): p. 1-12.

22. Ben-Avi, R., et al., *Establishment of adoptive cell therapy with tumor infiltrating lymphocytes for non-small cell lung cancer patients.* Cancer Immunology, Immunotherapy, 2018. **67**(8): p. 1221-1230.

23. Radvanyi, L.G., *Tumor-infiltrating lymphocyte therapy: addressing prevailing questions.* The Cancer Journal, 2015. **21**(6): p. 450-464.

24. Rosenberg, S.A. and N.P. Restifo, *Adoptive cell transfer as personalized immunotherapy for human cancer.* Science, 2015. **348**(6230): p. 62-68.

25. Yee, C., et al., *Adoptive T cell therapy using antigen-specific CD8+ T cell clones for the treatment of patients with metastatic melanoma: in vivo persistence, migration, and antitumor effect of transferred T cells.* Proceedings of the National Academy of Sciences, 2002. **99**(25): p. 16168-16173.

26. Johnson, L.A., et al., *Gene therapy with human and mouse T-cell receptors mediates cancer regression and targets normal tissues expressing cognate antigen.* Blood, 2009. **114**(3): p. 535-546.

27. Eshhar, Z., et al., *Specific activation and targeting of cytotoxic lymphocytes through chimeric single chains consisting of antibody-binding domains and the gamma or zeta subunits of the immunoglobulin and T-cell receptors.* Proceedings of the National Academy of Sciences, 1993. **90**(2): p. 720-724.

28. Maude, S.L., E.J. Shpall, and S.A. Grupp, *Chimeric antigen receptor T-cell therapy for ALL.* Hematology 2014, the American Society of Hematology Education Program Book, 2014. **2014**(1): p. 559-564.

29. June, C.H., et al., *CAR T cell immunotherapy for human cancer.* Science, 2018. **359**(6382): p. 1361-1365.

30. Shah, N.N. and T.J. Fry, *Mechanisms of resistance to CAR T cell therapy.* Nature reviews Clinical oncology, 2019. **16**(6): p. 372-385.

31. Sun, S., et al., *Immunotherapy with CAR-modified T cells: toxicities and overcoming strategies.* Journal of immunology research, 2018. **2018**.

32. Ribas, A. and R.C. Koya, *Adoptive cell transfer of T-cell receptor-engineered lymphocytes: lessons from recent modeling.* Future Oncology, 2010. **6**(11): p. 1671-1673.

33. Vantourout, P. and A. Hayday, *Six-of-the-best: unique contributions of γδ T cells to immunology.* Nature Reviews Immunology, 2013. **13**(2): p. 88-100.

34. Chien, Y.-h., C. Meyer, and M. Bonneville, *γδ T cells: first line of defense and beyond.* Annual review of immunology, 2014. **32**: p. 121-155.

35. Kunzmann, V., et al., *Stimulation of γδ T cells by aminobisphosphonates and induction of antiplasma cell activity in multiple myeloma.* Blood, 2000. **96**(2): p. 384-392.

36. Braza, M.S., et al., *γδ T lymphocytes count is normal and expandable in peripheral blood of patients with follicular lymphoma, whereas it is decreased in tumor lymph nodes compared with inflammatory lymph nodes.* The journal of immunology, 2010. **184**(1): p. 134-140.

37. Mayassi, T. and B. Jabri, *Human intraepithelial lymphocytes.* Mucosal immunology, 2018. **11**(5): p. 1281-1289.

38. Kabelitz, D., D. Wesch, and W. He, *Perspectives of γδ T Cells in Tumor Immunology.* Cancer research, 2007. **67**(1): p. 5.

39. Bubeník, J., *Tumour MHC class I downregulation and immunotherapy (Review).* Oncology reports, 2003. **10**(6): p. 2005-2008.

40. Pennington, D.J., et al., *The integration of conventional and unconventional T cells that characterizes cell-mediated responses.* Advances in immunology, 2005. **87**: p. 27-59.

41. Roberts, S. and M. Girardi, *Conventional and unconventional T cells.* Clinical and basic immunodermatology, 2008: p. 85-104.

42. Marrack, P., et al., *Evolutionarily conserved amino acids that control TCR-MHC interaction.* Annu. Rev. Immunol., 2008. **26**: p. 171-203.

43. Christopher Garcia, K., et al., *The molecular basis of TCR germline bias for MHC is surprisingly simple.* Nature immunology, 2009. **10**(2): p. 143-147.

44. Girardi, M., *Cutaneous biology of gammadelta T cells.* Advances in Dermatology, 2004. **20**: p. 203-215.

45. Kronenberg, M. and I. Engel, *On the road: progress in finding the unique pathway of invariant NKT cell differentiation.* Current opinion in immunology, 2007. **19**(2): p. 186-193.

46. Wesch, D., T. Hinz, and D. Kabelitz, *Analysis of the TCR Vgamma repertoire in healthy donors and HIV-1-infected individuals.* International immunology, 1998. **10**(8): p. 1067-1075.

47. Deusch, K., et al., *A major fraction of human intraepithelial lymphocytes simultaneously expresses the γ/δ T cell receptor, the CD8 accessory molecule and preferentially uses the Vδ1 gene segment.* European journal of immunology, 1991. **21**(4): p. 1053-1059.

48. Kalyan, S. and D. Kabelitz, *Defining the nature of human γδ T cells: a biographical sketch of the highly empathetic.* Cellular & molecular immunology, 2013. **10**(1): p. 21-29.

49. Kazen, A.R. and E.J. Adams, *Evolution of the V, D, and J gene segments used in the primate γδ T-cell receptor reveals a dichotomy of conservation and diversity.* Proceedings of the National Academy of Sciences, 2011. **108**(29): p. E332-E340.

50. Paul, S., et al., *Phenotypic and Functional Plasticity of Gamma–Delta (γδ) T Cells in Inflammation and Tolerance.* International reviews of immunology, 2014. **33**(6): p. 537-558.

51. Groh, V., et al., *Broad tumor-associated expression and recognition by tumor-derived γδ T cells of MICA and MICB.* Proceedings of the National Academy of Sciences, 1999. **96**(12): p. 6879-6884.

52. Airoldi, I., et al., *γδ T-cell reconstitution after HLA-haploidentical hematopoietic transplantation depleted of TCR-αβ+/CD19+ lymphocytes.* Blood, 2015. **125**(15): p. 2349-2358.

53. Wesch, D., A. Glatzel, and D. Kabelitz, *Differentiation of resting human peripheral blood γδ T cells toward Th1-or Th2-phenotype.* Cellular immunology, 2001. **212**(2): p. 110-117.

54. Ness-Schwickerath, K.J., C. Jin, and C.T. Morita, *Cytokine requirements for the differentiation and expansion of IL-17A–and IL-22–producing human Vγ2Vδ2 T cells.* The Journal of Immunology, 2010. **184**(12): p. 7268-7280.

55. Caccamo, N., et al., *Differentiation, phenotype, and function of interleukin-17–producing human Vγ9Vδ2 T cells.* Blood, 2011. **118**(1): p. 129-138.

56. Peters, C., et al., *Human Vδ2 T cells are a major source of interleukin-9.* Proceedings of the National Academy of Sciences, 2016. **113**(44): p. 12520-12525.

57. Ramstead, A.G. and M.A. Jutila, *Complex role of γδ T-cell-derived cytokines and growth factors in cancer.* Journal of Interferon & Cytokine Research, 2012. **32**(12): p. 563-569.

58. Bonneville, M., R.L. O'Brien, and W.K. Born, *γδ T cell effector functions: a blend of innate programming and acquired plasticity.* Nature Reviews Immunology, 2010. **10**(7): p. 467-478.

59. Sicard, H. and J.-J. Fournie, *Metabolic routes as targets for immunological discrimination of host and parasite.* Infection and immunity, 2000. **68**(8): p. 4375-4377.

60. Hintz, M., et al., *Identification of (E)-4-hydroxy-3-methyl-but-2-enyl pyrophosphate as a major activator for human γδ T cells in Escherichia coli.* FEBS letters, 2001. **509**(2): p. 317-322.

61. Nerdal, P.T., et al., *Butyrophilin 3A/CD277–Dependent Activation of Human γδ T Cells: Accessory Cell Capacity of Distinct Leukocyte Populations.* The Journal of Immunology, 2016. **197**(8): p. 3059-3068.

62. Espinosa, E., et al., *Chemical synthesis and biological activity of bromohydrin pyrophosphate, a potent stimulator of human γδ T cells.* Journal of Biological Chemistry, 2001. **276**(21): p. 18337-18344.

63. Chien, Y.h. and Y. Konigshofer, *Antigen recognition by γδ T cells.* Immunological reviews, 2007. **215**(1): p. 46-58.

64. Fiore, F., et al., *Enhanced ability of dendritic cells to stimulate innate and adaptive immunity on short-term incubation with zoledronic acid.* Blood, 2007. **110**(3): p. 921-927.

65. Dieli, F., et al., *Induction of γδ T-lymphocyte effector functions by bisphosphonate zoledronic acid in cancer patients in vivo.* Blood, 2003. **102**(6): p. 2310-2311.

66. Gossman, W. and E. Oldfield, *Quantitative structure− activity relations for γδ T cell activation by phosphoantigens.* Journal of medicinal chemistry, 2002. **45**(22): p. 4868-4874.

67. Thurnher, M., G. Gruenbacher, and O. Nussbaumer, *Regulation of mevalonate metabolism in cancer and immune cells.* Biochimica et Biophysica Acta (BBA)-Molecular and Cell Biology of Lipids, 2013. **1831**(6): p. 1009-1015.

68. Gruenbacher, G., et al., *Stress-related and homeostatic cytokines regulate Vγ9Vδ2 T-cell surveillance of mevalonate metabolism.* Oncoimmunology, 2014. **3**(8): p. e953410.

69. Rigau, M., et al., *Butyrophilin 2A1 is essential for phosphoantigen reactivity by γδ T cells.* Science, 2020. **367**(6478).

70. Sandstrom, A., et al., *The intracellular B30. 2 domain of butyrophilin 3A1 binds phosphoantigens to mediate activation of human Vγ9Vδ2 T cells.* Immunity, 2014. **40**(4): p. 490-500.

71. Yang, Y., et al., *A structural change in butyrophilin upon phosphoantigen binding underlies phosphoantigen-mediated Vγ9Vδ2 T cell activation.* Immunity, 2019. **50**(4): p. 1043-1053. e5.

72. Karunakaran, M.M., et al., *Butyrophilin-2A1 directly binds germline-encoded regions of the Vγ9Vδ2 TCR and is essential for phosphoantigen sensing.* Immunity, 2020. **52**(3): p. 487-498. e6.

73. Scotet, E., et al., *Tumor recognition following Vγ9Vδ2 T cell receptor interactions with a surface F1-ATPase-related structure and apolipoprotein AI.* Immunity, 2005. **22**(1): p. 71-80.

74. Mo, C., et al., *Ectopic expression of human MutS homologue 2 on renal carcinoma cells is induced by oxidative stress with interleukin-18 promotion via p38 mitogen-*

activated protein kinase (MAPK) and c-Jun N-terminal kinase (JNK) signaling pathways. Journal of Biological Chemistry, 2012. **287**(23): p. 19242-19254.

75. Dai, Y., et al., *Ectopically expressed human tumor biomarker MutS homologue 2 is a novel endogenous ligand that is recognized by human γδ T cells to induce innate anti-tumor/virus immunity.* Journal of Biological Chemistry, 2012. **287**(20): p. 16812-16819.

76. Aggarwal, R., et al., *Human Vγ2Vδ2 T cells limit breast cancer growth by modulating cell survival-, apoptosis-related molecules and microenvironment in tumors.* International Journal of Cancer, 2013. **133**(9): p. 2133-2144.

77. Norell, H., et al., *At the Bench: Preclinical rationale for exploiting NK cells and γδ T lymphocytes for the treatment of high-risk leukemias.* Journal of leukocyte biology, 2013. **94**(6): p. 1123-1139.

78. Wrobel, P., et al., *Lysis of a Broad Range of Epithelial Tumour Cells by Human γδ T Cells: Involvement of NKG2D ligands and T-cell Receptor-versus NKG2D-dependent Recognition.* Scandinavian journal of immunology, 2007. **66**(2-3): p. 320-328.

79. Rincon-Orozco, B., et al., *Activation of Vγ9Vδ2 T cells by NKG2D.* The Journal of Immunology, 2005. **175**(4): p. 2144-2151.

80. Correia, D.V., A.C. Lopes, and B. Silva-Santos, *Tumor cell recognition by γδ T lymphocytes: T-cell receptor vs. NK-cell receptors.* Oncoimmunology, 2013. **2**(1): p. e22892.

81. Todaro, M., et al., *Efficient killing of human colon cancer stem cells by γδ T lymphocytes.* The Journal of Immunology, 2009. **182**(11): p. 7287-7296.

82. Li, X., et al., *Generation of human regulatory γδ T cells by TCRγδ stimulation in the presence of TGF-β and their involvement in the pathogenesis of systemic lupus erythematosus.* The Journal of Immunology, 2011. **186**(12): p. 6693-6700.

83. Niu, C., et al., *In vitro analysis of the proliferative capacity and cytotoxic effects of ex vivo induced natural killer cells, cytokine-induced killer cells, and gamma-delta T cells.* BMC immunology, 2015. **16**(1): p. 1-10.

84. Poonia, B. and C.D. Pauza, *Gamma delta T cells from HIV+ donors can be expanded in vitro by zoledronate/interleukin-2 to become cytotoxic effectors for antibody-dependent cellular cytotoxicity.* Cytotherapy, 2012. **14**(2): p. 173-181.

85. He, Y., et al., *γδ T cell and other immune cells crosstalk in cellular immunity.* Journal of immunology research, 2014. **2014**.

86. Maniar, A., et al., *Human γδ T lymphocytes induce robust NK cell–mediated antitumor cytotoxicity through CD137 engagement.* Blood, The Journal of the American Society of Hematology, 2010. **116**(10): p. 1726-1733.

87. Lafont, V., et al., *Isopentenyl pyrophosphate, a mycobacterial non-peptidic antigen, triggers delayed and highly sustained signaling in human γδ T lymphocytes without inducing down-modulation of T cell antigen receptor.* Journal of Biological Chemistry, 2001. **276**(19): p. 15961-15967.

88. Anderson, J., et al., *Licensing of γδT cells for professional antigen presentation: a new role for antibodies in regulation of antitumor immune responses.* Oncoimmunology, 2012. **1**(9): p. 1652-1654.

89. Gertner-Dardenne, J., et al., *Bromohydrin pyrophosphate enhances antibody-dependent cell-mediated cytotoxicity induced by therapeutic antibodies.* Blood, The Journal of the American Society of Hematology, 2009. **113**(20): p. 4875-4884.

90. Braza, M.S., et al., *γδ T-cell killing of primary follicular lymphoma cells is dramatically potentiated by GA101, a type II glycoengineered anti-CD20 monoclonal antibody.* Haematologica, 2011. **96**(3): p. 400.

91. Tokuyama, H., et al., *Vγ9Vδ2 T cell cytotoxicity against tumor cells is enhanced by monoclonal antibody drugs—rituximab and trastuzumab.* International journal of cancer, 2008. **122**(11): p. 2526-2534.

92. Capietto, A.-H., L. Martinet, and J.-J. Fournié, *Stimulated γδ T cells increase the in vivo efficacy of trastuzumab in HER-2+ breast cancer.* The Journal of Immunology, 2011. **187**(2): p. 1031-1038.

93. Benzaïd, I., et al., *High phosphoantigen levels in bisphosphonate-treated human breast tumors promote Vγ9Vδ2 T-cell chemotaxis and cytotoxicity in vivo.* Cancer research, 2011. **71**(13): p. 4562-4572.

94. Kabelitz, D., et al., *Characterization of tumor reactivity of human Vγ9Vδ2 γδ T cells in vitro and in SCID mice in vivo.* The Journal of Immunology, 2004. **173**(11): p. 6767-6776.

95. Joalland, N., et al., *IL-21 increases the reactivity of allogeneic human Vγ9Vδ2 T cells against primary glioblastoma tumors.* Journal of Immunotherapy, 2018. **41**(5): p. 224-231.

96. D'Asaro, M., et al., *Vγ9Vδ2 T lymphocytes efficiently recognize and kill zoledronate-sensitized, imatinib-sensitive, and imatinib-resistant chronic myelogenous leukemia cells.* The Journal of Immunology, 2010. **184**(6): p. 3260-3268.

97. Cui, Q., et al., *Targeting myeloma–osteoclast interaction with Vγ9Vδ2 T cells.* International journal of hematology, 2011. **94**(1): p. 63-70.

98. Ross, J., et al., *A systematic review of the role of bisphosphonates in metastatic disease.* Health technology assessment (Winchester, England), 2004. **8**(4): p. 1-176.

99. Coleman, R.E. and E.V. McCloskey, *Bisphosphonates in oncology.* Bone, 2011. **49**(1): p. 71-76.

100. Oades, G., J. Coxon, and K. Colston, *The potential role of bisphosphonates in prostate cancer.* Prostate cancer and prostatic diseases, 2002. **5**(4): p. 264-272.

101. Solomayer, E.-F., et al., *Influence of zoledronic acid on disseminated tumor cells in primary breast cancer patients.* Annals of oncology, 2012. **23**(9): p. 2271-2277.

102. Gober, H.-J., et al., *Human T cell receptor γδ cells recognize endogenous mevalonate metabolites in tumor cells.* The Journal of experimental medicine, 2003. **197**(2): p. 163-168.

103. Braza, M.S. and B. Klein, *Anti-tumour immunotherapy with Vγ9Vδ2 T lymphocytes: from the bench to the bedside.* British journal of haematology, 2013. **160**(2): p. 123-132.

104. Dunford, J.E., et al., *Structure-activity relationships for inhibition of farnesyl diphosphate synthase in vitro and inhibition of bone resorption in vivo by nitrogen-containing bisphosphonates.* Journal of Pharmacology and Experimental Therapeutics, 2001. **296**(2): p. 235-242.

105. Jiang, P., et al., *Anti-cancer effects of nitrogen-containing bisphosphonates on human cancer cells.* Oncotarget, 2016. **7**(36): p. 57932.

106. Fleisch, H., et al., *Bisphosphonates: mechanisms of action.* Principles of bone biology, 2002: p. 1361-XLIII.

107. Coxon, F.P., et al., *Visualizing mineral binding and uptake of bisphosphonate by osteoclasts and non-resorbing cells.* Bone, 2008. **42**(5): p. 848-860.

108. Pazianas, M., S. van der Geest, and P. Miller, *Bisphosphonates and bone quality.* BoneKEy reports, 2014. **3**.

109. Lehenkari, P.P., et al., *Further insight into mechanism of action of clodronate: inhibition of mitochondrial ADP/ATP translocase by a nonhydrolyzable, adenine-containing metabolite.* Molecular pharmacology, 2002. **61**(5): p. 1255-1262.

110. Caraglia, M., et al., *The farnesyl transferase inhibitor R115777 (Zarnestra®) synergistically enhances growth inhibition and apoptosis induced on epidermoid cancer cells by Zoledronic acid (Zometa®) and Pamidronate.* Oncogene, 2004. **23**(41): p. 6900-6913.

111. Ibrahim, A., et al., *Approval summary for zoledronic acid for treatment of multiple myeloma and cancer bone metastases.* Clinical Cancer Research, 2003. **9**(7): p. 2394-2399.

112. Chen, T., et al., *Pharmacokinetics and pharmacodynamics of zoledronic acid in cancer patients with bone metastases.* The Journal of Clinical Pharmacology, 2002. **42**(11): p. 1228-1236.

113. Skerjanec, A., et al., *The pharmacokinetics and pharmacodynamics of zoledronic acid in cancer patients with varying degrees of renal function.* The Journal of Clinical Pharmacology, 2003. **43**(2): p. 154-162.

114. Lin, J., *Bisphosphonates: a review of their pharmacokinetic properties.* Bone, 1996. **18**(2): p. 75-85.

115. Caraglia, M., et al., *Emerging anti-cancer molecular mechanisms of aminobisphosphonates.* Endocrine-related cancer, 2006. **13**(1): p. 7-26.

116. Russell, R.G.G., et al., *Bisphosphonates: an update on mechanisms of action and how these relate to clinical efficacy.* Annals of the New York Academy of Sciences, 2007. **1117**(1): p. 209-257.

117. Saunders, Y., et al., *Systematic review of bisphosphonates for hypercalcaemia of malignancy.* Palliative medicine, 2004. **18**(5): p. 418-431.

118. Tamura, T., et al., *Zoledronic acid, a third-generation bisphosphonate, inhibits cellular growth and induces apoptosis in oral carcinoma cell lines.* Oncology reports, 2011. **25**(4): p. 1139-1143.

119. Tsubaki, M., et al., *Reduction of metastasis, cell invasion, and adhesion in mouse osteosarcoma by YM529/ONO-5920-induced blockade of the Ras/MEK/ERK and Ras/PI3K/Akt pathway.* Toxicology and applied pharmacology, 2012. **259**(3): p. 402-410.

120. Stresing, V., et al., *Nitrogen-containing bisphosphonates can inhibit angiogenesis in vivo without the involvement of farnesyl pyrophosphate synthase.* Bone, 2011. **48**(2): p. 259-266.

121. Lin, J.-F., et al., *Zoledronic acid induces autophagic cell death in human prostate cancer cells.* The Journal of urology, 2011. **185**(4): p. 1490-1496.

122. Lan, Y.-C., et al., *Zoledronic acid-induced cytotoxicity through endoplasmic reticulum stress triggered REDD1-mTOR pathway in breast cancer cells.* Anticancer research, 2013. **33**(9): p. 3807-3814.

123. Matsumoto, S., et al., *Efficacy of the third-generation bisphosphonate, zoledronic acid alone and combined with anti-cancer agents against small cell lung cancer cell lines.* Lung Cancer, 2005. **47**(1): p. 31-39.

124. Luo, K.-W., et al., *Anti-tumor and anti-osteolysis effects of the metronomic use of zoledronic acid in primary and metastatic breast cancer mouse models.* Cancer letters, 2013. **339**(1): p. 42-48.

125. Croucher, P.I., et al., *Zoledronic Acid Treatment of 5T2MM-Bearing Mice Inhibits the Development of Myeloma Bone Disease: Evidence for Decreased Osteolysis, Tumor Burden and Angiogenesis, and Increased Survival.* Journal of Bone and Mineral Research, 2003. **18**(3): p. 482-492.

126. Jeong, J., et al., *Preventive effects of zoledronic acid on bone metastasis in mice injected with human breast cancer cells.* Journal of Korean medical science, 2011. **26**(12): p. 1569.

127. Ory, B., et al., *Zoledronic acid suppresses lung metastases and prolongs overall survival of osteosarcoma-bearing mice.* Cancer: Interdisciplinary International Journal of the American Cancer Society, 2005. **104**(11): p. 2522-2529.

128. Koto, K., et al., *Clinically relevant dose of zoledronic acid inhibits spontaneous lung metastasis in a murine osteosarcoma model.* Cancer letters, 2009. **274**(2): p. 271-278.

129. Giraudo, E., M. Inoue, and D. Hanahan, *An amino-bisphosphonate targets MMP-9–expressing macrophages and angiogenesis to impair cervical carcinogenesis.* The Journal of clinical investigation, 2004. **114**(5): p. 623-633.

130. Labrinidis, A., et al., *Zoledronic acid inhibits both the osteolytic and osteoblastic components of osteosarcoma lesions in a mouse model.* Clinical cancer research, 2009. **15**(10): p. 3451-3461.

131. Labrinidis, A., et al., *Zoledronic acid protects against osteosarcoma-induced bone destruction but lacks efficacy against pulmonary metastases in a syngeneic rat model.* International journal of cancer, 2010. **127**(2): p. 345-354.

132. Kremer, R., et al., *Effect of oral bisphosphonates for osteoporosis on development of skeletal metastases in women with breast cancer: results from a pharmaco-epidemiological study.* Journal Of The National Cancer Institute, 2014. **106**(11): p. dju264.

133. Coleman, R.E., et al., *Breast-cancer adjuvant therapy with zoledronic acid.* N Engl J Med, 2011. **365**: p. 1396-1405.

134. Morgan, G.J., et al., *First-line treatment with zoledronic acid as compared with clodronic acid in multiple myeloma (MRC Myeloma IX): a randomised controlled trial.* The Lancet, 2010. **376**(9757): p. 1989-1999.

135. Mhaskar, R., et al., *Bisphosphonates in multiple myeloma: a network meta-analysis.* Cochrane Database of Systematic Reviews, 2012(5).

136. Okegawa, T., et al., *Zoledronic acid improves clinical outcomes in patients with bone metastatic hormone-naive prostate cancer in a multicenter clinical trial.* Anticancer research, 2014. **34**(8): p. 4415-4420.

137. Van Acker, H.H., et al., *Bisphosphonates for cancer treatment: mechanisms of action and lessons from clinical trials.* Pharmacology & therapeutics, 2016. **158**: p. 24-40.

138. Wiemer, D.F. and A.J. Wiemer, *Opportunities and challenges in development of phosphoantigens as Vγ9Vδ2 T cell agonists.* Biochemical pharmacology, 2014. **89**(3): p. 301-312.

139. Roelofs, A.J., et al., *Peripheral blood monocytes are responsible for γδ T cell activation induced by zoledronic acid through accumulation of IPP/DMAPP.* British journal of haematology, 2009. **144**(2): p. 245-250.

140. Kato, Y., et al., *Targeting of tumor cells for human γδ T cells by nonpeptide antigens.* The Journal of Immunology, 2001. **167**(9): p. 5092-5098.

141. Dieli, F., et al., *Targeting human γδ T cells with zoledronate and interleukin-2 for immunotherapy of hormone-refractory prostate cancer.* Cancer research, 2007. **67**(15): p. 7450-7457.

142. Bryant, N.L., et al., *Preclinical evaluation of ex vivo expanded/activated γδ T cells for immunotherapy of glioblastoma multiforme.* Journal of neuro-oncology, 2011. **101**(2): p. 179-188.

143. Jarry, U., et al., *Stereotaxic administrations of allogeneic human Vγ9Vδ2 T cells efficiently control the development of human glioblastoma brain tumors.* Oncoimmunology, 2016. **5**(6): p. e1168554.

144. Nishio, N., et al., *Zoledronate sensitizes neuroblastoma-derived tumor-initiating cells to cytolysis mediated by human γδ T cells.* Journal of Immunotherapy, 2012. **35**(8): p. 598-606.

145. Li, Z., et al., *Sensitization of human osteosarcoma cells to Vγ9Vδ2 T-cell-mediated cytotoxicity by zoledronate.* Journal of Orthopaedic Research, 2012. **30**(5): p. 824-830.

146. Dhar, S. and S.V. Chiplunkar, *Lysis of aminobisphosphonate-sensitized MCF-7 breast tumor cells by Vγ9Vδ2 T cells.* Cancer Immunity Archive, 2010. **10**(1): p. 10.

147. Mao, T.L., et al., *Ex vivo expanded human Vγ9vδ2 T-cells can suppress epithelial ovarian cancer cell growth.* International journal of molecular sciences, 2019. **20**(5): p. 1139.

148. Sato, K., et al., *Cytotoxic effects of γδ T cells expanded ex vivo by a third generation bisphosphonate for cancer immunotherapy.* International journal of cancer, 2005. **116**(1): p. 94-99.

149. Mattarollo, S.R., et al., *Chemotherapy and zoledronate sensitize solid tumour cells to Vγ9Vδ2 T cell cytotoxicity.* Cancer Immunology, Immunotherapy, 2007. **56**(8): p. 1285-1297.

150. Wilhelm, M., et al., *γδ T cells for immune therapy of patients with lymphoid malignancies.* Blood, 2003. **102**(1): p. 200-206.

151. To, W.C., et al., *Systemic adoptive T-cell immunotherapy in recurrent and metastatic carcinoma of the head and neck: a phase 1 study.* Archives of Otolaryngology–Head & Neck Surgery, 2000. **126**(10): p. 1225-1231.

152. Lang, J.M., et al., *Pilot trial of interleukin-2 and zoledronic acid to augment γδ T cells as treatment for patients with refractory renal cell carcinoma.* Cancer Immunology, Immunotherapy, 2011. **60**(10): p. 1447-1460.

153. Meraviglia, S., et al., *In vivo manipulation of Vγ9Vδ2 T cells with zoledronate and low-dose interleukin-2 for immunotherapy of advanced breast cancer patients.* Clinical & Experimental Immunology, 2010. **161**(2): p. 290-297.

154. Otto, M., et al., *Combination immunotherapy with clinical-scale enriched human γδ T cells, hu14. 18 antibody, and the immunocytokine Fc-IL7 in disseminated neuroblastoma.* Clinical cancer research, 2005. **11**(23): p. 8486-8491.

155. Kang, N., et al., *Adoptive immunotherapy of lung cancer with immobilized anti-TCRγδ antibody-expanded human γδ T Cells in peripheral blood.* Cancer biology & therapy, 2009. **8**(16): p. 1540-1549.

156. Buccheri, S., et al., *Efficacy and safety of γδT cell-based tumor immunotherapy: a meta-analysis.* J Biol Regul Homeost Agents, 2014. **28**(1): p. 81-90.

157. Fournié, J.-J., et al., *What lessons can be learned from γδ T cell-based cancer immunotherapy trials?* Cellular & molecular immunology, 2013. **10**(1): p. 35-41.

158. Gan, Y., M. Wallace, and M. Malkovsky, *Fas-dependent, activation-induced cell death of gammadelta cells.* Journal of biological regulators and homeostatic agents, 2001. **15**(3): p. 277-285.

159. Kondo, M., et al., *Expansion of human peripheral blood γδ T cells using zoledronate.* JoVE (Journal of Visualized Experiments), 2011(55): p. e3182-e3182.

160. Kobayashi, H., et al., *Phase I/II study of adoptive transfer of γδ T cells in combination with zoledronic acid and IL-2 to patients with advanced renal cell carcinoma.* Cancer Immunology, Immunotherapy, 2011. **60**(8): p. 1075-1084.

161. Kakimi, K., et al., *Adoptive transfer of zoledronate-expanded autologous Vγ9Vδ2 T-cells in patients with treatment-refractory non-small-cell lung cancer: a multicenter, open-label, single-arm, phase 2 study.* Journal for immunotherapy of cancer, 2020. **8**(2).

162. Alnaggar, M., et al., *Allogenic Vγ9Vδ2 T cell as new potential immunotherapy drug for solid tumor: a case study for cholangiocarcinoma.* Journal for immunotherapy of cancer, 2019. **7**(1): p. 1-7.

163. Kunzmann, V., et al., *Tumor-promoting versus tumor-antagonizing roles of γδ T cells in cancer immunotherapy: results from a prospective phase I/II trial.* Journal of immunotherapy, 2012. **35**(2): p. 205-213.

164. Zhao, Y., C. Niu, and J. Cui, *Gamma-delta (γδ) T cells: friend or foe in cancer development?* Journal of translational medicine, 2018. **16**(1): p. 1-13.

165. Mukai, S., et al., *Infiltration of tumors by systemically transferred tumor-reactive T lymphocytes is required for antitumor efficacy.* Cancer research, 1999. **59**(20): p. 5245-5249.

166. Carlos, T., *Leukocyte recruitment at sites of tumor: dissonant orchestration.* Journal of Leukocyte Biology, 2001. **70**(2): p. 171-184.

167. Fisher, D.T., et al., *IL-6 trans-signaling licenses mouse and human tumor microvascular gateways for trafficking of cytotoxic T cells.* The Journal of clinical investigation, 2011. **121**(10): p. 3846-3859.

168. Peres, E., et al., *High-dose chemotherapy and adoptive immunotherapy in the treatment of recurrent pediatric brain tumors.* Neuropediatrics, 2008. **39**(03): p. 151-156.

169. Visioni, A., et al., *Intra-arterial versus intravenous adoptive cell therapy in a mouse tumor model.* Journal of Immunotherapy (Hagerstown, Md.: 1997), 2018. **41**(7): p. 313.

170. Fisher, B., et al., *Tumor localization of adoptively transferred indium-111 labeled tumor infiltrating lymphocytes in patients with metastatic melanoma.* Journal of Clinical Oncology, 1989. **7**(2): p. 250-261.

171. Nicol, A., et al., *Clinical evaluation of autologous gamma delta T cell-based immunotherapy for metastatic solid tumours.* British journal of cancer, 2011. **105**(6): p. 778-786.

172. Nieda, M., et al., *Therapeutic activation of Vα24+ Vβ11+ NKT cells in human subjects results in highly coordinated secondary activation of acquired and innate immunity.* Blood, 2004. **103**(2): p. 383-389.

173. Schmidts, A. and M.V. Maus, *Making CAR T cells a solid option for solid tumors.* Frontiers in immunology, 2018. **9**: p. 2593.

174. Keilholz, U., et al., *Regional administration of lymphokine-activated killer cells can be superior to intravenous application.* Cancer, 1992. **69**(8): p. 2172-2175.

175. Rosenberg, S.A., et al., *Cell transfer therapy for cancer: lessons from sequential treatments of a patient with metastatic melanoma.* Journal of immunotherapy (Hagerstown, Md.: 1997), 2003. **26**(5): p. 385.

176. Katz, S.C., et al., *HITM-SIR: phase Ib trial of intraarterial chimeric antigen receptor T-cell therapy and selective internal radiation therapy for CEA+ liver metastases.* Cancer gene therapy, 2020. **27**(5): p. 341-355.

177. Adusumilli, P.S., et al., *Regional delivery of mesothelin-targeted CAR T cell therapy generates potent and long-lasting CD4-dependent tumor immunity.* Science translational medicine, 2014. **6**(261): p. 261ra151-261ra151.

178. Adusumilli, P.S., et al., *Abstract CT036: A phase I clinical trial of malignant pleural disease treated with regionally delivered autologous mesothelin-targeted CAR T cells: Safety and efficacy.* Cancer Research, 2019. **79**(13 Supplement): p. CT036-CT036.

179. Choi, B.D., et al., *Intracerebral delivery of a third generation EGFRvIII-specific chimeric antigen receptor is efficacious against human glioma.* Journal of clinical neuroscience, 2014. **21**(1): p. 189-190.

180. Han, J., et al., *CAR-engineered NK cells targeting wild-type EGFR and EGFRvIII enhance killing of glioblastoma and patient-derived glioblastoma stem cells.* Scientific reports, 2015. **5**(1): p. 1-13.

181. Priceman, S.J., et al., *Regional delivery of chimeric antigen receptor–engineered T cells effectively targets HER2+ breast Cancer metastasis to the brain.* Clinical Cancer Research, 2018. **24**(1): p. 95-105.

182. Brown, C.E., et al., *Regression of glioblastoma after chimeric antigen receptor T-cell therapy.* New England Journal of Medicine, 2016. **375**(26): p. 2561-2569.

183. van Schalkwyk, M.C., et al., *Design of a phase I clinical trial to evaluate intratumoral delivery of ErbB-targeted chimeric antigen receptor T-cells in locally advanced or recurrent head and neck cancer.* Human gene therapy clinical development, 2013. **24**(3): p. 134-142.

184. Dedrick, R.L., et al., *Pharmacokinetic rationale for peritoneal drug administration.* Cancer Treat. Rep, 1978. **62**: p. 1-13.

185. Wada, I., et al., *Intraperitoneal injection of in vitro expanded Vγ9Vδ2 T cells together with zoledronate for the treatment of malignant ascites due to gastric cancer.* Cancer medicine, 2014. **3**(2): p. 362-375.

186. Li, J., et al., *Implantable and Injectable Biomaterial Scaffolds for Cancer Immunotherapy.* Frontiers in Bioengineering and Biotechnology, 2020. **8**: p. 1363.

187. Smith, T.T., et al., *Biopolymers codelivering engineered T cells and STING agonists can eliminate heterogeneous tumors.* The Journal of clinical investigation, 2017. **127**(6): p. 2176-2191.

188. Rosenberg, S.A., *Cell transfer immunotherapy for metastatic solid cancer—what clinicians need to know.* Nature reviews Clinical oncology, 2011. **8**(10): p. 577-585.

189. Tumeh, P.C., et al., *The impact of ex vivo clinical grade activation protocols on human T cell phenotype and function for the generation of genetically modified cells for adoptive cell transfer therapy.* Journal of immunotherapy (Hagerstown, Md.: 1997), 2010. **33**(8): p. 759.

190. Stephan, S.B., et al., *Biopolymer implants enhance the efficacy of adoptive T-cell therapy.* Nature biotechnology, 2015. **33**(1): p. 97-101.

191. Dunn, Z.S., J. Mac, and P. Wang, *T cell immunotherapy enhanced by designer biomaterials.* Biomaterials, 2019. **217**: p. 119265.

192. Peppas, N.A. and A.G. Mikos, *Preparation methods and structure of hydrogels.* Hydrogels in medicine and pharmacy, 1986. **1**: p. 1-27.

193. Singh, A. and N.A. Peppas, *Hydrogels and scaffolds for immunomodulation.* Advanced Materials, 2014. **26**(38): p. 6530-6541.

194. Leach, D.G., S. Young, and J.D. Hartgerink, *Advances in immunotherapy delivery from implantable and injectable biomaterials.* Acta biomaterialia, 2019. **88**: p. 15-31.

195. Tsao, C.-T., et al., *Thermoreversible poly (ethylene glycol)-g-chitosan hydrogel as a therapeutic T lymphocyte depot for localized glioblastoma immunotherapy.* Biomacromolecules, 2014. **15**(7): p. 2656-2662.

196. Monette, A., et al., *Chitosan thermogels for local expansion and delivery of tumor-specific T lymphocytes towards enhanced cancer immunotherapies.* Biomaterials, 2016. **75**: p. 237-249.

197. Youssef, A., S.J. Hollister, and P.D. Dalton, *Additive manufacturing of polymer melts for implantable medical devices and scaffolds.* Biofabrication, 2017. **9**(1): p. 012002.

198. Papalamprou, A., et al., *Xenogeneic cardiac extracellular matrix scaffolds with or without seeded mesenchymal stem cells exhibit distinct in vivo immunosuppressive and regenerative properties.* Acta biomaterialia, 2016. **45**: p. 155-168.

199. Zysk, A., et al., *Adoptive transfer of ex vivo expanded Vγ9Vδ2 T cells in combination with zoledronic acid inhibits cancer growth and limits osteolysis in a murine model of osteolytic breast cancer.* Cancer letters, 2017. **386**: p. 141-150.

200. Zysk, A., et al., *Zoledronate Enhances the Cytotoxicity of Gamma Delta T Cell Immunotherapy in an Orthotopic Mouse Model of Osteolytic Osteosarcoma.* Journal of Cancer Science & Therapy, 2018.

201. Goto, H., et al., *Potent antitumor activity of zoledronic acid-induced Vγ9Vδ2 T cells against primary effusion lymphoma.* Cancer letters, 2013. **331**(2): p. 174-182.

202. Carpenito, C., et al., *Control of large, established tumor xenografts with genetically retargeted human T cells containing CD28 and CD137 domains.* Proceedings of the National Academy of Sciences, 2009. **106**(9): p. 3360-3365.

203. Song, D.-G., et al., *In vivo persistence, tumor localization, and antitumor activity of CAR-engineered T cells is enhanced by costimulatory signaling through CD137 (4-1BB).* Cancer research, 2011. **71**(13): p. 4617-4627.

204. Parente-Pereira, A.C., et al., *Trafficking of CAR-engineered human T cells following regional or systemic adoptive transfer in SCID beige mice.* Journal of clinical immunology, 2011. **31**(4): p. 710-718.

205. Morita, C.T., et al., *Nonpeptide antigens, presentation mechanisms, and immunological memory of human Vγ2Vδ2 T cells: discriminating friend from foe through the recognition of prenyl pyrophosphate antigens.* Immunological reviews, 2007. **215**(1): p. 59-76.

206. Benzaïd, I., et al., *In vivo phosphoantigen levels in bisphosphonate-treated human breast tumors trigger Vγ9Vδ2 T-cell antitumor cytotoxicity through ICAM-1 engagement.* Clinical Cancer Research, 2012. **18**(22): p. 6249-6259.

207. Weigelin, B. and P. Friedl, *A three-dimensional organotypic assay to measure target cell killing by cytotoxic T lymphocytes.* Biochemical pharmacology, 2010. **80**(12): p. 2087-2091.

208. Siegers, G.M., et al., *Functional Plasticity of Gamma Delta T Cells and Breast Tumor Targets in Hypoxia.* Frontiers in Immunology, 2018. **9**(1367).

209. Zinonos, I., et al., *Anticancer efficacy of Apo2L/TRAIL is retained in the presence of high and biologically active concentrations of osteoprotegerin in vivo.* Journal of Bone and Mineral Research, 2011. **26**(3): p. 630-643.

210. Zinonos, I., et al., *Doxorubicin overcomes resistance to drozitumab by antagonizing inhibitor of apoptosis proteins (IAPs).* Anticancer Research, 2014. **34**(12): p. 7007-7020.

211. Dharmapatni, A.A., et al., *Elevated expression of caspase-3 inhibitors, survivin and xIAP correlates with low levels of apoptosis in active rheumatoid synovium.* Arthritis research & therapy, 2009. **11**(1): p. 1-11.

212. Mahvi, D.A., et al., *Local cancer recurrence: the realities, challenges, and opportunities for new therapies.* CA: a cancer journal for clinicians, 2018. **68**(6): p. 488-505.

213. Restifo, N.P., M.E. Dudley, and S.A. Rosenberg, *Adoptive immunotherapy for cancer: harnessing the T cell response.* Nature Reviews Immunology, 2012. **12**(4): p. 269-281.

214. Gentles, A.J., et al., *The prognostic landscape of genes and infiltrating immune cells across human cancers.* Nature medicine, 2015. **21**(8): p. 938.

215. Muraro, M., et al., *Osteosarcoma cell line growth inhibition by zoledronate-stimulated effector cells.* Cellular immunology, 2007. **249**(2): p. 63-72.

216. Hoeres, T., et al., *Improving the efficiency of Vγ9Vδ2 T-cell immunotherapy in Cancer.* Frontiers in immunology, 2018. **9**: p. 800.

217. Jauhiainen, M., et al., *Analysis of endogenous ATP analogs and mevalonate pathway metabolites in cancer cell cultures using liquid chromatography–electrospray ionization mass spectrometry.* Journal of Chromatography B, 2009. **877**(27): p. 2967-2975.

218. Fisher, J.P., et al., *γδ T cells for cancer immunotherapy: a systematic review of clinical trials.* Oncoimmunology, 2014. **3**(1): p. e27572.

219. Nakajima, J., et al., *A phase I study of adoptive immunotherapy for recurrent non-small-cell lung cancer patients with autologous γδ T cells.* 2010. **37**(5): p. 1191-1197.

220. McTaggart, S., *Isoprenylated proteins.* Cellular and Molecular Life Sciences CMLS, 2006. **63**(3): p. 255-267.

221. Coxon, F.P., K. Thompson, and M.J. Rogers, *Recent advances in understanding the mechanism of action of bisphosphonates.* Current opinion in pharmacology, 2006. **6**(3): p. 307-312.

222. Kubista, B., et al., *Anticancer effects of zoledronic acid against human osteosarcoma cells.* Journal of orthopaedic research, 2006. **24**(6): p. 1145-1152.

223. Nicodemus, G.D. and S.J. Bryant, *Cell encapsulation in biodegradable hydrogels for tissue engineering applications.* Tissue Engineering Part B: Reviews, 2008. **14**(2): p. 149-165.

224. Kleinman, H.K. and G.R. Martin. *Matrigel: basement membrane matrix with biological activity*. in *Seminars in cancer biology*. 2005. Elsevier.

225. Knight, E. and S. Przyborski, *Advances in 3D cell culture technologies enabling tissue-like structures to be created in vitro.* Journal of anatomy, 2015. **227**(6): p. 746-756.

226. Caliari, S.R. and J.A. Burdick, *A practical guide to hydrogels for cell culture.* Nature methods, 2016. **13**(5): p. 405-414.

227. Polykandriotis, E., et al., *To matrigel or not to matrigel.* The American journal of pathology, 2008. **172**(5): p. 1441-1442.

228. Janmey, P.A., J.P. Winer, and J.W. Weisel, *Fibrin gels and their clinical and bioengineering applications.* Journal of the Royal Society Interface, 2009. **6**(30): p. 1-10.

229. Ramshaw, J.A., et al., *Collagens as biomaterials.* Journal of Materials Science: Materials in Medicine, 2009. **20**(Suppl 1): p. 3.

230. Shaikh, F.M., et al., *Fibrin: a natural biodegradable scaffold in vascular tissue engineering.* Cells Tissues Organs, 2008. **188**(4): p. 333-346.

231. Jackson, M.R., *Fibrin sealants in surgical practice: an overview.* The American journal of surgery, 2001. **182**(2): p. S1-S7.

232. De Boer, M.T., et al., *Role of fibrin sealants in liver surgery.* Digestive surgery, 2012. **29**(1): p. 54-61.

233. Jackson, M.R., *New and potential uses of fibrin sealants as an adjunct to surgical hemostasis.* The American journal of surgery, 2001. **182**(2): p. S36-S39.

234. Ogunnaike, E.A., et al., *Fibrin gel enhances the antitumor effects of chimeric antigen receptor T cells in glioblastoma.* Science Advances, 2021. **7**(41): p. eabg5841.

235. Weiden, J., et al., *Injectable biomimetic hydrogels as tools for efficient T cell expansion and delivery.* Frontiers in immunology, 2018. **9**: p. 2798.

236. Hayday, A.C., *γδ cells: a right time and a right place for a conserved third way of protection.* Annual review of immunology, 2000. **18**(1): p. 975-1026.

237. Park, J.H. and H.K. Lee, *Function of γδ T cells in tumor immunology and their application to cancer therapy.* Experimental & Molecular Medicine, 2021: p. 1-10.

238. Eberl, M., et al., *Microbial isoprenoid biosynthesis and human γδ T cell activation.* FEBS letters, 2003. **544**(1-3): p. 4-10.

239. Gu, S., et al. *Butyrophilin3A proteins and Vγ9Vδ2 T cell activation*. in *Seminars in cell & developmental biology*. 2018. Elsevier.

240. Moulin, M., et al., *Vγ9Vδ2 T cell activation by strongly agonistic nucleotidic phosphoantigens.* Cellular and Molecular Life Sciences, 2017. **74**(23): p. 4353-4367.

241. Sebestyen, Z., et al., *Translating gammadelta (γδ) T cells and their receptors into cancer cell therapies.* Nature reviews Drug discovery, 2020. **19**(3): p. 169-184.

242. Abe, Y., et al., *Clinical and immunological evaluation of zoledronate-activated Vγ9γδ T-cell-based immunotherapy for patients with multiple myeloma.* Experimental hematology, 2009. **37**(8): p. 956-968.

243. Noguchi, A., et al., *Zoledronate-activated Vγ9γδ T cell-based immunotherapy is feasible and restores the impairment of γδ T cells in patients with solid tumors.* Cytotherapy, 2011. **13**(1): p. 92-97.

244. Aoki, T., et al., *Adjuvant combination therapy with gemcitabine and autologous γδ T-cell transfer in patients with curatively resected pancreatic cancer.* Cytotherapy, 2017. **19**(4): p. 473-485.

245. Wilhelm, M., et al., *Successful adoptive transfer and in vivo expansion of haploidentical γδ T cells.* Journal of translational medicine, 2014. **12**(1): p. 1-5.

246. Sakamoto, M., et al., *Adoptive immunotherapy for advanced non-small cell lung cancer using zoledronate-expanded γδ T cells: a phase I clinical study.* 2011. **34**(2): p. 202-211.

247. Jungbluth, A.A., et al., *Immunohistochemical detection of γ/δ T lymphocytes in formalin-fixed paraffin-embedded tissues.* Applied Immunohistochemistry & Molecular Morphology, 2019. **27**(8): p. 581-583.

248. Sun, S., et al., *Fluorescent bisphosphonate and carboxyphosphonate probes: a versatile imaging toolkit for applications in bone biology and biomedicine.* Bioconjugate chemistry, 2016. **27**(2): p. 329-340.

249. Cremers, S. and S. Papapoulos, *Pharmacology of bisphosphonates.* Bone, 2011. **49**(1): p. 42-49.

250. Junankar, S., et al., *Real-time intravital imaging establishes tumor-associated macrophages as the extraskeletal target of bisphosphonate action in cancer.* Cancer discovery, 2015. **5**(1): p. 35-42.

251. Roelofs, A.J., et al., *Molecular mechanisms of action of bisphosphonates: current status.* Clinical Cancer Research, 2006. **12**(20): p. 6222s-6230s.

252. Thompson, K., et al., *Cytosolic entry of bisphosphonate drugs requires acidification of vesicles after fluid-phase endocytosis.* Molecular pharmacology, 2006. **69**(5): p. 1624-1632.

253. Caraglia, M., et al., *Zoledronic acid: an unending tale for an antiresorptive agent.* Expert opinion on pharmacotherapy, 2010. **11**(1): p. 141-154.

254. Freire, E., D.R. Vega, and R. Baggio, *Zoledronate complexes. III. Two zoledronate complexes with alkaline earth metals:[Mg (C5H9N2O7P2) 2 (H2O) 2] and [Ca (C5H8N2O7P2)(H2O)] n.* Acta Crystallographica Section C: Crystal Structure Communications, 2010. **66**(6): p. m166-m170.

255. Zlatev, H.P., et al., *Uptake of free, calcium-bound and liposomal encapsulated nitrogen containing bisphosphonates by breast cancer cells.* European Journal of Pharmaceutical Sciences, 2016. **86**: p. 58-66.

256. Han, H.-K., H.-J. Shin, and D.H. Ha, *Improved oral bioavailability of alendronate via the mucoadhesive liposomal delivery system.* European journal of pharmaceutical sciences, 2012. **46**(5): p. 500-507.

257. van Rooijen, N. and E. van Kesteren-Hendrikx, *Clodronate liposomes: perspectives in research and therapeutics.* Journal of liposome research, 2002. **12**(1-2): p. 81-94.

258. Marra, M., et al., *Nanotechnologies to use bisphosphonates as potent anticancer agents: the effects of zoledronic acid encapsulated into liposomes.* Nanomedicine: Nanotechnology, Biology and Medicine, 2011. **7**(6): p. 955-964.

259. Marra, M., et al., *New self-assembly nanoparticles and stealth liposomes for the delivery of zoledronic acid: a comparative study.* Biotechnology advances, 2012. **30**(1): p. 302-309.

260. Salzano, G., et al., *Self-assembly nanoparticles for the delivery of bisphosphonates into tumors.* International journal of pharmaceutics, 2011. **403**(1-2): p. 292-297.

261. De Rosa, G., D. De Stefano, and A. Galeone, *Oligonucleotide delivery in cancer therapy.* Expert opinion on drug delivery, 2010. **7**(11): p. 1263-1278.

262. Louis, D.N., et al., *The 2007 WHO classification of tumours of the central nervous system.* Acta neuropathologica, 2007. **114**(2): p. 97-109.

263. Davis, M.E., *Glioblastoma: overview of disease and treatment.* Clinical journal of oncology nursing, 2016. **20**(5): p. S2.

264. Surawicz, T.S., et al., *Brain tumor survival: results from the National Cancer Data Base.* Journal of neuro-oncology, 1998. **40**(2): p. 151-160.

265. Weiss, H.M., et al., *Biodistribution and plasma protein binding of zoledronic acid.* Drug Metabolism and Disposition, 2008. **36**(10): p. 2043-2049.

266. Wang, H., et al., *Different T-cell subsets in glioblastoma multiforme and targeted immunotherapy.* Cancer Letters, 2021. **496**: p. 134-143.

267. Buckner, J.C., et al. *Central nervous system tumors*. in *Mayo Clinic Proceedings*. 2007. Elsevier.

268. Wang, P.P., J. Frazier, and H. Brem, *Local drug delivery to the brain.* Advanced drug delivery reviews, 2002. **54**(7): p. 987-1013.

269. Bregy, A., et al., *The role of Gliadel wafers in the treatment of high-grade gliomas.* Expert review of anticancer therapy, 2013. **13**(12): p. 1453-1461.

270. Chung, D.-S., H.-J. Shin, and Y.-K. Hong, *A new hope in immunotherapy for malignant gliomas: adoptive T cell transfer therapy.* Journal of immunology research, 2014. **2014**.

271. Nakazawa, T., et al., *Cytotoxic human peripheral blood-derived γδT cells kill glioblastoma cell lines: implications for cell-based immunotherapy for patients with glioblastoma.* Journal of neuro-oncology, 2014. **116**(1): p. 31-39.

272. Bryant, N.L., et al., *Characterization and immunotherapeutic potential of γδ T-cells in patients with glioblastoma.* Neuro-oncology, 2009. **11**(4): p. 357-367.

273. Chauvin, C., et al., *NKG2D controls natural reactivity of Vγ9Vδ2 T lymphocytes against mesenchymal glioblastoma cells.* Clinical Cancer Research, 2019. **25**(23): p. 7218-7228.

274. Fujimiya, Y., et al., *In vitro interleukin 12 activation of peripheral blood CD3 (+) CD56 (+) and CD3 (+) CD56 (-) gammadelta T cells from glioblastoma patients.* Clinical cancer research, 1997. **3**(4): p. 633-643.

275. Lamb, L.S., *γδ T cells as immune effectors against high-grade gliomas.* Immunologic research, 2009. **45**(1): p. 85-95.

276. Silva-Santos, B., K. Serre, and H. Norell, *γδ T cells in cancer.* Nature reviews immunology, 2015. **15**(11): p. 683-691.

277. Nakazawa, T., et al., *Antitumor effects of minodronate, a third-generation nitrogen-containing bisphosphonate, in synergy with γδT cells in human glioblastoma in vitro and in vivo.* Journal of neuro-oncology, 2016. **129**(2): p. 231-241.

278. Russell, R.G.G., *Bisphosphonates: from bench to bedside.* Annals of the New York Academy of Sciences, 2006. **1068**(1): p. 367-401.

279. Clézardin, P., *Bisphosphonates' antitumor activity: an unravelled side of a multifaceted drug class.* Bone, 2011. **48**(1): p. 71-79.

280. Harwood Jr, H., et al., *In vivo regulation of human leukocyte 3-hydroxy-3-methylglutaryl coenzyme A reductase: increased enzyme protein concentration and catalytic efficiency in human leukemia and lymphoma.* Journal of lipid research, 1991. **32**(8): p. 1237-1252.

281. Asslan, R., et al., *Epidermal growth factor stimulates 3-hydroxy-3-methylglutaryl-coenzyme A reductase expression via the ErbB-2 pathway in human breast adenocarcinoma cells.* Biochemical and biophysical research communications, 1999. **260**(3): p. 699-706.

282. Cimini, E., et al., *Zoledronic acid enhances Vδ2 T-lymphocyte antitumor response to human glioma cell lines.* International journal of immunopathology and pharmacology, 2011. **24**(1): p. 139-148.

283. Gronich, N. and G. Rennert, *Beyond aspirin—cancer prevention with statins, metformin and bisphosphonates.* Nature reviews Clinical oncology, 2013. **10**(11): p. 625-642.

284. Clézardin, P., *Mechanisms of action of bisphosphonates in oncology: a scientific concept evolving from antiresorptive to anticancer activities.* BoneKEy reports, 2013. **2**.

285. Göbel, A., et al., *Cholesterol and beyond-The role of the mevalonate pathway in cancer biology.* Biochimica et Biophysica Acta (BBA)-Reviews on Cancer, 2020. **1873**(2): p. 188351.

286. Hiraga, T., et al., *Zoledronic acid inhibits visceral metastases in the 4T1/luc mouse breast cancer model.* Clinical cancer research, 2004. **10**(13): p. 4559-4567.

287. Gnant, M. and P. Clézardin, *Direct and indirect anticancer activity of bisphosphonates: a brief review of published literature.* Cancer treatment reviews, 2012. **38**(5): p. 407-415.

288. Buhaescu, I. and H. Izzedine, *Mevalonate pathway: a review of clinical and therapeutical implications.* Clinical biochemistry, 2007. **40**(9-10): p. 575-584.

289. Brown, J.E., H. Neville-Webbe, and R.E. Coleman, *The role of bisphosphonates in breast and prostate cancers.* Endocrine-related cancer, 2004. **11**(2): p. 207-224.

290. Goffinet, M., et al., *Zoledronic acid treatment impairs protein geranyl-geranylation for biological effects in prostatic cells.* BMC cancer, 2006. **6**(1): p. 1-10.

291. Senaratne, S., J. Mansi, and K. Colston, *The bisphosphonate zoledronic acid impairs Ras membrane [correction of impairs membrane] localisation and induces cytochrome c release in breast cancer cells.* British Journal of Cancer, 2002. **86**(9): p. 1479-1486.

292. Oades, G.M., et al., *Nitrogen containing bisphosphonates induce apoptosis and inhibit the mevalonate pathway, impairing Ras membrane localization in prostate cancer cells.* The Journal of urology, 2003. **170**(1): p. 246-252.

293. Idrees, A.S., et al., *Comparison of γδ T cell responses and farnesyl diphosphate synthase inhibition in tumor cells pretreated with zoledronic acid.* Cancer science, 2013. **104**(5): p. 536-542.

294. Butt, S., et al., *The target for statins, HMG-CoA reductase, is expressed in ductal carcinoma-in situ and may predict patient response to radiotherapy.* Annals of surgical oncology, 2014. **21**(9): p. 2911-2919.

295. de Wolf, E., et al., *Dietary geranylgeraniol can limit the activity of pitavastatin as a potential treatment for drug-resistant ovarian cancer.* Scientific reports, 2017. **7**(1): p. 1-10.

296. Greenaway, J.B., et al., *Ovarian tumour growth is characterized by mevalonate pathway gene signature in an orthotopic, syngeneic model of epithelial ovarian cancer.* Oncotarget, 2016. **7**(30): p. 47343.

297. Qiu, Z., et al., *HMGCR positively regulated the growth and migration of glioblastoma cells.* Gene, 2016. **576**(1): p. 22-27.

298. Mo, H. and C.E. Elson, *Studies of the isoprenoid-mediated inhibition of mevalonate synthesis applied to cancer chemotherapy and chemoprevention.* Experimental biology and medicine, 2004. **229**(7): p. 567-585.

299. Gruenbacher, G. and M. Thurnher, *Mevalonate metabolism governs cancer immune surveillance.* Oncoimmunology, 2017. **6**(10): p. e1342917.

300. Horie, N., et al., *Combined effects of a third-generation bisphosphonate, zoledronic acid with other anticancer agents against murine osteosarcoma.* British journal of cancer, 2007. **96**(2): p. 255-261.

301. Koto, K., et al., *Zoledronic acid inhibits proliferation of human fibrosarcoma cells with induction of apoptosis, and shows combined effects with other anticancer agents.* Oncology reports, 2010. **24**(1): p. 233-239.

302. Fromigue, O., L. Lagneaux, and J.J. Body, *Bisphosphonates induce breast cancer cell death in vitro.* Journal of bone and mineral research, 2000. **15**(11): p. 2211-2221.

303. Boissier, S., et al., *Bisphosphonates inhibit breast and prostate carcinoma cell invasion, an early event in the formation of bone metastases.* Cancer research, 2000. **60**(11): p. 2949-2954.

304. Montague, R., et al., *Differential inhibition of invasion and proliferation by bisphosphonates: anti-metastatic potential of Zoledronic acid in prostate cancer.* European urology, 2004. **46**(3): p. 389-402.

305. Gouin, F., et al., *Zoledronic acid slows down rat primary chondrosarcoma development, recurrent tumor progression after intralesional curretage and increases overall survival.* International journal of cancer, 2006. **119**(5): p. 980-984.

306. Wakchoure, S., et al., *Bisphosphonates inhibit the growth of mesothelioma cells in vitro and in vivo.* Clinical cancer research, 2006. **12**(9): p. 2862-2868.

307. Merrell, M.A., et al., *Differential effects of Ca2+ on bisphosphonate-induced growth inhibition in breast cancer and mesothelioma cells.* European journal of pharmacology, 2007. **559**(1): p. 21-31.

308. Ottewell, P.D., et al., *Sustained inhibition of tumor growth and prolonged survival following sequential administration of doxorubicin and zoledronic acid in a breast cancer model.* International journal of cancer, 2010. **126**(2): p. 522-532.

309. Santolaria, T., et al., *Repeated systemic administrations of both aminobisphosphonates and human Vγ9Vδ2 T cells efficiently control tumor development in vivo.* The Journal of Immunology, 2013. **191**(4): p. 1993-2000.

310. J Roelofs, A., et al., *Bisphosphonates: molecular mechanisms of action and effects on bone cells, monocytes and macrophages.* Current pharmaceutical design, 2010. **16**(27): p. 2950-2960.

311. Costa, L., et al., *Anticancer evidence for zoledronic acid across the cancer continuum.* Critical reviews in oncology/hematology, 2011. **77**: p. S31-S37.

312. Clézardin, P., F.H. Ebetino, and P.G. Fournier, *Bisphosphonates and cancer-induced bone disease: beyond their antiresorptive activity.* Cancer Research, 2005. **65**(12): p. 4971-4974.

313. Stresing, V., et al., *Bisphosphonates in cancer therapy.* Cancer letters, 2007. **257**(1): p. 16-35.

314. Marra, M., et al., *Cutting the limits of aminobisphosphonates: new strategies for the potentiation of their anti-tumour effects.* Current cancer drug targets, 2009. **9**(7): p. 791-800.

315. Yuasa, T., et al., *Zoledronic acid-a multiplicity of anti-cancer action.* Current medicinal chemistry, 2007. **14**(20): p. 2126-2135.

316. Mönkkönen, H., et al., *Bisphosphonate-induced ATP analog formation and its effect on inhibition of cancer cell growth.* Anti-cancer drugs, 2008. **19**(4): p. 391-399.

317. Mönkkönen, H., et al., *Zoledronic acid induced IPP/ApppI accumulation in different cancer cell lines.* Bone, 2006. **3**(38): p. 58.

318. Tanaka, Y., *Human γδ T cells and tumor immunotherapy.* Journal of Clinical and Experimental Hematopathology, 2006. **46**(1): p. 11-23.

319. Shmeeda, H., et al., *Liposome encapsulation of zoledronic acid results in major changes in tissue distribution and increase in toxicity.* Journal of Controlled Release, 2013. **167**(3): p. 265-275.

320. Rommasi, F. and N. Esfandiari, *Liposomal Nanomedicine: Applications for Drug Delivery in Cancer Therapy.* Nanoscale Research Letters, 2021. **16**(1): p. 1-20.

321. Hodgins, N.O., J.T.-W. Wang, and K.T. Al-Jamal, *Nano-technology based carriers for nitrogen-containing bisphosphonates delivery as sensitisers of γδ T cells for anticancer immunotherapy.* Advanced drug delivery reviews, 2017. **114**: p. 143-160.

322. Chebbi, I., et al., *In vitro assessment of liposomal neridronate on MDA-MB-231 human breast cancer cells.* International journal of pharmaceutics, 2010. **383**(1-2): p. 116-122.

323. Shmeeda, H., et al., *Delivery of zoledronic acid encapsulated in folate-targeted liposome results in potent in vitro cytotoxic activity on tumor cells.* Journal of Controlled Release, 2010. **146**(1): p. 76-83.

324. Edmonds, S., et al., *Exploiting the metal-chelating properties of the drug cargo for in vivo positron emission tomography imaging of liposomal nanomedicines.* ACS nano, 2016. **10**(11): p. 10294-10307.

325. Rajan, R., et al., *Liposome-induced immunosuppression and tumor growth is mediated by macrophages and mitigated by liposome-encapsulated alendronate.* Journal of Controlled Release, 2018. **271**: p. 139-148.

326. Hodgins, N.O., et al., *Investigating in vitro and in vivo αvβ6 integrin receptor-targeting liposomal alendronate for combinatory γδ T cell immunotherapy.* Journal of controlled release, 2017. **256**: p. 141-152.

327. Hodgins, N.O., et al., *In vitro potency, in vitro and in vivo efficacy of liposomal alendronate in combination with γδ T cell immunotherapy in mice.* Journal of Controlled Release, 2016. **241**: p. 229-241.

328. Parente-Pereira, A.C., et al., *Adoptive immunotherapy of epithelial ovarian cancer with Vγ9Vδ2 T cells, potentiated by liposomal alendronic acid.* The Journal of Immunology, 2014. **193**(11): p. 5557-5566.

329. Wiemer, A.J., et al., *Pivaloyloxymethyl-modified isoprenoid bisphosphonates display enhanced inhibition of cellular geranylgeranylation.* Bioorganic & medicinal chemistry, 2008. **16**(7): p. 3652-3660.

330. van Beek, E., et al., *Structural requirements for bisphosphonate actions in vitro.* Journal of bone and mineral research, 1994. **9**(12): p. 1875-1882.

331. Hirabayashi, H., et al., *Relationship between physicochemical and osteotropic properties of bisphosphonic derivatives: rational design for osteotropic drug delivery system (ODDS).* Pharmaceutical research, 2001. **18**(5): p. 646-651.

332. Zhang, Y., et al., *Lipophilic bisphosphonates as dual farnesyl/geranylgeranyl diphosphate synthase inhibitors: an X-ray and NMR investigation.* Journal of the American Chemical Society, 2009. **131**(14): p. 5153-5162.

333. Zhang, Y., et al., *Lipophilic pyridinium bisphosphonates: potent γδ T cell stimulators.* Angewandte Chemie International Edition, 2010. **49**(6): p. 1136-1138.

334. Adams, E.J., S. Gu, and A.M. Luoma, *Human gamma delta T cells: evolution and ligand recognition.* Cellular immunology, 2015. **296**(1): p. 31-40.

335. Harly, C., C.-M. Peigné, and E. Scotet, *Molecules and mechanisms implicated in the peculiar antigenic activation process of human Vγ9Vδ2 T cells.* Frontiers in immunology, 2015. **5**: p. 657.